Hydraulic Analysis of Ice-covered River Flow

Md. Azizul Hoque

A thesis

In

The Department of Building, Civil and Environmental Engineering

Presented in Partial Fulfillment of the Requirements

for the Degree of Master of Applied Science (Civil Engineering) at

Concordia University

Montreal, Quebec, Canada

April 2009

Your file Votre référence
ISBN: 978-0-494-63326-7
Our file Notre référence
ISBN: 978-0-494-63326-7

Abstract

Hydraulic Analysis of Ice -covered River Flow

Md. Azizul Hoque

For a substantial portion of the year many Canadian rivers are frozen. River ice is known to have an important impact on the water cycle and hydraulic engineering infrastructures. From the hydraulics perspective, the formation of an ice cover on the river surface causes an increase in resistance to flow and therefore a decrease in discharge to downstream.

In the subject area of ice covered river hydraulics, there have been limited studies. In this study we have quantified the differences in flow velocity, discharge and flow energy distributions between conditions with and without the ice cover. We have also estimated the roughness of the ice cover underside using the boundary layer theory. Based on our flow analysis of a larger number of ice-covered rivers in Canada, the boundary layer profiles beneath the ice cover and above the channel bed are rarely symmetric, i.e. the dynamic effect of the ice cover and that of the channel bed differ. Many of the observed velocity profiles are too complicated to be described using simple analytical functions.

The presence of the ice cover can reduce the hydraulic radius of a cross section by as much as 46% and flow discharge by 60%, in comparisons to the corresponding values associated with open channel conditions. Under ice covered conditions the flow is very sensitive to the friction parameter. For a given river cross section, the difference in flow velocities with and without an ice cover is between 39% and 60%.

Acknowledgements

I am glad to express my sincere gratitude to my thesis supervisor, Prof. S. S. Li, the Department of Building, Civil and Environmental Engineering (BCEE), Concordia University, Montreal, QC, for his relentless support and illustrious guidance. Prof. Li always encouraged me to do something that is almost new in my field of research. I appreciate his guidance at different stages of this research work.

I would like to thank Mr. Ashiqur Rahman Khan, a M.A.Sc. student in BCEE for his help on some hydraulic engineering experiments, which was very helpful in course of my thesis. I also thank Mr. Sangsoo Han, a Ph.D. student in BCEE, for his valuable demonstration on HEC-RAS modelling, which has been used in this thesis.

I would like to thank the faculty members and administrative staff of BCEE for their suggestions and guidance towards accomplishment of my thesis.

I would like to thank my father who always encouraged me to complete the degree in the field of Hydraulic Engineering, especially in Water Resources Engineering.

I specifically thank my wife, Mumtaz Begum, and two sons, Md. Afnan Hoque and Md. Afsan Hoque, for their encouragement and support to complete my thesis.

Finally, I would like to thank my colleagues, for their encouragement and help during the research period.

Md Azizul Hoque
M.A.Sc. in Civil Engineering
Dept. of Building, Civil & Environmental Engineering, Concordia University
1455 de Maisonneuve Blvd. West
Montréal, Québec, Canada, H3G 1M8

Table of Contents

Chapter Four: Flow Resistance in Ice-covered Rivers

List of Figures

List of Tables

List of Symbols

English Symbols

Symbol	Definition
A	Cross sectional area (m^2)
A_i	Ice affected area (m^2)
A_b	Channel bed affected area (m^2)
a	Ratio of wetted perimeter exerted by ice to the wetted perimeter exerted at bottom
b_x	Horizontal distance at the point, x (m)
C	Coefficient of expansion or contraction loss; integration constant
h_e	Energy head loss
K_o	Coefficient
k_i	Ice roughness height , (m)
L	Reach length, (m)
m_b	The power coefficient for the bed flow layer,
m_i	The power coefficient for the ice-cover underside flow layer
n	Manning's roughness coefficient
n_o	Manning's composite roughness coefficient

n_i	Manning's roughness coefficient for ice cover
n_b	Manning's roughness coefficient for channel bed
P	Wetted perimeter (m)
p_i	Wetted perimeter exerted by ice (m)
p_b	Wetted perimeter exerted at channel bottom (m)
Q	Discharge (m^3/s)
q_x	Discharge through sub section x, (m^3/s)
q_1	Discharge through sub section 1, (m^3/s)
R_h	Hydraulic radius (m)
S	Channel bed slope
$\overline{S}_f$	Average friction slope between the two cross sections
V	Depth-averaged velocity m/s
V_i	Mean velocity at the zone of ice-cover, (m/s)
V_b	Mean velocity at the zone of channel bed, (m/s)
V_o	Maximum free stream velocity under ice-cover (m/s)
V_{mb}	Depth-averaged velocity at the zone of channel bed (m/s)
V_{mi}	Depth-averaged velocity at the zone of Ice (m/s)

v	Flow velocity under the zone of ice affected area (m/s)
v_{sb}	Related to the average velocity for the bed flow layer
v_{si}	Related to the average velocity for ice-cover flow layer
v_x	M ean velocity at vertical x (m/s)
Y	The depth of water, (m)
y_o	Depth below underside of the ice-cover to the poin of maximum velocity (m)
y_i	The depth below ice underside to the maximum velocity
y_b	The depth from channel bed to the maximum velocity

Greek Symbols

Symbol	Definition
κ	Von Karman's constant
υ	Molecular viscosity of water (1.5×10^{-6} m^2/s)
δ_m	The logarithmic velocity distribution.
τ_w	Shear stress of water (N/m^2)
v_τ	Wall friction velocity (m/s)
ρ	Density of water (gm/cm^3)
α	Energy coefficient
β	Momentum coefficient,

Abbreviations

ASCE	American Society of Civil Engineers
HEC-RAS	Hydraulic Engineering Center's River Analysis System
USGS	United States Geographical System
WSC	Water Survey of Canada
m	meter
m^3/s	Cubic meter per second

Chapter One: Introduction

1.1 Background

River ice processes affect river ecology as well as fish, and the winter habitats are more complex than ice free hydrodynamics (Power *et al.*, 1993; Beltaos, 1995; Cunjak, 1996; Heggenes and Dokk, 2001; Prowse 2001). The Canadian oil sands industry, federal and provincial departments and aboriginal groups are working jointly through the Cumulative Environmental Management Association to establish appropriate flow management regimes and monitoring programs for the lower Athabasca River. According to Hamilton (2003), river ice is involved in 38% of the cases of extremely low discharge and 9.3% of maximum flow events. The impact of river ice on flood levels may be even greater in connection with stage. One-third of the floods in eastern Canada are related to ice jams (Beltaos, 1995).

Almost all the rivers in Canada and other countries of cold climate are ice-covered in the winter. The Canadian subarctic region from Labrador nearly to the Bering Sea is dotted with many lakes and crossed by innumerable rivers, where winters are long and harsh. When the winter temperatures drop below the freezing level, ice covers form on the river surface. The formation of ice covers has social, economic and environmental implications. In winter time, river ice jams can cause river floods, threat navigation safety, interrupt hydropower operation and affect the health of the ecology system. River floods can also result from river ice melting in the spring.

There have been numerous examples of river floods as a direct result of ice jam. An example is shown in Figure 1.1. In the winter of 2008, ice jam took place in the Nechako River and the Fraser River and caused river floods in the City of Prince George in British

Columbia. Such events would lead to not only the execution of expensive emergency response for human being safety, but also potentially caused damage to infrastructures such as bridges (Figure 1.2). From the infrastructure design point of view, river ice is an important factor in ice-affected rivers. This is because the thickness of the ice cover produces impacts on the channel flow under the ice.

As another example, ice jam induced flood occurred in Lemhi River in Salmon, Idaho in 1984 (Figure 1.3). The flooded area included 92 homes and businesses. Water flowed into some homes to depths of over 2 feet, and then formed thick layers of ice that remained in buildings when the floodwaters receded. Flood damages were estimated about $1.8 millions (Source: US Army Corps of Engineers).

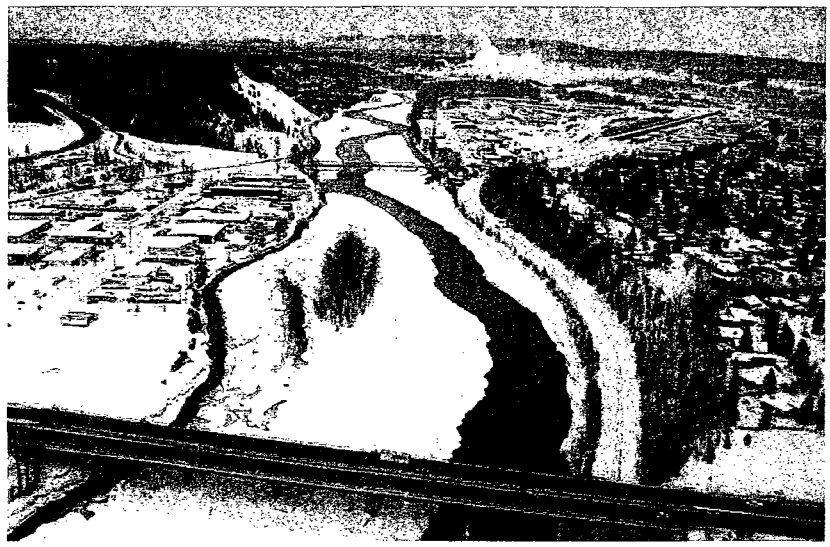

Fig. 1.1 River areas along the Nechako River and the Fraser River in British Columbia, which were affected by the ice jam and floods in the winter of 2008 (City of Prince Geroge, 2008).

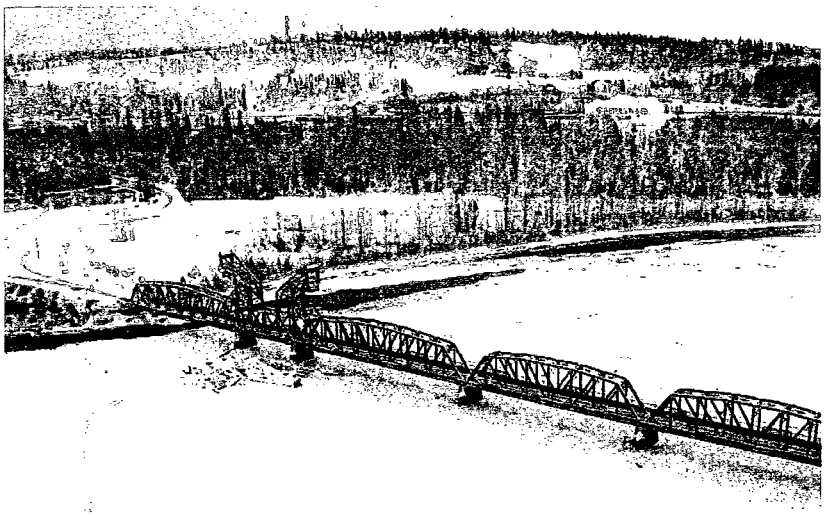

Fig. 1.2 Floods due to ice jam led to water level fluctuations and affected the Foothills Bridge and the Morning Place areas (City of Prince George, 2008).

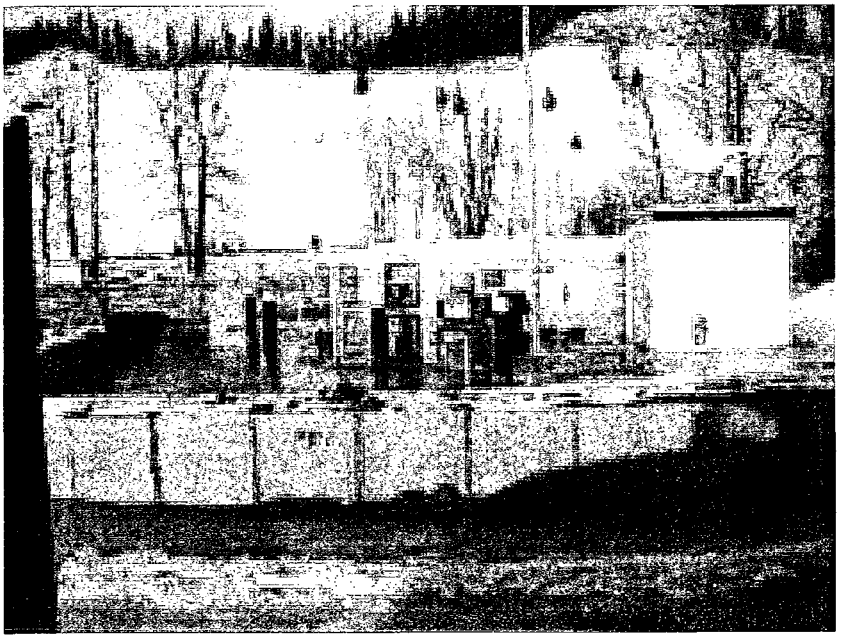

Fig. 1.3 Ice jam induced floods in Lehmi River, Salmon, Idaho, in 1984. Homes and businesses were damaged by the event (Source: U.S. Army Corps of Engineers).

The above examples have demonstrated the importance of the study of ice-covered rivers. In fact, sub-arctic channel flows typically reach a minimum at the end of the cold season just before the onset of spring melts. Late winter channel flows are relatively unaffected by meteorological influences, leaving storage elements (in the form of ice which would melt as the temperature rises) in the contributing area as the dominant source of flow.

For the hydraulics perspective, ice-covered rivers behave differently from rivers with a free surface. The presence of ice covers reduces the water cross sectional areas, increases the wetted perimeter and hence increases the flow resistance. This amounts to reductions of flow velocity and hence discharge capacity. The presence of the ice covers also change the distribution of the flow velocities from point to point at a given cross section. This altered velocity distribution has important implications to the application of the energy principle to river flow hydraulics.

Much of the previous studies on river hydraulics have dealt with open channels that have a free surface. Little research work has been done for ice-covered rivers. As a result, our understanding of the hydraulics of ice-covered rivers is limited, mainly because of the difficulty in obtaining field data from ice-covered rivers. Field measurements by Water Survey Canada have provided valuable velocity profiles from river stations across the country. These field measurements represent the unique opportunity to carry out a thorough analysis.

1.2 Thesis Objectives

The general goal of this research work is to enhance our understanding of the hydraulics of ice-covered rivers. Our objectives are:

1. To evaluate the applicability of some existent formulae for the determination of channel discharge under ice-covered conditions,
2. To compare the differences in flow velocity and channel discharge between free surface and ice-covered conditions,
3. To determine the changes in flow resistance due to the presence of ice covers, and
4. To quantify the reduction in flow area due to ice covers.

1.3 Organisation of Thesis

In this thesis we will compile available ice-covered river data including velocity profiles, ice cover thickness and channel geometry from a large number of Canadian river stations. Quality control will be performed to detect and/or eliminate data that are physically unreasonable. We will conduct statistics analysis in order to produce roughness coefficients for the ice cover underside. It is expected that the estimation of the coefficients for ice-covered rivers is much more complex than that for open channels. Difficulties in applying certain river hydraulics methods such as the direct method for determining the roughness of ice covers and the indirect method will be identified. In addition, we will examine the characteristics of ice-covered rivers in connection with boundary layers as well as important implications.

The remaining parts of this thesis are organized as follows. In Chapter Two a review of the literature pertinent to the hydraulics of ice-covered rivers is provided. This

is followed by a description of the field data and measurement of flow from ice-covered rivers in Chapter Three. In Chapter Four, we perform statistics and resistance analyses of the field measurements. These analyses produce discharge, velocity profile structures, reduction in flow area and roughness height of the ice cover underside. Results and discussion are presented in Chapter Five. Chapter Six discusses the parameterization in numerical modelling of ice-covered river flow. The discussion includes brief theoretical considerations and parameter specifications. In Chapter Seven we draw conclusions before presenting suggestions and recommendations for future research on the topic of ice-covered river hydraulics in Chapter Eight.

Chapter Two: Literature Review

2.1 Ice-covered Rivers

Rivers and streams in Canada and other northern countries typically have an ice cover in the winter season. Field observations have indicated ice covers of various configurations. Ashton (1986) classified the ice cover configurations as follows (Figures 2.1a-g): (a) frazil produced in the channel, and anchor ice formed on the channel bed and banks, with the onset of severe winter conditions; (b, c) partial ice covers, which develop in the early stages of formation of a complete river ice cover; (d-g) continuous ice covers. The continuous ice covers are further classified into four different types: consolidated ice covers, fragmented ice covers, hanging dams and aufeis.

In this thesis we are interested in stream flows under the consolidated ice covers, which are new or which form through the reconsolidation and subsequent smoothing of fragmented ice covers. Fragmented ice covers refer to the condition where an existing ice is broken up but the large ice masses remain wedged with each other (Ashton, 1986). The ice covers of interest are characterized by a smooth underside or an underside with small ripples. The hydraulics of river channels with a smooth cover would be less complicated; the hydraulic analysis of such a condition will help reveal some fundamental aspects of the ice-covered river flow problem.

2.2 Velocity Distribution in Ice-covered Rivers

It is constructive to consider the simplest case where natural rivers and streams are straight channels. Uzuner (1975) discussed the two-layer hypothesis that the flow in an ice-covered straight channel may be treated as a sandwich of two free-surface streams.

One of them is associated with the channel bed, whereas the other is associated with the underside of the ice cover. Urroz and Ettema (1994) extended the two-layer hypothesis to ice-covered, curved channels.

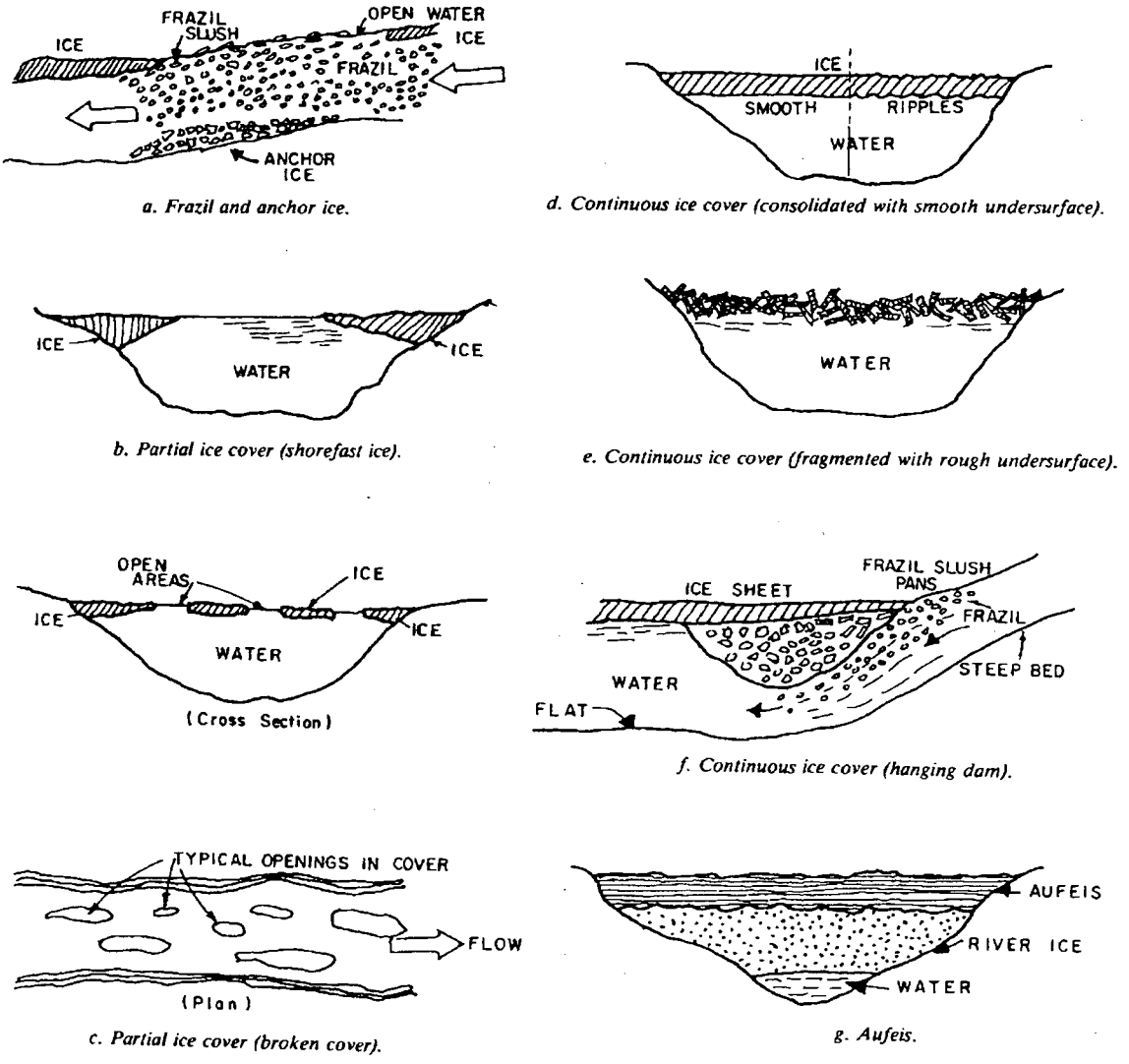

Fig. 2.1: Configurations of river ice covers (adopted from Ashton, 1986). A hanging dam refers to a relatively large accretion underneath the cover. Aufeis refers to massive surface ice, which can completely block the channel cross section and ice-covered curved channels.

They concluded that the hypothesis is inadequate for the analysis of flow in ice-covered natural rivers and streams that are not straight. The hypothesis gives only preliminary estimates in order of magnitude and direction of channel-wise and transverse flow components.

Consider ice-covered flow as two streams that are formed by the underside of the ice cover and the channel bottom. The vertical distribution of stream-wise velocity, v, of the two streams can be expressed by the fundamental power laws (Dolgopolova, 2002)

$$v = v_{sb}\left(\frac{Y-y}{y_b}\right)^{1/m_b} \tag{2.1}$$

$$v = v_{si}\left(\frac{y}{Y-y_b}\right)^{1/m_i} \tag{2.2}$$

where y is the vertical coordinate of a given point below the ice-cover, measured positive downward, Y is the total flow depth, y_b is the depth of the bed flow layer, m_b is the power coefficient for the bed flow layer, m_i is the power coefficient for the ice-cover underside flow layer, v_{sb} is related to the average velocity for the bed flow layer, and v_{si} is related to the average velocity for ice-cover flow layer. The power laws can also be expressed as (see e.g. Urroz and Ettema, 1994)

$$v = K_o\left(\frac{y}{Y}\right)^{1/m_b}\left(1-\frac{y}{Y}\right)^{1/m_i} \tag{2.3}$$

where K_o is a coefficient. Equation (2.3) is an extension of the power law expression by Tsai and Ettema (1994).

An important use of the power laws is for estimating the channel average velocity. Together channel cross section geometry, one can further calculate the discharge. For this and other applications, we must determine the coefficients and parameters in the

equations. A reliable way to determine the coefficients and parameters is to make field measurements from ice-covered rivers and streams. It is our intention to examine how well the above-mentioned theoretical velocity variations describe measured flow conditions to be presented in chapters of this thesis to follow.

2.3 Flow Measurements under Ice-Covered Conditions

To measure channel flow from ice-covered rivers is known as a challenging and sometime dangerous task. Traditionally, one drills a series of holes through the ice cover across the wetted channels and ice thickness (see e.g. Wang, 1993; Walker and Wang, 1997). Adjacent holes are typically some tens of meters apart; more than twenty holes may be necessary, depending on the width of the channel of interest. These holes represent measurement stations. Through the holes current meters are lowered into the flowing water and are suspended by either a lowering rod or cable at selected depths in the water column.

Usually the water level is used as the reference elevation when making ice-covered measurements. Walker and Wang (1997) suggested that measurements are made at selected discrete depths of $0.05Y$, $0.1Y$... $0.95Y$, where Y is the total depth between the ice-cover underside and the channel bed. Current meters suspended at the selected depths produce measurements of flow velocities. These velocities varying with depth describe velocity profiles of certain shape. The actual number of selected depths where measurements are made depends on the total flow depth at a given station.

To our knowledge the most systematic measurements of flow in ice-covered rivers and streams have been made by USGS and Water Survey Canada (Walker and Wang,

1997; Wang, 1993). Other flow measurements from ice-covered rivers in Canada include Burrell and Davar (1980). Techniques for flow measurements from ice-covered rivers have been improved over the recent years. An Acoustic Doppler Current Profiler mounted on the channel bed can record virtually continuous 3-D flow velocities over the entire water column (see e.g. Morse *et al.*, 2005).

2.4 Determination of River Discharge under Ice-covered Conditions

A need exits to determine channel discharges not only in the open-water season but also in the ice-covered season. This is particularly relevant to rivers and channels in Quebec. The following review covers the rating curve method and the velocity-area method for the determination of river discharges in the ice-covered season.

2.4.1 Rating Curve Method

A rating curve is a depth–discharge relationship for a given channel. The depth-discharge rating curve is established by fitting depth and flow rate measurements from a hydrometric gauging station as a regression problem. The idea of establishing the rate curve is to convert flow depth, which is relatively easy to measure, to discharge. Water Survey Canada has established rating curves for many gauging stations in Canadian rivers. The rating curves are believed to provide discharges of acceptable accuracy in the open-water season.

However, rating curves that are derived for open-water conditions may not provide accurate discharges in the ice covered season. Due to the effects of an ice cover, a unique stage–discharge relationship may not even exist. At the same time, because of the statistic nature of a rating curve, to establish it requires a large amount of depth and

flow data, which usually are not available in ice-covered rivers and streams. Obviously, the most accurate method for determining ice-covered discharge is by making direct measurements, but this entails field programs that are expensive and technically difficult to carry out.

River flow researchers have attempted to develop alternative methods for winter discharge determination. Hicks and Healy (2003) investigated the approach of hydraulic modelling of simple ice covers. They applied the approach to the Mackenzie River near Fort Providence in Northwest Territories and the Athabasca River at Fort McMurray in Alberta, and showed error percentages as low as 3% in discharge. This accuracy is apparently site specific. The suitability of the approach would depend on the availability of a sufficient amount of field data from the channel of interest, in order to calibrate the model. An interesting potential of Hicks and Healy (2003) is the development of rating curves using model output of water level and discharge under ice-covered conditions.

The question arises as to how to properly specify the ice thickness and roughness for the purpose of hydraulic modelling, given that these parameters tend to vary with time and space. The characterization of the ice cover parameters would be a contribution to advancing our understanding of ice-covered channels through numerical modelling. Ice cover characteristics partly depend on channel cross section shape, flow depth and discharge magnitude. More complicated factors would include climate and ice growth mechanism, which is beyond the scope of the present study.

2.4.2 Flow Area under Ice-covered Conditions

River discharge can be directly determined as the product of the cross sectional average velocity and the cross sectional area. This is so-called the velocity-area method. The question becomes how to obtain reliable estimates of the area as well as the average velocity from field measurements. As illustrated in Figure 2.1, ice covers exhibit different configurations. Also the configuration of a given channel can vary with time. This makes it difficult to precisely estimate the effective area of the cross section. In a review paper, Pelletier (1988) identified the uncertainty in the determination of the cross-sectional area under ice covered conditions as one of the major factors that affect the accuracy of discharge determinations.

For a given cross section, the comparison of the flow area between ice-covered conditions and open water conditions should reveal to what extent the ice cover affects the flow area. Although the result is expected to be different from year to year, it would be possible to characterize the percentage of reduction in flow area by the ice cover. Such characterization helps improve the planning and management of freshwater resources in the winter low flow season.

It is equally important to obtain the cross sectional average velocity of good accuracy. Obviously the most reliable way to do so is to make extensive field measurements. However, this is often not feasible because of high cost, technical difficulties and operation safety. The following review describes various methods for determining the cross-sectional average velocity or depth-averaged velocity from a reduced amount of field measurements.

2.4.3 Index Velocity Method

The work by Healy and Hicks (2004) indicated a unique relationship between the cross sectional average velocity and the maximum point-velocity of the cross-section. The investigators defined the maximum point-velocity as an index velocity. The idea is to measure this velocity at a single point in the cross section, and then to calculate the average channel velocity using the relationship. This is the so-called index velocity method for winter discharge determination. The use of this method encounters the practical difficulty that we do not have prior knowledge of location of the maximum point-velocity in a measurement section. Morse *et al.* (2005) provided a guide to optimize the locations of sensor installation in the field.

It is not surprising that flow velocities vary from point to point in a channel section, particularly in the presence of an ice cover. The maximum point-velocity ought to be different from the average channel velocity. To what degree they differ and to what degree velocities vary from point to point can be revealed by the evaluation of the energy and momentum coefficients. This evaluation is part of the analyses presented in this thesis.

2.4.4 Point Velocity

Commonly used point-velocity methods include the two-point velocity method and the single point-velocity method (Rantz *et al.*, 1982). The former refers to the estimation of the depth-averaged velocity at a given station as the average of the point velocities at depths of 0.2Y and at 0.8Y below the ice cover underside, where Y represents the total flow depth at the station. The latter involves finding the depth-averaged velocity by

multiplying the point velocity at 0.5Y or 0.6Y by a coefficient. These two methods are employed by the USGS and Water Survey Canada to determine river discharges under ice covered conditions (Rantz *et al.*, 1982; Walker and Wang, 1997).

Teal *et al.* (1994) studied the accuracy of the two-point method for estimating average velocity in a channel-section vertical. They suggested that the average of velocities measured at 0.2 and 0.8 of flow depth should be taken as the average velocity, with a percentage error of about 2% for a wide range of bed and ice cover roughness. They suggested the error can be further reduced by introducing a coefficient of 0.98. Their work suffers the limitation that the velocity profiles are generated numerically using the two-power law. It remains a question as to how well the procedures fit field measurements.

A value of 0.88 for the coefficient has widely been applied to the 0.5Y point-velocity in order to convert the point velocity to the depth-averaged velocity (Rantz *et al.*, 1982). However, the application of this widely used value does not provide satisfactory conversions, as evidenced in flow measurements from a large number of ice covered rivers (Walker and Wang, 1997). The measurements also highlight the temporal variations at a given station. The discharge calculation for individual stations through conversion can contain considerable errors.

Issues regarding the accuracy of the point-velocity methods for winter discharge calculations were also raised in investigations by other researchers (e.g. Melcher and Walker, 1992; Pelletier, 1989; Spitzer, 1988). Alford and Carmack (1988) provided field evidence that coefficients for point velocity at 0.4Y are more stable than those at 0.5Y or 0.6Y. Given that there are the significant uncertainties in sampling and analyzing the

depth-averaged velocities and hence cross-sectional average velocities in time and in space (Pelletier, 1988), further research work would be worth our while.

2.4.5 Flow Resistance Methods

The Manning's equation (in S.I. unit) of the form

$$Q = \frac{1}{n_o} A R_h^{2/3} S^{1/2} \tag{2.4}$$

is typically used to estimate discharge, Q, in open channel flow. The equation allows the calculation of discharge for given Manning's roughness coefficient, n_o, hydraulic radius, R_h, and channel bed slope, S. The hydraulic radius is defined as the ratio of the cross sectional area A ($= A_i + A_b$) to the wetted channel perimeter p ($= p_b + p_i$), as illustrated in Figure 2.2. Strictly speaking, this empirical formula is applicable for uniform channels only (Henderson, 1966), whereas natural rivers and stream are rarely uniform channels. However, we may consider the calculated discharge as the first order approximation of the actual discharge of a given river cross section.

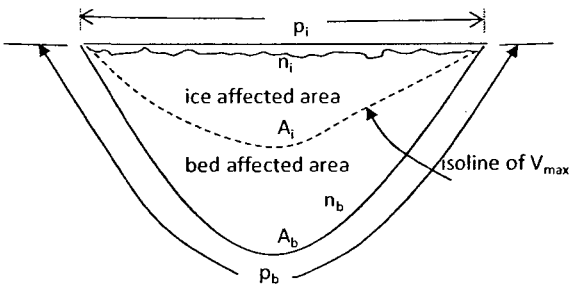

Fig. 2.2: Definition sketch of an ice-covered cross section, showing two parts. The composite friction coefficient, n_o, are associated with the ice cover friction coefficient, n_i, and the channel bed friction coefficient, n_b, respectively. For a wide channel, the effects of the channel sides on the coefficients are negligible.

Note that for a given discharge and channel slope, the formation of an ice cover increases the resistance to flow and therefore flow depth. The increased flow depth would lead to the increased discharge from an open water rating curve being greater than the actual discharge, with an ice cover. The presence of the additional ice cover boundary almost doubles the wetted perimeter for wide channels.

Ashton (1986) considered that the cross section could be divided into two parts, Figures 2.2 and 2.3, with one section exerting shear on the bed, and the other section exerting shear on the ice cover underside. The boundary between these two sections is considered as zero shears within the flow, and therefore this boundary is not included in either the wetted perimeter p_b or the wetted perimeter p_i. The formulas for hydraulic radius, channel bed and ice underside roughness coefficients can be applied to each section as if it were a channel by itself.

The Manning's equation (Eq. 2.4) has the advantage that knowledge of the actual flow velocities is not needed for the calculation of discharge. Given the difficulties in measuring flow velocities in ice covered rivers, the equation is attractive. However, we must specify the appropriate value for the Manning's coefficient. This is in addition to the specifications of the geometric quantities of the cross section, i.e. the cross sectional area, wetted perimeter and the channel bed slope. The challenge to determine the quantities under ice covered conditions has been discussed earlier.

The Manning's roughness coefficient in equation (2.4) should be considered as a composite coefficient that incorporates the frictional effect of the ice cover underside and that of the channel bed, Figure 2.3. Extensive investigations regarding only channel bed roughness have been carried out in the past. In this section we focus on the situation

where an ice cover exists. Ice cover roughness can be estimated by the following two methods: The first method is to estimate the composite roughness by performing a gradually varied flow analysis over the study reach using channel geometry, water surface elevations and ice thicknesses. The second method is to locally estimate the roughness from vertical velocity profile distributions (Larsen, 1969; Calkins *et al.*, 1982).

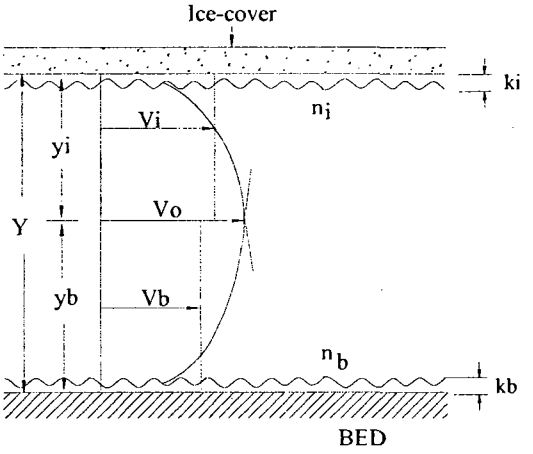

Fig. 2.3 Determination of composite roughness under ice-covered channels.

A number of formulations for the composite roughness coefficient have been proposed, based on the two boundary-layer approach. A summary of the formulations is given in Uzuner (1973). Some of the formulae are listed below:

$$n_o^2 = \frac{n_b^2 + a n_i^2}{1 + a} \tag{2.5}$$

$$\frac{n_o}{n_b} = \frac{a + 1}{1 + a(n_b / n_i)} \tag{2.6}$$

$$\frac{n_o}{n_b} = \frac{1}{\sqrt{1 + a}} (n_i / n_b) \left[a^{3/4} + (n_i / n_b)^{3/2} \right]^{2/3} \tag{2.7}$$

$$\frac{n_o}{n_b} = \frac{0.63(y_i / y_b + 1)^{5/3}}{n_b / n_i (y_i / y_b)^{5/3} + 1} \tag{2.8}$$

Equations (2.7) and (2.8) were given by Chow (1959) and Larsen (1969), respectively. In the above expressions (Figure 2.3), Y is the effective flow depth, κ is Von Karman's constant, δ_m is the logarithmic velocity distribution, R_o (= R_i + R_b) is the hydraulic radius, y_i is the depth below the ice cover underside to the maximum velocity, y_b is the depth from the maximum velocity to the channel bed, a is the ratio of wetted perimeter exerted by ice to the wetted perimeter exerted at bottom, V_b is the average velocity in the bed section, and V_i is the average velocity in the ice-cover section.

According to Sabaneev (1948), equation (2.5) is valid for the roughness of bed that is less than 0.04 and the channel depth is more than 2 m. The accuracy of this approach came 1% or better.

Key assumptions made in the derivation of the above formulae are described in Netzhikhovskiy (1964). Most of them make use of the Manning equation or the Chézy equation. For given values of n_i and n_b, the composite roughness can be determined. Typical values for n_i and n_b were reported in Carey (1966). The significance of determining the composite roughness is to allow predicting the shear stress exerted on the ice cover by the flow. This is essential for applications to the calculation of stage-discharge relations for ice-covered rivers, the predictions of river-ice breakup and the analysis of ice jams.

Table 2.1 presents calculated composite roughness of river bed and ice underside for the St. Croix River, Wisconsin, using Levi's (1948), Cary's (1966), Hancu's (1967) and Larsen's (1969) formulations. The values for n_i and n_b are also given.

Table 2.1: Comparison of n_0 values by different authors calculations

Y(m)	n_b	n_i	Levi (1948) n_0	Carey (1967) n_0	Hancu (1966) n_0	Larsen (1969) n_0
0.07	0.0249	0.01	0.0201	0.0182	0.0203	0.0182
0.07	0.024	0.0122	0.0198	0.0191	0.0207	0.0184
0.08	0.0259	0.0177	0.0223	0.0215	0.0246	0.0219
0.07	0.0248	0.0154	0.0209	0.0204	0.0228	0.0203
0.07	0.0249	0.0135	0.0206	0.0196	0.0222	0.0195
0.07	0.025	0.0161	0.0212	0.0208	0.0233	0.0207
0.07	0.025	0.0145	0.0208	0.0201	0.0224	0.02
0.07	0.0253	0.0199	0.0228	0.0227	0.0256	0.0227
0.07	0.0253	0.0299	0.0277	0.0241	0.0328	0.0242
0.08	0.0252	0.0245	0.0249	0.0248	0.0288	0.0248
0.09	0.0252	0.0281	0.0267	0.0266	0.0312	0.0266
0.08	0.0251	0.024	0.0246	0.0246	0.0284	0.0245
0.08	0.0252	0.0244	0.0248	0.0248	0.0287	0.0248
0.09	0.025	0.023	0.024	0.024	0.0277	0.024

We caution that the proposed formulae for the determination of the composite roughness coefficient are subject to errors. Some of the factors that have lead to the errors are:

(1) The calculations involve the poor accuracy of measuring instruments, field procedures and computational methods for winter discharge measurement.

(2) The two-layer hypothesis in curved ice-covered channels does not satisfy the three-dimensional curved channel flow.

(3) The formulae are empirical relationships.

(4) The results are site-specific.

Chapter Three: Field Measurements of Ice-covered River Flow

3.1 Measurement Stations

In the winter period of 1989 to 1990, four Water Survey Canada's regional offices (Atlantic, Ontario, Western & Northern and Pacific & Yukon) participated in the field data collection activities. Twenty six river sites were selected in the first year of operation (Walker and Wang, 1997). In Table 3.1, we list the river stations, with information about station codes, geographic locations, mean flow depth and bottom slope. Altogether 70 field surveys of ice-covered river flow were conducted.

At each river station, the cross section was typically divided into 20 to 25 sub-sections across the river (Figure 3.1). Each sub-section is a vertical strip that extends from the ice cover underside to the channel bottom. Within a given sub-section, flow velocities were measured at different vertical distances from the ice cover underside, producing vertical profiles of ice covered flow. Such velocity profiles (that show the vertical structure of velocities) were measured at an approximate frequency of once every three to four weeks. From 1989 to 1990, a total of 1539 vertical velocity profiles were obtained (Walker and Wang, 1997), some of which are shown in Appendix B.

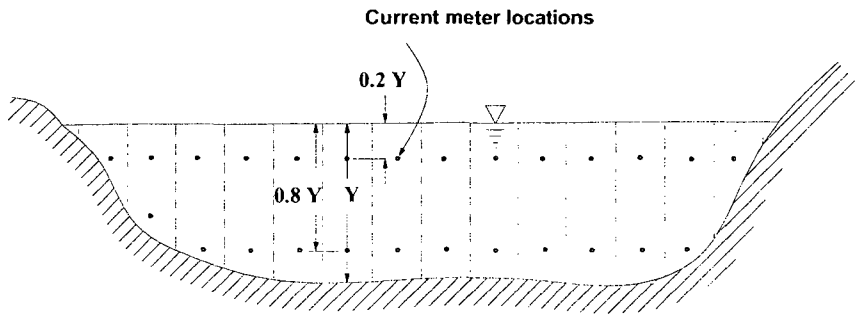

Fig. 3.1 Flow velocity measurement by point velocity method (modified from Hwang and Houghtalen, 1996).

Table 3.1: Water Survey Canada's stations of ice-covered flow measurements in the winter period of 1989 to 1990 (Walker and Wang, 1997). Channel slope values for some of the rivers are not available to us.

Sl. No.	Name of River with Province	Representing Station No.	Latitude & Longitude	Mean Depth (m)	Bottom Slope
1	Salmon R. at Castaway, NB	01AN002	(46°17'28" N & 65°43'24" W)	0.7	No data
2	S.W Miramichi, NB	01BO001	(46°44'10" N & 65°49'36" W)	2	No data
3	River John, NS	01DO001	(45°43'42" N & 63°03'09" W)	0.3	No data
4	Kaministiquia, ON	02AB006	(48°31'58" N & 89°35'39" W)	1.4	0.0001
5	Saugeen, ON	02FC002	(44°7'13" N & 81°6'55" W)	1.5	0.000035
6	Nith River, ON	02GA038	(43°29'2" N & 80°50'6" W)	0.4	No data
7	Burnt River, ON	02HF003	(44°42'03" N & 78°40'40" W)	2.2	0.00004
8	Eels Creek, ON	02HH001	(44°38'30" N & 78°8'7" W)	0.55	0.00003
9	Moira River, ON	02HL005	(44°30'0" N & 77°37'3" W)	0.7	0.00003
10	Salmon R. Shannonville, ON	02HM003	(44°12'28" N & 77°12'35" W)	1.7	0.00002
11	Upper Humber River, NF	02YL001	(49°14'26" N & 57°21'45" W)	1.4	No data
12	Terra Nova River, NF	02YS005	(48°39'43" N & 54°01'05" W)	2	No data
13	groundhog River, ON	04LD001	(49°19'07" N & 82°02'25" W)	2.5	0.00034
14	Oldman River, AB	05AA023	(49°48'50" N & 114°11'0" W)	0.25	0.0038
15	Red Deer River, AB	05CE001	(51°28'02" N & 112°42'38" W)	0.98	0.00035
16	North Saskatchewan, SK	05GG001	(53°12'10" N & 105°46'06" W)	1.25	No data
17	Ou Appelle River, SK	05JF001	(50°39'16" N & 104°51'06" W)	0.4	No data
18	Beaver Rivere, AB	06AD006	(54°21'15" N & 110°13'0" W)	1.1	0.00021
19	Pembina River, AB	07BC002	(54°27'05" N & 113°59'30" W)	0.7	0.0001
20	Halfway River, BC	07FA006	(56°15'04" N & 121°37'39" W)	0.54	0.0008
21	Litle Smoky River, AB	07GH002	(55°27'25" N & 117°09'40" W)	0.8	0.00094
22	Peace River, NWT	07KC001	(59°06'50" N & 112°25'35" W)	4.5	No data
23	Yellowknife River, NWT	07SB002	(62°31'21" N & 114°09'32" W)	3	0.00001
24	Fraser River, BC	08KA005	(53°17'10" N & 120°06'46" W)	1.3	No data
25	Takhini River, YT	09AC001	(60°51'08" N & 135°44'21" W)	1.4	No data
26	Yukon River, YT	09AH001	(62°05'45" N & 136°16'18" W)	2.5	0.0004

3.2 Field Conditions

The flow measurements from ice covered river stations by Water Survey Canada were the first set of measurements in Canadian hydrometric history. Water Survey Canada divides the river stations into three groups based on the channel depth. The first group has flow depth from 0.3 to 1.0 m; the second group has flow depth from 1 to 2 m; the third

group has flow depth greater than 2.0 m. It is not surprising that velocity profiles from different groups have different shape. Other considerations of station selection are:

(1) A station has a complete ice cover (see Figure 2.1).

(2) There is no evidence of slush (frazil ice). The presence of slush under the ice cover makes it difficult to obtain reliable measurements of discharge in ice covered rivers. Flow through the slush-filled portions of the river channel is often assumed to be negligible.

(3) A river reach is straight. The reason is that we prefer to avoid any river bend so as to minimize spatial variations in thickness of the ice cover.

(4) The bed material is homogeneous, i.e. sediments are of more or less uniform size.

(5) There is no obstruction above or below. This is to isolate the effects of the ice cover and the channel bed on the flow.

(6) The river cross section is relatively uniform, in which case the flow is less complicated.

3.3 Measurements

The instruments used for the profile measurements were conventional Water Survey Canada-style Price winter meters equipped with metallic rotors. The penta counters were removed to reduce frictional resistance at low velocity (Walker and Wang, 1997). These meters were used in combination with winter rods or standard winter weights. The current meters were calibrated individually in the towing tank with the same suspension assembly used in the field. The meters were heated between each vertical to ensure that the ice did not adhere to the meter, particularly the pivot.

The measurements provide velocity profiles that show the changes in flow speed with depth. In Figure 3.2, we show examples of the velocity profiles from each of the three depth groups. The effective depth is the vertical distance from the underside of the ice cover to the channel bed. The depth of a point on the profile is a relative depth, i.e. the depth below the ice cover underside divided by the effective depth. Typically there are profiles every a few meters from one river bank to other river bank. Flow measurements at key depths and derivation of friction coefficients are of relevance to this analysis.

3.4 Data Accuracy

There are uncertainties in the Price winter meter that Water Survey Canada used to make the flow measurements. In terms of repeatability, Herschy (1975) reported uncertainty of ±1.5% for velocity above 0.3 m/s and ±16% for velocity below 0.3 m/s. Smoot and Carter (1968) found that the uncertainty was less than 2% for velocity above 0.3 m/s. The uncertainty increases as the velocity decreases. As shown in Appendix B, almost all the point velocities exceed 0.3 m/s. Therefore, we consider the velocity data that we use in this study contain insignificantly small repeatability uncertainty.

Pelletier (1988) pointed out that the effects of boundaries (ice cover underside and channel bottom) on the accuracy of flow measurements can be significant in very shallow water. This is particularly the case when the flow depth is less than 0.6 m. It is necessary to apply correction factors to velocities obtained by current meters when used in shallow water of less than 0.6 m deep. The vast majority of the velocity profiles that we analyze are from stations where the depths are larger than 0.6 m.

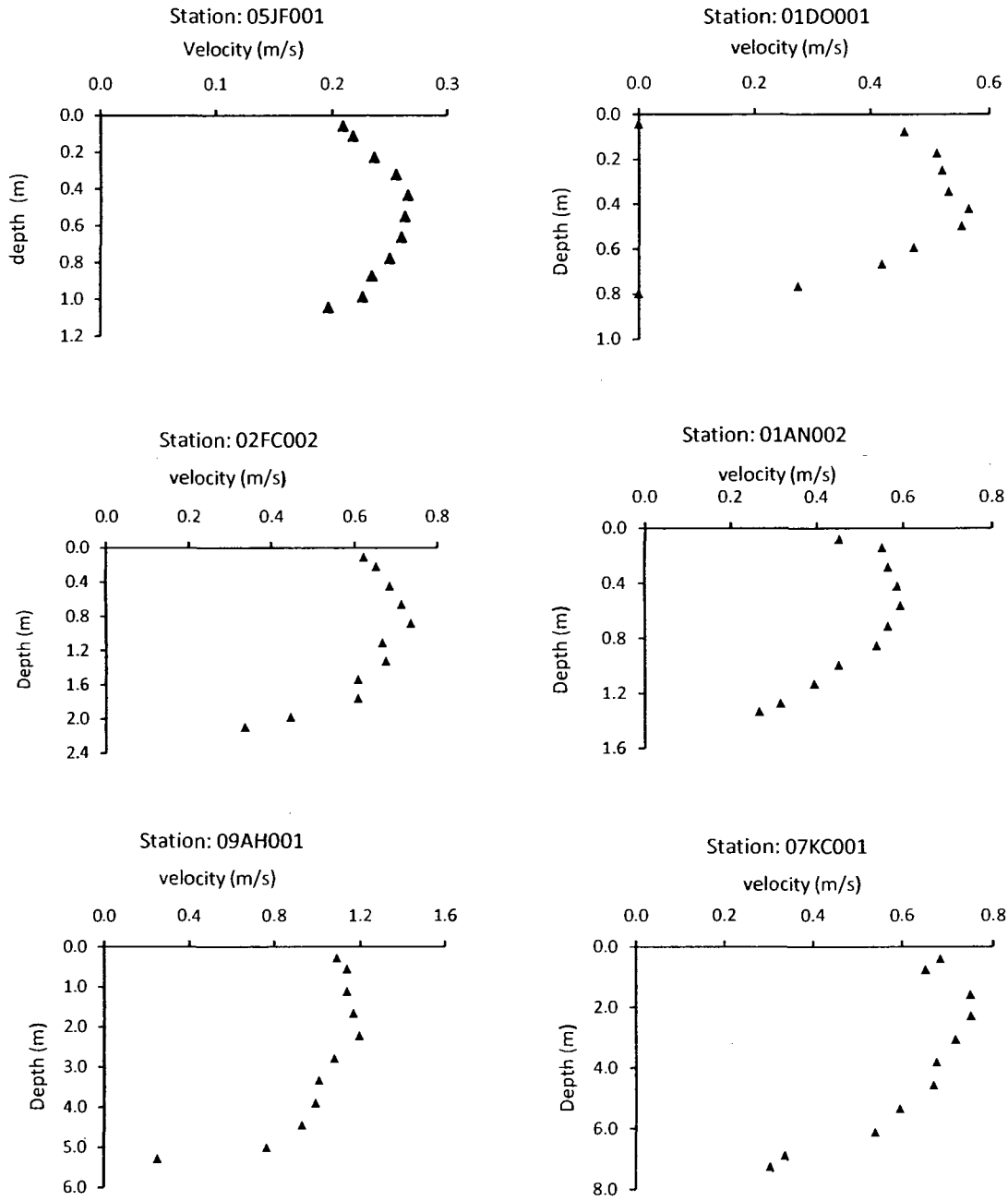

Fig. 3.2 Observed velocity profiles from ice-covered river stations.

Chapter Four: Flow Resistance in Ice-Covered Rivers

4.1 Introduction

In northern countries with cold winters most rivers and their receiving estuaries are ice-covered for certain periods of the year. Beltaos (2007) reported ice-covered time periods of up to several months for some Canadian rivers. It has been well-documented that the presence of an ice cover caused interruptions to winter navigation, major floods, the erosion of the riverbank and riparian areas, and hazards in the development and operation of hydropower. Thus, ice-covered river flow is an important issue. Since the early 1930s, river ice problems and engineering solutions to the problems have attracted continuous attentions from river engineering researchers. However, our understanding of ice-covered river hydraulics is still limited.

The hydraulic behaviour of an ice-covered river differs substantially from that of the river when its surface is exposed to the atmosphere. In Chapter Three we describe winter flow data from a large collection of Canadian rivers. These data include flow velocities as well as ice cover thickness. In this chapter we will analyze the data, in order to reveal the differences in hydraulic behaviour with and without ice covers. Obviously, the presence of an ice cover in winter can significantly increase the resistance to flow and therefore reduce the hydraulic conveyance capacity.

In the analysis of the resistance to flow the roughness at solid boundaries is the most important parameter. As Ashton (1986) pointed out, it is difficult to measure directly the roughness of the underside of an ice cover and the roughness of the channel bed. We do expect the overall roughness under ice-covered condition to be substantially different from the corresponding roughness when the surface of the channel is exposed to

the atmosphere. Field observations (Hicks *et al.*, 1995) show that river ice floats with about 90% of its thickness submerged and resists the flow of water. The wetted perimeter is approximately doubled for an ice cover with underside roughness usually not equal to the bed roughness. The water level would be about 30% higher, compared to that for the same discharge under open water condition.

In the following we determine discharge in ice-covered rivers by using various methods and compare the results.

4.2 Determination of Ice-covered River Discharge

Traditionally, current meters measure flow velocity at a point in a river cross section. In the cross-river direction the cross section is divided into a series of sub-sections, each of which extends from the water surface (for open channel flow) or the ice cover underside to the channel bed. Discharge can be determined by measuring flow velocities in short spatial intervals throughout the whole cross section. If the flow is steady, the discharge will be the product of the overall cross-sectional mean velocity and the area of the cross section. The computational procedures involve the determination of the depth average velocity for each sub-section. This depth average velocity is obtained from velocity observations at many points in that vertical sub-section.

Rantz and others (1982) summarised various methods for estimating depth average velocity:

a) Vertical-velocity curve (0.1Y increment),

b) Two-point velocity,

c) Six-tenths depth,

d) Three-point velocity,

e) Two-tenths depth,

f) Sub-surface velocity,

g) Surface-velocity,

h) Integration,

i) Five-point velocity and

j) Six-point velocity measurement.

Among the above-mentioned methods, the first four methods are point velocity measurement techniques.

The vertical-velocity curve method involves making point-velocity measurements at 0.1Y depth increments. It entails flow measurements at 100 different points between the ice cover underside and the channel bed. It is rarely used in the field because it is time consuming.

The two-point method is extensively used in the field. Observations of flow velocities at 0.2Y and 0.8Y below the ice cover underside are made. The average of these two velocities is taken as the depth average velocity for a given channel sub-section.

For the six-tenths depth method, the mean vertical velocity is taken as the measured velocity at 0.6Y, multiplied by a correction coefficient of 0.92 to allow for the effects of the ice cover on the flowing water.

When the two-point method cannot be used due to slush, debris or a sounding weight preventing measurement at 0.2Y or 0.8Y or the stage is changing rapidly, the six-tenths depth method is a better choice. The three-point velocity method combines the

two-point (0.2Y and 0.8Y) method and the six tenths (0.6Y) method, i.e. measurements of flow are made at the three depths below the ice cover underside.

The two-tenths depth method is used for measuring flows of such high velocities that is not possible to obtain depth soundings or to position the instrument at 0.8 or 0.6 of the flow depths. Sub-surface and surface velocity method is used only when it is difficult to obtain soundings and depths. The integration, five-point and six-point methods are rarely used.

4.2.1 Vertical Velocity Curve Method

The vertical-velocity curve method is a series of velocity observations at points well distributed between the water surface and the channel bed, which are made at each of the verticals. The observed velocities are plotted against depth. Normally, the observations are taken at 0.1-depth increments between 0.1 and 0.9 of the depth. Since observations are always taken at 0.2, 0.6 and 0.8 of the depth, the results may be compared to the other methods of velocity observations. Figure 4.1 shows the typical profiles of channel wise velocity in open water and ice-covered channels.

The vertical-velocity curve method is valuable in determining coefficients for applications to the results obtained by other methods but is not generally adapted to routine discharge measurements because of extra time required to collect field data and to compute the average velocity.

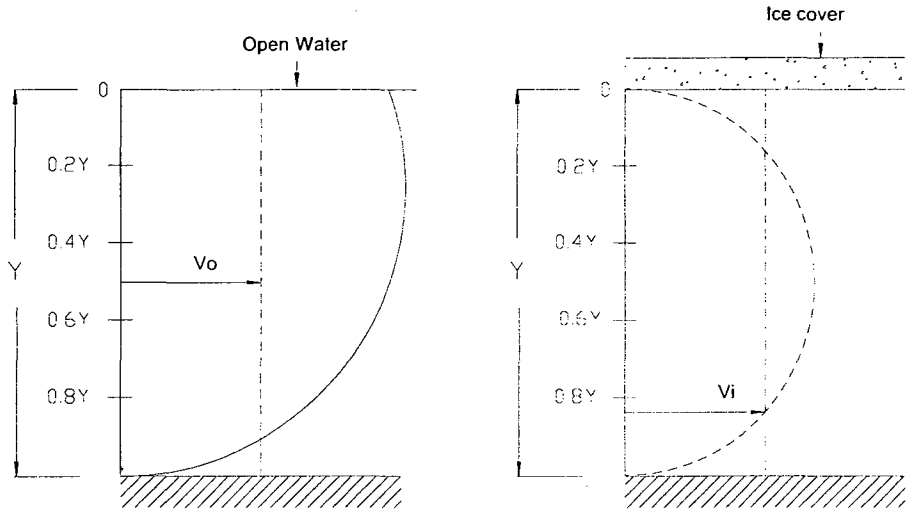

Fig. 4.1 Velocity measurement in open water and ice cover conditions. V_o represents the depth average velocity in open channel flow. V_i represents the depth average velocity in ice-covered channel flow.

4.2.2 Mid-section Method

We determine the discharge using the so-called mid-section method. This is a conventional current-meter method and belongs to the vertical velocity curve category. In this method the current meter measures the velocity at each vertical and represents the average velocity in a rectangular channel sub-section. The sub-section area extends laterally from half the distance from the preceding observation vertical to half the distance to the next, and vertically from the ice cover underside to the sounded depth.

The cross section is defined by depths (Figure 4.2) at verticals Y_1, Y_2, Y_3, Y_4 ..., and Y_n. At each vertical, the velocities are sampled by a current meter in order to obtain the mean velocity for each sub-section. The sub-section discharge is then computed using the following equations.

$$q_x = \left[\frac{(b_x - b_{x-1})}{2} + \frac{(b_{x+1} - b_x)}{2}\right] Y_x \tag{4.1}$$

or

$$q_x = v_x \left[\frac{(b_{x+1} - b_{x-1})}{2}\right] Y_x \tag{4.2}$$

where q_x is the discharge through sub-section x, (x = 1, 2, 3,... n), v_x is mean velocity at vertical x, b_x is the horizontal distance from a point on the shoreline, P_o, to vertical x, b_{x-1} is the horizontal distance from the point, P_o, to the preceding vertical, b_{x+1} is the horizontal distance from the point, P_o, to the next vertical and d_x is the depth of water at vertical x.

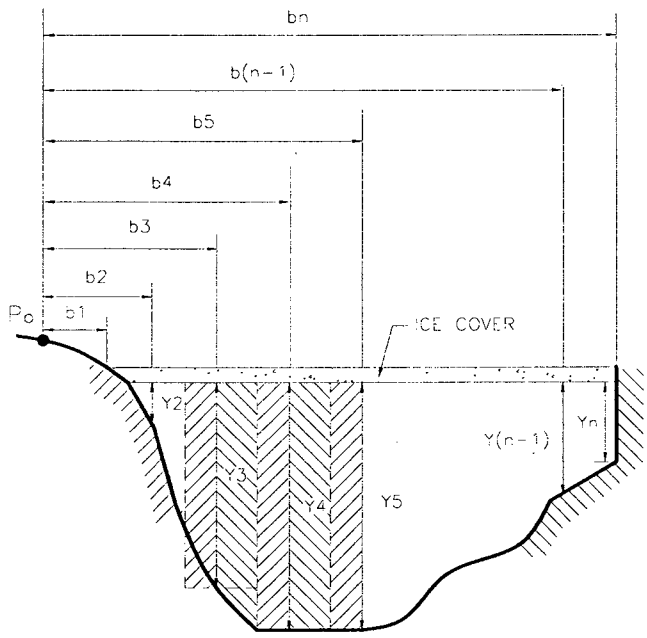

Fig. 4.2 Mid-section method for computing cross section area and discharge.

The total discharge of a cross section is the sum of the discharges for individual sub-sections. For example, the discharge of sub-section one is

$$q_1 = v_1 \left[\frac{b_2 - b_1}{2}\right] Y_1 \tag{4.3}$$

where q_1 is the discharge of sub section 1, v_1 is the mean velocity at vertical 1, b_1 is the horizontal distance from an initial point to vertical 1, b_2 is the horizontal distance of vertical 2, Y_1 is the depth of water at the observation vertical 1. Normally, the discharge of sub- section one is zero because the depth at observation vertical one is zero. Hence , the total discharge of the entire cross section is

$$Q = \sum (q_1 + q_2 + ... + q_n) \tag{4.4}$$

This is the appropriate method for discharge determination from measurements because it covers the whole area through sub-sections and for each vertical the mean velocity is converted to area-weighted mean velocity.

4.3 Estimate of Flow Area

4.3.1 Effective Flow Area

We calculate the effective flow area (Figure 4.3) under ice-covered condition by evaluating the following integral

$$A = \int_{x_1}^{x_2} [y(x) - i(x)] dx \tag{4.5}$$

where A is the flow area, y is the outer depth as if the ice-covered were not present, i is the thickness of the ice-cover and x_1 and x_2 are the coordinates across the river. We have ignored the thermal expansion as water changes from liquid to solid phases.

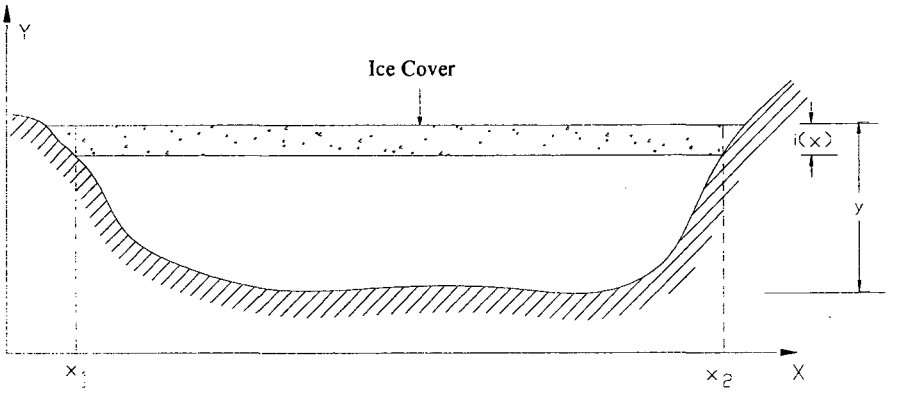

Fig. 4.3 Cross section showing the effective flow area.

4.3.2 Flow Area Reduction

We evaluate the percentage of the reduced area covered by ice (Figure 4.3) in each of the water conveyance cross-sectional area by the following method

$$\Delta A = \frac{\int_{x_1}^{x_2} i(x)dx}{\int_{x_1}^{x_2} y(x)dx} \times 100 \qquad (4.6)$$

where Δa is the cross sectional area of flow reduced by the ice thickness. Integrals (4.5) and (4.6) are evaluated using Matlab. Figure 4.4 shows a calculation example of the flow reduction area.

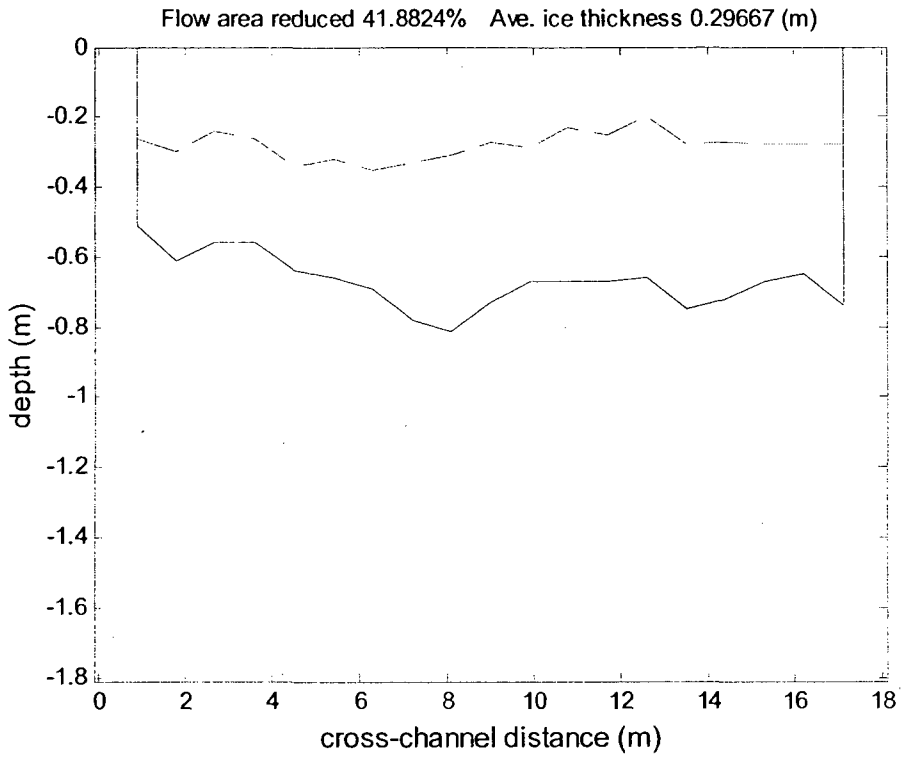

Fig. 4.4 Reduction of flow area due to the presence of an ice cover.

4.4 Resistance to Flow

4.4.1 Estimate of the Manning's Friction Coefficient

The channel-wise velocity near a solid boundary (e.g. ice covers with a smooth underside) varies logarithmically with distance from the solid surface (Figure 4.5). According to the well-known law of the wall, the relationship between the velocity and wall distance is given by

$$v = \frac{v_\tau}{\kappa} ln\left(\frac{y v_\tau}{\nu}\right) + C \qquad (4.7)$$

where v is the flow velocity within the zone of influence by the ice cover, v_τ is friction velocity, κ (= 0.40) is the Karman's Constant, y is the vertical coordinate of a given point below the ice-cover, measured positive downward, ν is the molecular viscosity of water

(1.5×10^{-6} m^2/s), and C is an integral coefficient. The value for C is in the range of 5 to 8. When applied to the region near the channel bed, the velocity function given by equation (4.7) can be approximated by equation (2.1). When applied to the region beneath the ice cover underside, it can be approximated by equation (2.2). The friction velocity is defined as

$$v_\tau = \sqrt{\frac{\tau_w}{\rho}} \tag{4.8}$$

where τ_w is the shear stress on the ice cover underside, and ρ is the density of water.

Equation (4.7) is often approximated by a simpler power law of the form

$$v = \frac{v_\tau m}{\kappa}\left(\frac{y}{y_i}\right)^{1/m} \tag{4.9}$$

where m (= 7) is an empirical slope, due to Prandt, of the best fit line, and y_i is the distance from the ice-cover underside to the point of maximum flow velocity (Figure 4.5). Note that y_i is equal to $Y - y_b$ so equation (4.9) is the same as equation (2.2).

The friction velocity is calculated using the relationship for uniform flow as (see e.g. Henderson, 1966)

$$v_\tau = \frac{n_i V}{y_i^{1/6}}\sqrt{g} \tag{4.10}$$

where V is the depth average velocity (Figure 4.5), whose value is determined from observed velocity profiles, and g is the gravitational acceleration (= 9.81 m/s^2). Equation (4.10) is derived from the Chézy equation $V = C\sqrt{R_h S}$, with the hydraulic radius R_h replaced by the flow depth for wide rivers. Note that the Chézy coefficient C is related to the Manning coefficient n_i as $C = y_i^{1/6}/n_i$, which yields a link between equation (4.10)

and the Manning's equation (eqs. 2.4 and 5.2). Our objective is to estimate the value for the Manning's friction coefficient by trial-and-error.

The idea is to initiate the Manning's friction coefficient with a guessed value. Then we substitute the guessed n value into equation (4.10) to calculate v_τ. In this step of the calculation, both the value for y_o and the depth average velocity, V, are calculated using observed velocity profile. Subsequently we can calculate the flow velocity, v, at any given depth y from equation (4.9). We adjust the Manning's friction coefficient so as to best fit the calculated distribution of flow velocity with the observed velocity profile. An example of the best fit is shown in Figure 4.6.

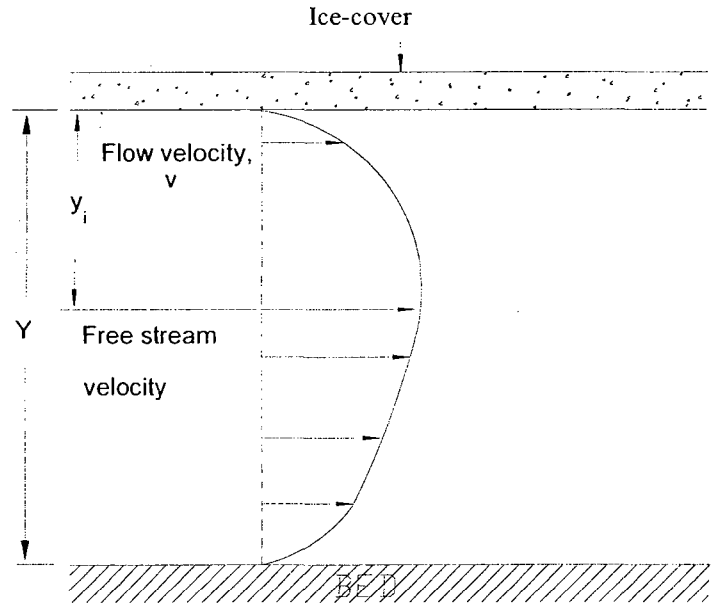

Fig. 4.5 Free flow velocity diagram

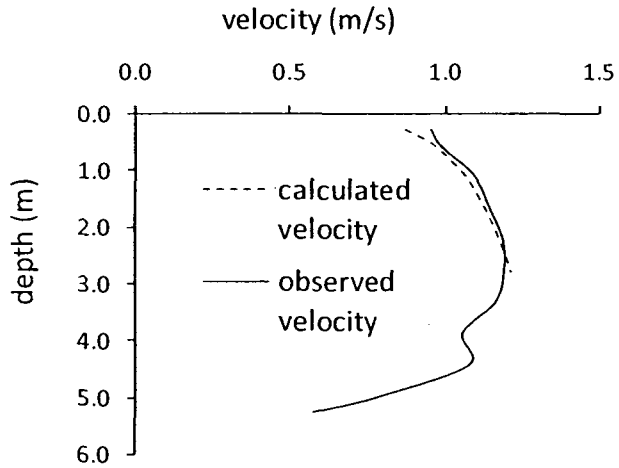

Fig. 4.6 Theoretical and observed velocity profile

Normally, the best fit to a collection of observed velocity profiles in the vicinity of the ice underside is obtained from the specification of the Manning's friction coefficient in the range of 0.011 to 0.018. We show some of the best fit calculated velocity and the observed velocity in Figure 4.7. Table 4.1 presents some values for n under ice-covered conditions.

Table 4.1: Manning's n values for ice-covered channels (Chow, 1959)

Ice condition	Velocity of flow (m/s)	n value
Smooth ice	0.4 to 0.6	0.010 to 0.012
Without drifting ice blocks	>0.6	0.014 to 0.017
With drifting ice blocks	0.4 to 0.6	0.016 to 0.018
	>0.6	0.017 to 0.020
Rough ice With drifting ice blocks		0.023 to 0.025

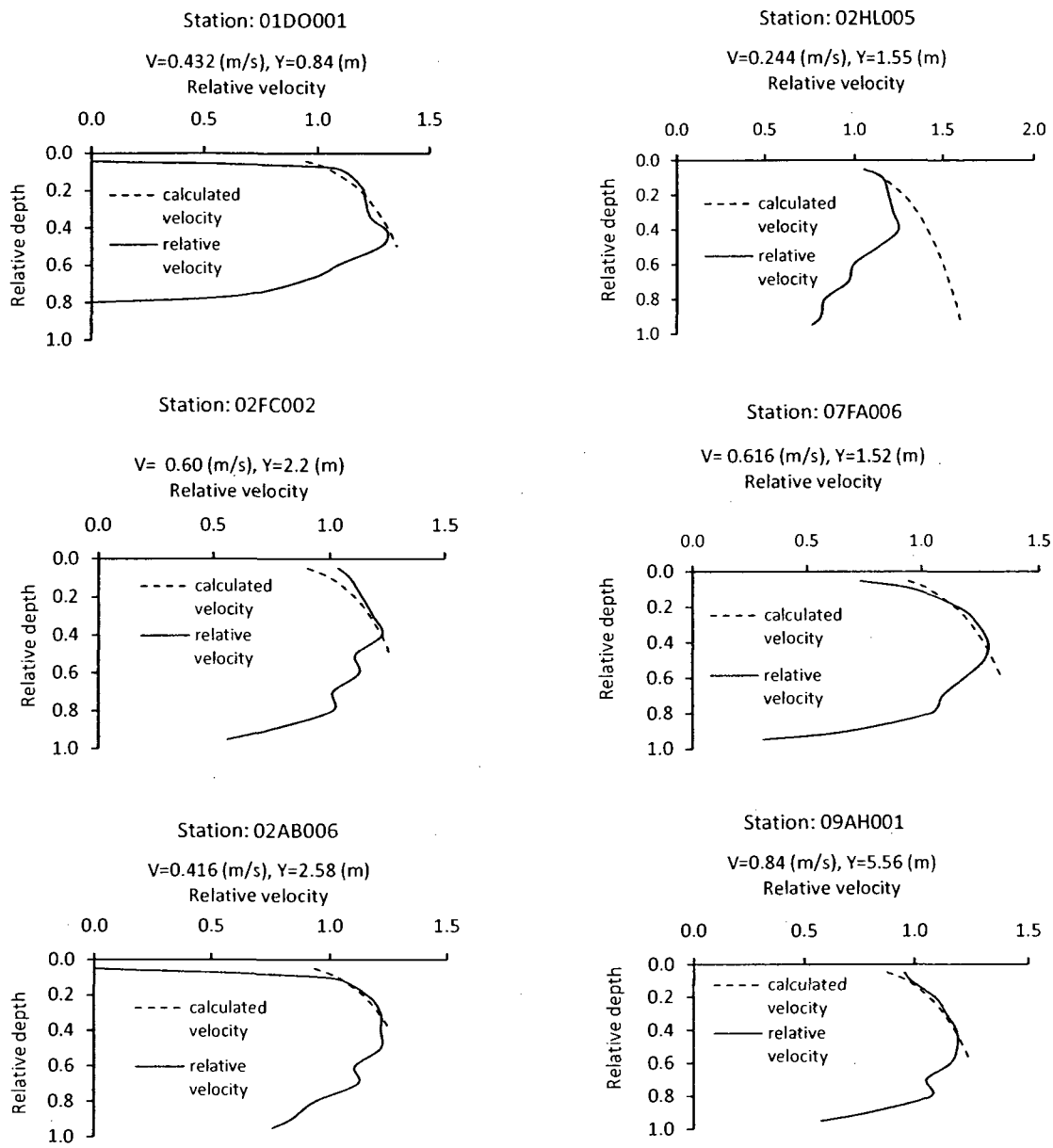

Fig. 4.7 Best fit between observed and calculated velocity profiles

4.4.2 Ice Cover Roughness

Ice roughness is a major component of flow resistance under the condition of ice-covered rivers. There are two methods for determining ice roughness height: direct determination and indirect determination of ice cover roughness. The direct determination of ice roughness height is very complex. The process requires several borings through ice covers. It is not a commonly used method (Ashton, 1986), although physically it is possible to bore several holes along the cross section. The problem with the direct determination is that the roughness can vary up to 100%. This is to say that the error is large.

The indirect determination of ice roughness height is a common practice, by which the roughness is determined from the velocity distribution (Figure 4.8). Generally, the flow of natural channels is fully turbulent. Therefore, it may be assumed that the Karman-Prandtl velocity distribution will hold from the boundary surface to the location of maximum velocity (Figure 4.8).

Larsen (1969) presented a method for estimating roughness height for the ice cover and for the channel bed separately. We estimate the roughness height under ice cover by the following equations

$$k_i = 30 y_i e^{-a_i} \tag{4.11}$$

$$a_i = \frac{V_\circ}{V_\circ - V_{mi}} \tag{4.12}$$

where k_i is the ice roughness height (m), y_i is the distance of the maximum velocity location that occurs between the channel bed and the ice cover, V_0 is the maximum velocity that occurs under the ice cover, V_{mi} is the mean velocity for the depth range

between the ice-cover underside and the point where the maximum velocity occurs, and a_i is the ratio of the maximum velocity of the vertical to the difference between the maximum velocity and the mean velocity.

We have selected fifteen profiles that have the shape of two boundary layers (Figure 4.8). The first one is the boundary layer caused by friction on the ice-cover underside. The second one is the boundary layer due to bed friction. We identify the point of the overlap of the boundary layer profiles as where the peak velocity occurs. The peak velocity gives V_o. We further calculate the mean velocity. These velocities allow us to calculate a_i. We also calculate the ratio of k_i/y_i and compare the limiting value as suggested by Calcins *et al.* (1982). The analysis results are shown in Table 4.8 in the Results Section.

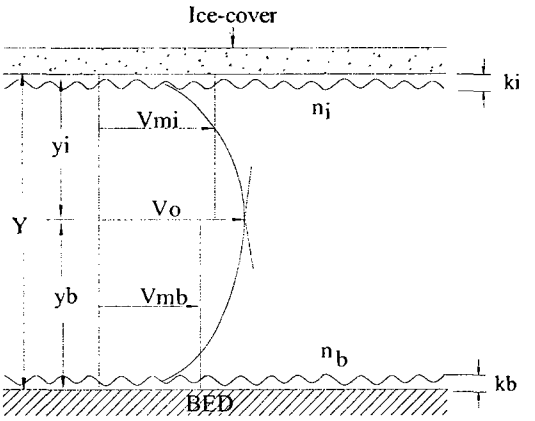

Fig. 4.8 Determination of Ice Roughness Height

Chapter Five: Results and Discussion

In this chapter we present the results of hydraulic radius, flow area, discharge, energy and momentum coefficients, depth-averaged velocity and ice roughness height. We calculate the hydraulic radius and discharge of the channels with and without ice-covered condition by using the Manning's uniform flow equation. The corresponding calculated values of ice-covered channels are compared with the channels where ice-cover is absent. This comparison reveals the effects of the ice cover.

5.1 Hydraulic Radius

Hydraulic radius is one of the most important parameters in channel flow because it affects the flow velocity and therefore the discharge. For example, if the hydraulic radius is larger, the flow velocity will be higher and therefore the discharge will be higher. On the other hand, if the hydraulic radius is smaller, the flow velocity will be lower and the discharge will be also lower. At a given cross section, the hydraulic radius, R_h, is defined as the ratio of the cross-sectional area, A, to the wetted perimeter, P, i.e.

$$R_h = \frac{A}{P} \tag{5.1}$$

The hydraulic radius decreases with increasing wetted perimeter. If the channel has a free surface, the wetted perimeter is the sum of the bottom boundary's length and the lengths of the channel sides. For a wide channel, the hydraulic radius is approximately equal to the flow depth, because the channel sides can be neglected in the calculation of R_h. The present study deals with small channels. Both the channel sides and the channel bed need to be taken into account.

If a channel has an ice cover, there will be an increase in the wetted perimeter, compared to the corresponding case of open water. The increase in the wetted perimeter leads to a decrease in the hydraulic radius. For a wide channel that is covered by ice, the hydraulic radius at a given cross section will be two times that for the case without ice.

For the 26 rivers listed in Table 3.1, the wetted perimeter includes the channel bed, channel sides and the underside of the ice cover in the calculation of the hydraulic radii. For comparison, the hydraulic radius with the ice-cover underside excluded is also estimated.

Based on the analysis of the ice covered rivers, the hydraulic radius (R_{hi}) ranges from 0.3 m to 1.9 m. The typical value is 1.0 m. Without an ice cover, the hydraulic radius ranges from 1.0 m to 4.6 m. The size of the rivers being small and shallow is reflected in the calculated hydraulic radius, ranging from slightly larger than 1.0 m to about 4.6 m. The typical value is 2.0 m. The results are presented in Table 5.1. The difference of percentage in the table is calculated as the ratio of the difference between R_{hi} and R_{ho}.

The analysis (see Table 5.1) shows that the hydraulic radius differs from a minimum of 54% to a maximum of 72% between conditions with and without ice-cover. Also, the ratio of the hydraulic radius with ice to that without ice ranges from a minimum of 28% to a maximum of 46%. Thus, there is a significant difference in the hydraulic radius between conditions with and without an ice cover. This is not surprising given that the channels of interest are wide.

Table 5.1: A comparison of hydraulic radii with and without an ice cover.

Station No.	Hydraulic Radius, R_h (m)		Difference, DR_h/R_{ho} = $(R_{ho}-R_{hi})/R_{ho}$ (%)	R_h Ratio = R_{hi}/R_{ho} (%)
	With ice-cover, R_{hi} (m)	Without ice-cover, R_{ho} (m)		
02AB006	0.93	2.22	58.1	41.9
02HF003	1.2	2.65	54.7	45.3
02HH001	0.61	1.64	62.8	37.2
02HL005	0.73	1.88	61.2	38.8
02HM003	1.13	2.55	55.7	44.3
04LD001	1.9	4.42	57.0	43.0
05AA023	0.3	1.07	72.0	28.0
05CE001	0.59	1.59	62.9	37.1
06AD006	0.4	1.2	66.7	33.3
07BC002	0.49	1.35	63.7	36.3
07FA006	0.67	1.82	63.2	36.8
07GH002	0.64	1.75	63.4	36.6
07SB002	1.72	3.75	54.1	45.9
09AH001	1.89	4.59	58.8	41.2

5.2 Flow Area

Measurements of the ice cover show that the ice cover has a finite thickness. For small river channels, the ice thickness is not negligible, compared to the channel depth. The percentage of flow area reduction is presented below.

The largest river is the Peace River in North West Territories (Table 5.2). The river has an average discharge of 1112 m^3/s in freezing season. The average flow velocity is 0.5 m/s. On average the flow area is reduced by 11% by an ice cover with an average ice thickness of 0.76 m. With the ice cover, the river has an effective mean depth of 4.5 m.

The second largest river is the Yukon River in Yukon Territories. The river has an average discharge of 355 m^3/s in freezing season with an average flow velocity of 0.85 m/s. The average flow reduction area is reduced by 21% with an average ice thickness of 1 m. The effective mean depth of the river is 2.5 m.

The smaller size rivers include the Saugeen River in Ontario (Table 5.2). The river has an average discharge of 29 m^3/s in freezing season, with an average flow velocity of 0.5 m/s. The average flow reduction area is reduced by 13% with an average ice thickness of 0.31 m. The effective mean depth of the river is 1.5 m.

The smallest size river is the River John in Nova Scotia. The river has an average discharge of 2.2 m^3/s in freezing season with an average flow velocity of 0.41 m/s. The average flow reduction area is reduced by 67% with an average ice thickness of 0.5 m. The effective mean depth of the river is 0.3 m. Detailed results are shown in Table 5.2.

Based on the analysis, we can see that the ice-cover leads to a reduction of the flow area by 11% for rivers with a larger mean flow depth and by 67% for rivers with a smaller mean flow depth. For example, analysis in this study, the Peace River has a mean depth of 4.5 m, and the flow reduction area is 11%. River John has a mean depth of 0.3 m and the flow reduction area is 67%. So, the flow reduction area depends on the mean flow depth. If the mean flow depth is larger, the flow reduction area is smaller. Conversely, if the mean flow depth is smaller, the flow reduction area is larger.

Table 5.2: Reductions to flow area due to ice covers, together with average (over time) ice cover thickness, mean depth, cross-sectional average velocity and total discharge.

Name of River	Reduced Flow Area(%)			Ice thickness (m)			Mean Depth (m)	Average Velocity (m/s)	average discharge (m3/s)
	upper limit	lower limit	average	upper limit	lower limit	average			
Salmon river at Castaway, NB	43.18	37.98	40.58	0.51	0.48	0.5	0.7	0.54	17
S.W Miramichi, NB	28.63	17.22	22.93	0.63	0.53	0.58	2	0.26	56
River John, NS	66.69	66.69	66.69	0.5	0.45	0.48	0.3	0.41	2.26
Kaministiquia, ON	20.82	20.82	20.82	0.55	0.42	0.42	1.4	0.32	42.56
Saugeen, ON	12.6	12.6	12.6	0.36	0.26	0.31	1.5	0.49	28.88
Nith river, ON	41.88	41.88	41.88	0.41	0.3	0.36	0.4	0.2	1.52
Burnt river, ON	17.36	15.67	16.52	0.47	0.4	0.44	2.2	0.2	11
Eels Creek, ON	48.82	41.07	44.945	0.61	0.5	0.56	0.55	0.18	5.82
Moira River, ON	47.04	40.32	43.68	0.62	0.54	0.58	0.7	0.14	4.45
Salmon river near Shannonville, ON	16.9	16.9	16.9	0.42	0.38	0.4	1.7	0.07	4.73
Upper Humber river, NF	49.66	18.02	33.84	0.54	0.42	0.48	1.4	0.6	46
Terra Nova River, NF	25.72	15.29	20.505	0.66	0.49	0.58	2	0.15	25
groundhog River, ON	23.51	16.98	20.245	0.8	0.73	0.77	2.5	0.16	65
Oldman River, AB	73.5	55.25	64.375	0.59	0.41	0.50	0.25	0.31	3.6
Red Deer River, AB	45.98	27.4	36.69	0.58	0.3	0.44	0.98	0.3	22.5
North Saskatchewan, SK	39.92	26.3	33.11	0.69	0.48	0.59	1.25	0.51	105
Ou Appelle River, SK	63.62	60.65	62.135	0.76	0.52	0.64	0.4	0.19	3.42
Beaver Rivere, AB	60.23	49.21	54.72	0.52	0.41	0.47	1.1	0.25	3.5
Pembina River, AB	50.66	28.25	39.455	0.49	0.29	0.39	0.7	0.28	17
Halfway River, BC	53.82	42.88	48.35	0.69	0.47	0.58	0.54	0.5	18
Litle Smoky River, AB	51.15	25.77	38.46	0.61	0.4	0.51	0.8	0.23	16
Peace River, NWT	14.18	8.1	11.14	0.81	0.7	0.76	4.5	0.47	1112
Yellowknife River, NWT	16.59	9.33	12.96	0.62	0.38	0.50	3	0.13	25
Fraser River, BC	25.47	12.92	19.195	0.4	0.22	0.31	1.3	0.26	32.15
Takhini River, YT	44.58	26.13	35.355	0.68	0.46	0.57	1.4	0.36	16.57
Yukon River, YT	25.65	15.75	20.7	1.1	0.76	0.93	2.50	0.85	355.23

5.3 Discharge

The direct effects of an ice cover at river cross section are the reduction to discharge through the cross section. Although the real conditions of the rivers of interest are far from uniform flow, it is constructive to examine the discharge with and without ice cover. As the first order approximation, we may estimate the flow velocity using Manning's equation (in S.I. units) for uniform flow. The equation is of the form

$$V = \frac{1}{n} R_h^{2/3} S_o^{1/2} \qquad (5.2)$$

The corresponding discharge will be

$$Q = VA \qquad (5.3)$$

We consider two levels of approximation: The first level of approximation is that the presence of the ice cover merely reduces the hydraulic radius, resulting in a decrease in the flow velocity and hence a reduction in discharge. Values for the Manning's coefficient used in discharge calculations are given in Table 5.3.

Table 5.3: Friction coefficients for ice cover and channel bed and calculated composite friction coefficient.

Station	Depth of the point of max. velocity, y_i (m)	$Y-y_i = y_b$ (m)	$a=y_i/y_b$	n_i (best fit value)	n_b (from database)	Calculated n_o by Chow (1959) method (eq. 2.7)	Calculated n_o by Larsen (1969) method (eq. 2.8)
02AB006	0.75	1.62	0.463	0.028	0.021	0.043	0.021
02HF003	0.74	1.59	0.465	0.026	0.023	0.037	0.022
02HH001	0.85	0.47	1.809	0.022	0.018	0.030	0.020
02HL005	0.77	0.69	1.116	0.0225	0.021	0.030	0.022
02HM003	0.8	1.75	0.457	0.0235	0.025	0.031	0.023
04LD001	2.14	2.93	0.730	0.027	0.03	0.034	0.028
05AA023	0.35	0.47	0.745	0.028	0.03	0.036	0.029
05CE001	0.19	0.76	0.250	0.02	0.028	0.023	0.022
06AD006	0.64	0.57	1.123	0.022	0.025	0.027	0.023
07BC002	0.51	0.72	0.708	0.019	0.02	0.025	0.019
07FA006	0.61	0.83	0.735	0.023	0.021	0.032	0.021
07GH002	0.44	0.93	0.473	0.02	0.029	0.023	0.025
07SB002	1.85	2.54	0.728	0.022	0.028	0.026	0.025
09AH001	1.67	3.61	0.463	0.032	0.03	0.044	0.028

In Table 5.4, the calculated velocities and discharges are shown in the presence of an ice cover. The strongest flow velocity is slightly larger than 1.0 m/s, the weakest flow velocity is 0.16 m/s, the average flow velocity is 0.51 m/s, and the typical flow velocity is slightly below 0.5 m/s. The corresponding discharges are given by equation (5.3).

The second level of approximation is that the presence of the ice cover not only reduces the hydraulic radius, but also increases the composite Manning's friction coefficient. For comparison, discharges, under the assumption that the ice cover is absent are also calculated using the Manning's uniform flow equation (eqs. 5.2 and 5.3).

In Table 5.4, the calculated maximum discharge without an ice cover is 769.16 m^3/s at River Station 09AH001, compared to the discharge of 425.16 m^3/s with an ice cover. The minimum discharge with an ice cover is around 2.89 m^3/s at River Station number 02HL005, compared to the minimum discharge of 5.42 m^3/s without an ice cover. The average (take into count all the stations in Table 5.4) discharge is 68 m^3/s with an ice cover, whereas it is slightly larger than 137 m^3/s without an ice cover. The typical discharge is larger than 13 m^3/s with an ice cover, and larger than 22 m^3/s without an ice cover. The estimates of cross-sectional average velocities using the Manning's equation are seen to be greater than the observed values, in some cases by a factor of two.

Table 5.4: A comparison of calculated velocity and discharge with and without ice cover. The Manning's coefficient is given the n_b values presented in Table 5.3.

Station No	With Ice-cover			Without Ice-cover		
	Hydraulic Radius (m)	Velocity (m/s)	Discharge (m^3/s)	Hydraulic Radius (m)	Velocity (m/s)	Discharge (m^3/s)
02AB006	0.93	0.45	60.52	2.22	0.81	108.48
02HF003	1.2	0.31	20.21	2.65	0.53	34.21
02HH001	0.61	0.22	3.28	1.64	0.42	6.32
02HL005	0.73	0.21	2.89	1.88	0.4	5.42
02HM003	1.13	0.19	13.33	2.55	0.33	22.9
04LD001	1.9	0.66	269.71	4.42	1.66	678.67
05AA023	0.3	0.93	8.13	1.07	2.15	18.79
05CE001	0.59	0.47	28.55	1.59	0.91	55.37
06AD006	0.4	0.31	3.26	1.2	0.66	6.84
07BC002	0.49	0.37	16.64	1.35	0.61	27.74
07FA006	0.67	1.04	18	1.82	2.01	34.89
07GH002	0.64	0.78	49.88	1.75	1.53	97.51
07SB002	1.72	0.16	33.91	3.75	0.27	57.12
09AH001	1.89	1.02	425.16	4.59	1.84	769.16

Table 5.5 shows the differences in flow velocity and discharge between ice-covered and open water conditions. Among all the stations listed in the table, the maximum difference in velocity ($V_o - V_i$, where V_o represents the depth average velocity without an ice cover and V_i represents the depth average velocity with an ice cover) between the two conditions is about 60% of V_o, the minimum difference in velocity is about 39% of V_o, the average difference in velocity is about 47% of V_o, and the typical difference in velocity is around 42% of V_o. Clearly the differences are significant.

In Table 5.5 we also present the ratio of the flow velocity with an ice cover to that without the ice cover. Of all the stations listed in the table, the maximum ratio is 61%. In other words, the presence of the ice cover has reduced the flow velocity by 39%. The minimum ratio is 40%, which means a greater percentage reduction. On average (over all the stations), the ratio is 53%. The typical ratio is about 51%.

In terms of the difference in discharge between ice-covered and open water conditions, we make the following observations (Table 5.5). The maximum ratio of the difference in discharge ($Q_o - Q_i$, where Q_o represents the discharge under open water condition and Q_i represents the discharge under ice-covered condition) between ice-covered and open water conditions is 60% of Q_o. The minimum ratio is 40%. The average (over all the listed stations) ratio is 47%. The typical ratio is around 48%. The ratio of the discharge under ice-covered condition to that under open water condition is 60% as the maximum, 40% as the minimum, and 53% as the average. Typically it is about 51%.

Table 5.5: Difference of velocity and discharge ratio between ice-free and ice-covered conditions.

Station No.	Velocity (m/s)				Discharge (m^3/s)			
	Calculated with ice-cover, V_i	Calculated without ice cover, V_o	Difference (%) DV/V_o = (Vo - Vi)/Vo	Ratio (%) = V_i/V_o	Calculated with ice-cover, Q_i	Calculated without ice cover, Q_o	Difference (%) DQ/Q_o = (Qo - Qi)/Qo	Ratio (%) = Q_i/Q_o
02AB006	0.45	0.81	44.44	55.56	60.52	108.48	44.21	55.79
02HF003	0.31	0.53	41.51	58.49	20.21	34.21	40.92	59.08
02HH001	0.22	0.42	47.62	52.38	3.28	6.32	48.10	51.90
02HL005	0.21	0.4	47.50	52.50	2.89	5.42	46.68	53.32
02HM003	0.19	0.33	42.42	57.58	13.33	22.9	41.79	58.21
04LD001	0.66	1.66	60.24	39.76	269.71	678.67	60.26	39.74
05AA023	0.93	2.15	56.74	43.26	8.13	18.79	56.73	43.27
05CE001	0.47	0.91	48.35	51.65	28.55	55.37	48.44	51.56
06AD006	0.31	0.66	53.03	46.97	3.26	6.84	52.34	47.66
07BC002	0.37	0.61	39.34	60.66	16.64	27.74	40.01	59.99
07FA006	1.04	2.01	48.26	51.74	18	34.89	48.41	51.59
07GH002	0.78	1.53	49.02	50.98	49.88	97.51	48.85	51.15
07SB002	0.16	0.27	40.74	59.26	33.91	57.12	40.63	59.37
09AH001	1.02	1.84	44.57	55.43	425.16	769.16	44.72	55.28

5.4 Energy Coefficient and Momentum Coefficient

The presence of an ice cover leads to the formation of a boundary layer immediately beneath the ice cover. This is similar to the formation of a boundary layer immediately above the channel bed. The flow velocity varies with distance from the ice underside. The variation in the flow velocity field is reflected in the energy coefficient, α, and momentum coefficient, β. These two coefficients are defined as

$$\alpha = \frac{\iint v^3 dA}{V_m{}^3 A} \tag{5.4}$$

and

$$\beta = \frac{\iint v^2 dA}{V_m{}^2 A} \tag{5.5}$$

where v is the flow velocity, V_m is the area-weighted mean velocity and A is the cross-sectional area. For comparison of two coefficients, are estimated from the measurements with the ice-cover excluded.

The energy coefficient α is more sensitive to velocity variations than β. The value of α and β are never less than 1.0. Both coefficients are equal to 1.0, if the flow of the channel section is uniform, and larger than 1.0, if the flow departs from uniform. According to Henderson (1966), α values derived from field observations are usually less than 1.15 for turbulent flow in a straight open channel that has a rectangular, trapezoidal or circular cross sections. In this study we obtained some α values that exceed 1.15. This is in part due to the presence of ice covers.

Chow (1959) reported that rivers under ice-covered condition have α values of 1.2 to 2.0, and β values of 1.07 to 1.33. Given that the data used by Chow (1959) could be subject to significant error due to poor measurement techniques, it would be interesting to make

comparisons with calculations using newly available field data. The calculated α values from this study indicate that four of the rivers are close to the lower limit of Chow (1959). However, most of the rivers seem to have α values below the lower limit of Chow (1959). The calculated β values from this study indicate that nine of the rivers are close to the lower limit of Chow (1959).

The analysis of field data in this thesis shows that the values of α ranges from a minimum of 1.09 to a maximum of 1.3, and the values of β ranges from a minimum of 1.03 to a maximum of 1.1. Calculated values for the two coefficients are listed in Table 5.6.

Table 5.6: Calculated values for the energy and momentum coefficients.

Station No.	Energy Coefficient, a	Momentum Coefficient, b
01AN002	1.1	1.03
01BO001	1.11	1.04
01DO001	1.3	1.08
02AB006	1.13	1.09
02FC002	1.16	1.06
02GA038	1.11	1.04
02HF003	1.1	1.03
02HH001	1.16	1.06
02HL005	1.15	1.05
02HM003	1.17	1.06
02YL001	1.19	1.07
02YS005	1.17	1.06
04LD001	1.12	1.04
05AA023	1.1	1.03
05CE001	1.14	1.05
05GG001	1.12	1.04
05JF001	1.13	1.1
06AD006	1.09	1.03
07BC002	1.12	1.07
07FA006	1.11	1.04
07GH002	1.11	1.04
07KC001	1.09	1.06
07SB002	1.1	1.03
08KA005	1.09	1.03
09AC001	1.1	1.04
09AH001	1.11	1.04

5.5 Depth-averaged Velocity

The significance of calculating depth-average flow velocity at a vertical is that the flow velocity is needed in order to obtain the cross-sectional mean flow velocity. This cross-sectional mean velocity in turn allows us to conveniently determine the discharge as the product of the mean flow velocity and the area of the cross section. We calculate depth-averaged velocity from observed velocity profiles by the following method:

$$V = \frac{1}{Y}\int_0^y v dy \tag{5.6}$$

where V is the depth-averaged velocity, y is the depth below ice surface, Y is the total depth of water and v is the observed velocity at given depths in the water column (Figure 4.5).

It is important to note that most of the velocity profiles are asymmetric profiles. The ice-underside boundary layers are thinner, compared to the bottom boundary layer. We show some examples of the asymmetric velocity profiles in Figure 5.1. In this case, the flow velocity changes more rapidly with distance from the ice-underside than with distance from the channel bottom. Just as right on the channel bed, the flow velocity must be zero right on the ice cover underside, because the flow is expected to satisfy the no-slid condition on the surface of a solid boundary.

As shown in Figure 5.1, the typical thicknesses of the ice covers for the river stations that we analyzed are about 30 cm. The ratio of the depth-averaged velocity to the maximum velocity in the water column is typically 85%.

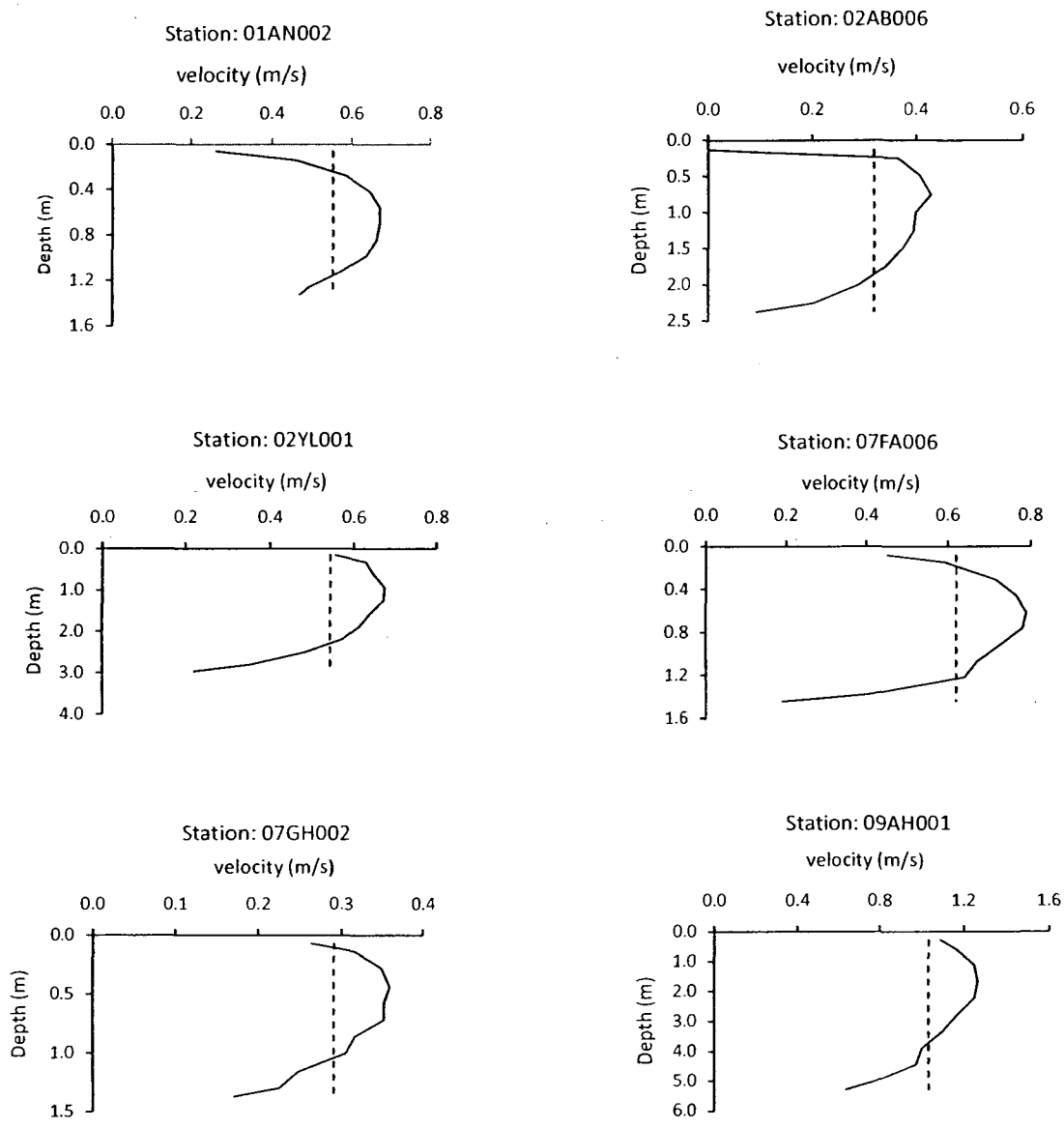

Fig. 5.1 Calculated depth-averaged velocity profiles within the observed velocity.

5.6 Ice Roughness Height

We have selected fifteen velocity profiles from the field measurements and calculated the ice roughness height by using equations (4.11) and (4.12). The calculated ice roughness heights are listed in Table 5.7. The roughness heights for profiles that appear to have the logarithmic velocity distribution are in the reasonable range of values. Calcins *et al.* (1982) suggested that equations (4.11) and (4.12) are not applicable for the case of fragmented ice covers or ice jams with very large value of k_i for the ice underside. Specifically, if the value of k_i/y_i is larger than 0.333, the methods are not applicable.

To illustrate this important point, we consider a couple sample profiles. Figures 5.2 (a) and (b) show examples of large values of k_i/y_i, which are unrealistic. As shown in Table 5.7, for Station 02AB006, the maximum velocity is 0.42 (m/s). The mean velocity is 0.30 (m/s). The ratio of the maximum velocity to the difference between the maximum velocity and the mean velocity for the depth range from the ice-underside and the depth of the maximum velocity [i.e. $V_\circ/(V_\circ - V_{mi})$] is 3.35. The distance from the ice-cover underside to the point of the maximum velocity is 0.75 m. The calculated ice roughness height is 0.789 m. The ratio k_i/y_i is 1.05, which is not acceptable. For Station 02GA038, the maximum velocity is 0.27 (m/s). The mean velocity is 0.14 (m/s). The $V_\circ/(V_\circ - V_{mi})$ ratio is 1.98. The distance from the ice-cover underside to the point of the maximum velocity is 0.16 m. Calculations of ice roughness height give 0.64 m. The ratio k_i/y_i is 4.0, which is also not acceptable.

Table 5.7: Ice roughness height as calculated using equations (4.11) and (4.12).

Station	Max. velocity beneath ice-cover, V_o (m/s)	Mean velocity V_{mi}, (m/s)	Depth average velocity V (m/s)	Actual depth of V_o or y_i (m)	Total depth, Y (m)	$a_i = V_o/(V_o - V_{mi})$	Ice roughness height, k_i (m)	k_i/y_i
01AN002	0.61	0.49	0.484	0.42	1.04	4.88	0.09437	0.2269
01BO001	0.34	0.31	0.246	1.26	4.2	11.50	0.00038	0.0003
02AB006	0.42	0.30	0.316	0.75	2.5	3.35	0.78940	1.0525
02FC002	0.72	0.65	0.579	0.65	2.16	11.27	0.00025	0.0004
02GA038	0.27	0.14	0.222	0.16	0.81	2.02	0.64686	3.9930
02HF003	0.27	0.23	0.196	0.74	2.46	6.36	0.03815	0.0517
02HM003	0.10	0.09	0.086	0.80	2.68	10.45	0.00070	0.0009
02YL001	0.67	0.62	0.543	0.94	3.12	13.78	0.00003	0.0000
05JF001	0.29	0.26	0.253	0.44	1.1	9.58	0.00091	0.0021
06AD006	0.37	0.32	0.303	0.26	1.28	6.47	0.01185	0.0463
07BC002	0.38	0.35	0.307	0.52	1.3	13.67	0.00002	0.0000
07FA006	0.79	0.67	0.616	0.61	1.52	6.40	0.03031	0.0498
07GH002	0.36	0.32	0.291	0.43	1.44	9.54	0.00093	0.0022
07SB002	0.17	0.14	0.136	1.85	4.62	5.59	0.20688	0.1119
07KC001	0.64	0.58	0.534	2.04	6.8	11.90	0.00042	0.0002

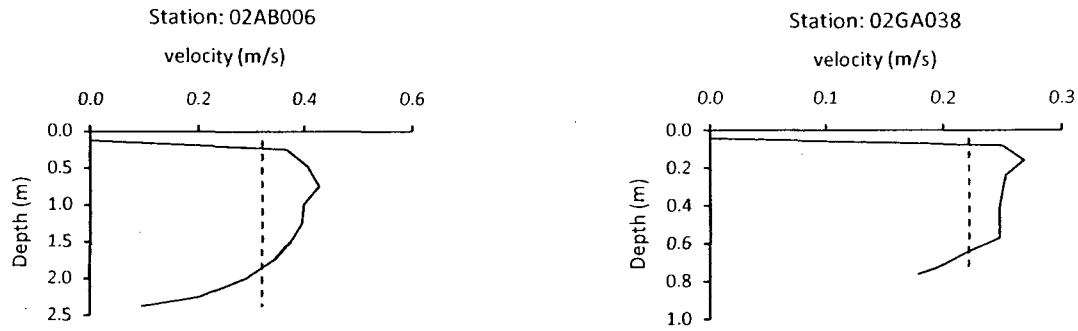

Fig. 5.2: Velocity Profiles which produce large values of k_i/y_i. The calculated ice roughness heights using equations (4.11) and (4.12) are not realistic.

5.7 Discussion

5.7.1 Hydraulic Radius

Hydraulic radius is a vital factor to estimating the flow velocity and thus discharge. In this study, hydraulic radius under open water condition, R_{ho}, and under ice-covered condition, R_{hi}, are calculated for the rivers listed in Table 3.1. The difference (R_{ho} - R_{hi}) ranges from a minimum of 54% of R_{ho} to a maximum of 72% of R_{ho}. For example, in Table 5.1, the R_{hi} of Cross Section 02AB006 is 0.93 m, whereas the R_{ho} of the cross section is 2.22 m, giving a difference of 1.29 m. This difference is 58% of the R_{ho} value. The presence of the ice cover has reduced the hydraulic radius by 42%, which reduces the flow velocity and discharge.

By definition the flow area of a cross section is related to its hydraulic radius and wetted perimeter as $R_h = A / P$. The larger the hydraulic depth, the smaller the reduced flow area. For example, Salmon River at Castaway, NB, the mean flow depth is 0.7 m (see Table 5.2) and reduced flow area is 43% of the cross sectional area under open water condition. As another example, S.W. Miramachi, NB, the mean flow depth is 2.0 m and the reduced flow area is about 29% of the cross sectional area under open water condition.

5.7.2 Manning's Friction Coefficient and Roughness Height

As an approximation we may use the Manning's uniform flow equation [eq. (5.2)] to calculate flow velocity. This calculation takes the Manning's friction coefficient (n) as an input parameter. Chow (1959) compiled some literature Manning's n values (Table 4.1) for ice-covered rivers. Take River Station 02AB006 as an example (Table 5.4). The

calculated flow velocity is 0.45 m/s under ice-covered condition and 0.81 m/s under open water condition (Table 5.4), giving a difference of 0.36 m/s. This velocity difference is 44.4% of the flow velocity under open water condition. The ratio of the flow velocity under ice-covered condition to that under open water condition is 56%.

In the calculations of flow velocities presented in Table 5.4, we have used Manning's n values in the range of 0.017 to 0.035. These Manning's n values are higher than the literature values (see Table 4.1) as compiled by Chow (1959). The use of the literature n values may is not accurate to determine the flow velocity under ice-covered condition.

For estimations of the roughness height of ice-cover underside, equations (4.11) and (4.12) are applicable for wide and deep channels. According to Calcins *et al.* (1982), shallow channels with relatively large values of boundary roughness are not a proper case where the equations can be applied. They also suggested that the equations are not applicable for the case of fragmented ice covers or for the case of ice jams with very large values of k_i ($k_i / y_i \succ 0.33$).

Almost all the cross sections listed in Table 5.7 have depth average velocities larger than 0.2 m/s. According to equations (4.11) and (4.12), the larger the depth average velocity, the larger the value for a_i, and therefore the smaller the value for k_i. The estimated values of k_i can be considered to be realistic since $k_i / y_i \prec 0.33$. There are two exceptions: Stations 02AB006 and 02GA038. We argue that if the mean velocity is larger than 0.2 m/s, we can use equations (4.11) and (4.12) to calculate the roughness height of ice-cover underside. However, although the equations (4.11) and (4.12) are quite reliable for the big channels with small roughness elements, they are not universally applicable.

5.7.3 Point Velocity Method

Calculating discharge by the point velocity method (conventional Mid-section method) is more accurate than other methods such as the two-point (0.2Y and 0.8Y) method, the six-tenths (0.6Y) depth and surface velocity method. Table 5.8 shows comparisons among velocity estimates using the different methods. The procedures involve the calculation of the cross-sectional sub-area of each vertical and horizontal sub-section and the multiplication of the sub-area by the area-weighted mean velocity. For individual verticals, the conventional Mid-section method is a discrete form of the depth average velocity given by equation (5.6). All the vertical profiles that we examined contain 11 velocity points, which accurately describe the asymmetry of the flow velocity. Some of the profiles are shown in Figure 3.2.

Table 5.8: Comparisons of depth-average velocity estimated using various methods

	Depth-average velocity (m/s) at selected stations						
	05JF001	01DO001	02FC002	01AN002	09AH001	07KC001	
Mid-section Method	0.235	0.417	0.616	0.482	0.987	0.610	
	Estimate of depth-average velocity (m/s)						Standard deviation (m/s)
0.2Y & 0.8Y Method	0.235	0.467	0.647	0.480	1.032	0.645	0.034
0.6Y Method	0.260	0.555	0.676	0.540	1.006	0.670	0.071
Surface Method	0.209	0.000	0.622	0.453	1.090	0.686	0.179

The asymmetry of velocity profiles results from the resistance to flow caused by an ice cover being not as strong as the resistance to flow caused by the channel bed. It is interesting to note that a single point depth of 70% of the water column is very close to the depth-averaged velocity. This is different from the two-point method (0.2Y and 0.8Y, where Y represents the total flow depth) for estimating depth average velocity, which is not always reliable.

Rouse (1961) suggested that the two-point method (0.2Y and 0.8Y) is applicable to open channel flow, with an error of about 2%. Similarly, Carter and Anderson (1963) reported errors of less than 2.2%. Other investigators (e.g. Pelletier, 1988; Herschy, 1975) reported somewhat higher error percentages, up to ± 6%. Using the two-point method, Lau (1982) estimated depth average velocity under ice-covered condition and indicated that the error was not more than 2 to 3%. However, it is not clear what experimental channel depths, and variations in ice-cover as well as in bed roughness are involved.

5.7.4 Energy and Momentum Coefficients

The energy coefficient, α, and the momentum coefficient, β, are the two indicators of the flow velocity distribution in a channel cross section. Values for α and β are never less than one, because the flow velocity in a channel section inevitably varies from one point to another. The mean velocity in a main channel section is larger than that on the channel sides or near the channel bottom. When applying the flow energy principle (see e.g. Henderson, 1966) to two cross sections in the path of the flow, one needs to use α as a correction factor.

If we are to apply a one-dimensional numerical model to a river channel, we need to specify the appropriate value for α. Based on our analysis, from which the results are presented in Chapter Five, Section 5.4, we realize that α values changes from one river cross section to another. The question is how significant the change of α values is. This question will be addressed in Chapter Six.

5.7.5 The Accuracy of the Two-Point Method

To investigate the accuracy of the two-point method for application to ice-covered rivers, we selected three channels of ice-covered conditions with different depth ranges. The depth ranges are: (1) 0.3 to 1.0 m, (2) 1.0 to 2.0 m, and (3) 2.0 m or deeper. In Figure 5.3(a) for Cross Section 01AN002, the flow depth is between 1.0 and 1.5 m. The cross sectional average velocity is 0.509 m/s, as determined using all the point velocity measurements. For all the sub-sections of the cross section, the overall average velocity based on the 0.2Y and 0.8Y point velocities is 0.514 m/s, being very close to 0.509 m/s based on all the point velocity measurements. However, for some individual vertical profiles of flow velocity, the average velocity based on the 0.2Y and 0.8Y point velocity can contain errors of up to ±7%, relative to the depth average velocity as determined using all the point velocity measurements from the individual verticals.

In Figure 5.3(b), the depth of the channel is between 1.0 and 1.4 m, the depth-average velocity using all the point velocity measurements is 0.664 m/s and the average velocity based on the 0.2Y and 0.8Y is 0.670 m/s. Similar to the case shown in Figure 5.3(a), for some individual profiles, the error associated with the two-point method can exceed 7%, relative to the depth average velocity as determined using all the point velocity measurements from the individual verticals.

In Figure 5.3(c), the depth is between 1.0 and 1.3 m. The depth average velocity using all the point velocity measurements is 0.462 m/s and the average velocity based on the 0.2Y and 0.8Y is 0.466 m/s. For some individual profiles, the error of the two-point method is slightly higher than the maximum errors shown in Figures 5.3(a) and (b). The errors shown in Figures 5.3(a-c) have implications to two-dimensional modelling of

depth average river flow. Here the two dimensions refer to the variations in flow across a river channel. The velocities are determined from discharge of 12.15 m^3/s and cross-sectional area of 24.82 m^2, (panel a), discharge of 15.63 m^3/s and cross-sectional area of 24.48 m^2 (panel b), and discharge of 9.43 m^3/s and cross-sectional area of 20.98 m^2 (panel c).

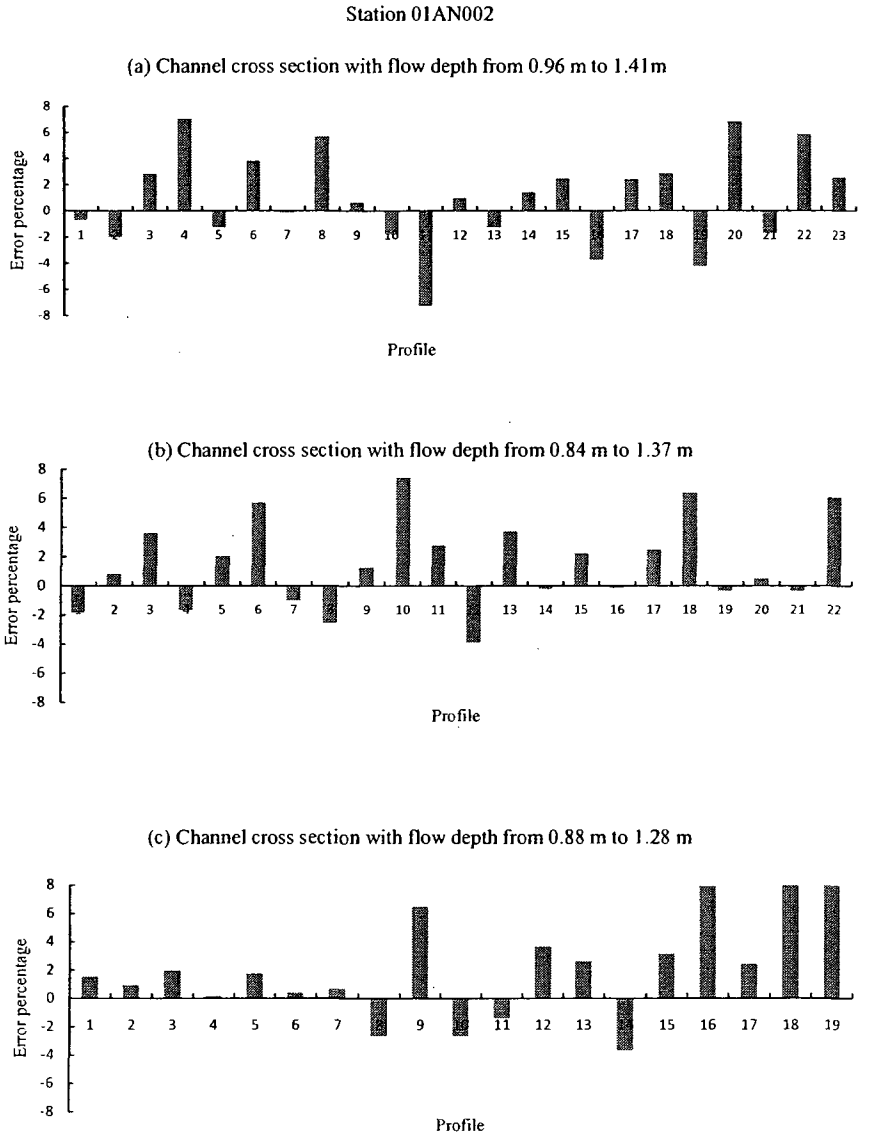

Fig. 5.3 Errors in depth average velocity as determined using the two-point method. The horizontal axis refers to a series of verticals across the channel. Positive and negative error percentages mean, respectively, over-estimates and under-estimates by the two-point methods, compared to the depth average flow velocity as determined using all the point velocity from an individual vertical. The measurements were made from 01AN002 on 23 Jan (panel a), 9 Feb. (panel b) and 15 Mar. (panel c) 1 990, respectively. The corresponding cross-sectional average velocities were respectively 0.49, 0.64 and 0.45 m/s.

In Figure 5.4(a) for Cross Section 01BO001, the flow depth is between 2 and 4 m. The average of the 0.2Y and 0.8Y velocities is 0.27 m/s, compared with the depth average velocity is 0.268 m/s using all the point velocity measurements from the cross section. For profile number 8, the error is 15.1%. The procedures for the determination of this error are identical to those described above for Cross Section 01AN002.

Figure 5.4(b), the depth is between 2.0 and 3.5 m, the average of the 0.2Y and 0.8Y velocities is 0.361 m/s, which is very close to the depth-averaged velocity of 0.354 m/s. For the cross section from which 23 profiles were obtained, the maximum error percentage associated with the two-point velocity method is 6.1%.

Figure 5.4 (c) shows the error percentage for a cross section where the depth is between 1.5 and 3 m. The depth averaged velocity is 0.393 m/s and the average velocity based on the 0.2Y and 0.8Y is 0.401 m/s. The maximum error percentage associated with the two-point method is 15.2%.

The above-discussed overall average velocities match Lau's (1982) numerical results that the average of the 0.2Y and 0.8Y velocities is only 2 to 3% higher than the actual mean velocity.

In Figure 5.5(a) for Station 04LD001, the flow depth is between 2.5 and 4.5 m. the depth-averaged velocity is 0.157 m/s, whereas the average velocity based on the 0.2Y and 0.8Y is 0.166 m/s. The maximum error percentage for this cross section by the two-point method is 18.7%. Figure 5.5(b) shows a cross section where the depth is between 2.0 and 4.0 m. The depth-averaged velocity is 0.113 m/s and the average velocity based on the 0.2Y and 0.8Y is 0.119 m/s. The maximum error percentage of this cross section by the two-point method is 14.31%. A similar maximum error associated with the two-

point method is shown in Figure 5.5(c) for a cross section where the depth is between 3.0 and 5 m.

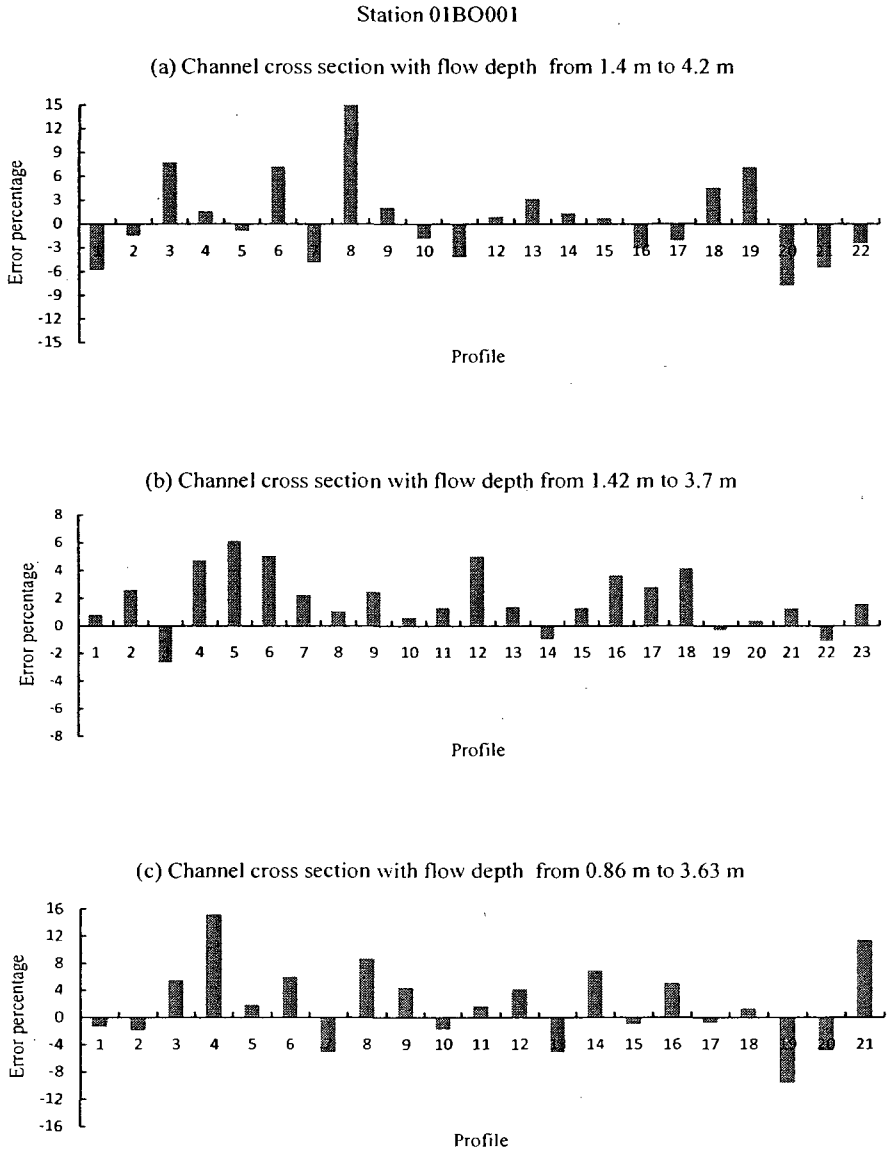

Fig. 5.4 Errors in depth average velocity as determined using the two-point method. The measurements were made from Station 01BO001 on 22 Jan (panel a), 8 Feb. (panel b) and 14 Mar. (panel c) 1990, respectively. The corresponding cross-sectional average velocities are 0.26, 0.34 and 0.28 m/s. (see the caption of Figure 5.3 for detailed explanation).

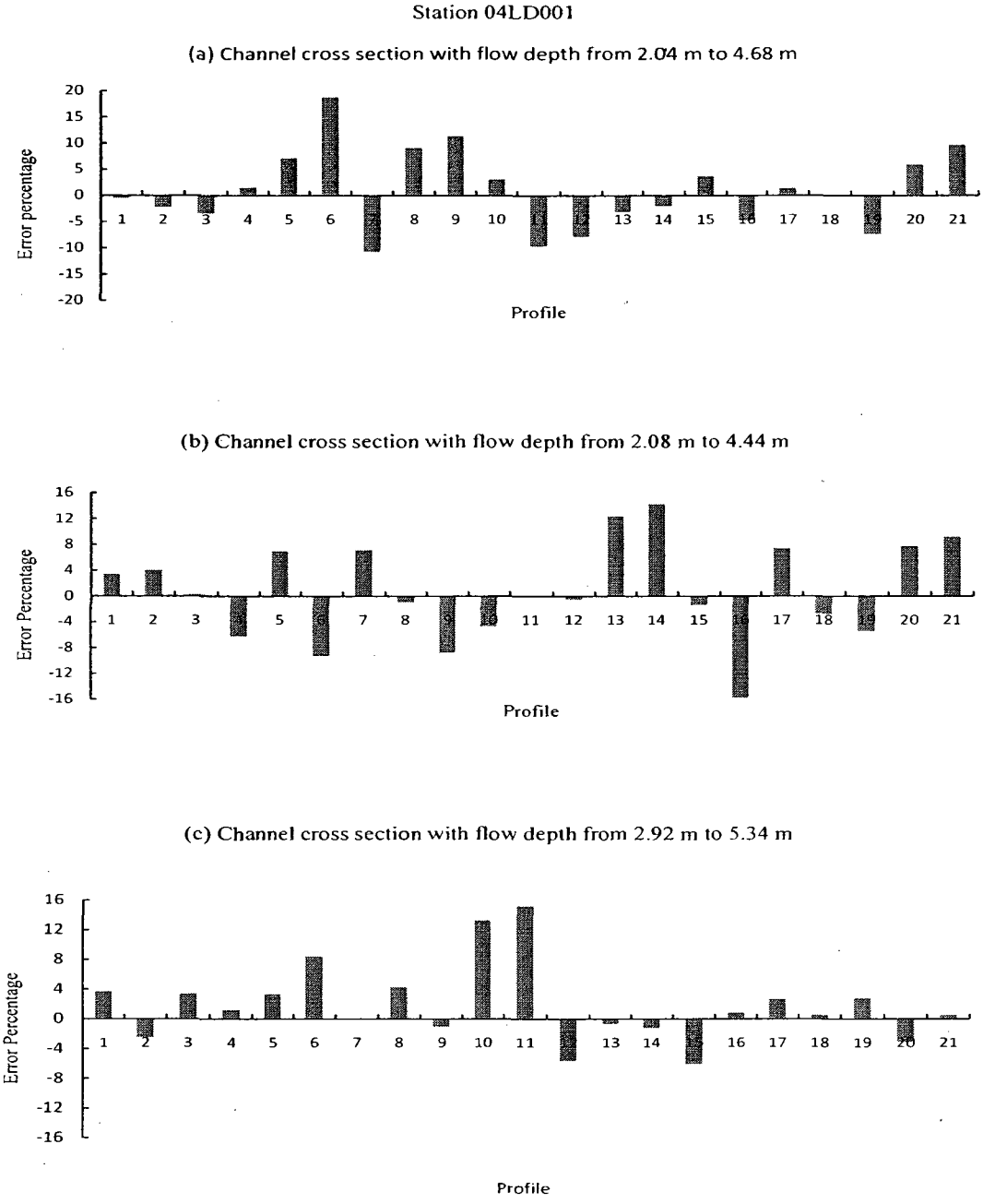

Fig. 5.5 Errors in depth average velocity as determined using the two-point method. The measurements were made from Station 04LD001 on 24 Jan (panel a), 28 Feb. (panel b) and 26 Mar. (panel c) 1990, respectively. The corresponding cross-sectional average velocities are 0.15, 0.11 and 0.30 m/s. (see the caption of Figure 5.3 for detailed explanation).

Chapter Six: Parameterization in Numerical Modelling of Ice-Covered River Flow

6.1 Parameters in the HEC-RAS Model

With a rapid increase in computational power, numerical modelling has proven a powerful tool for river flow simulations. Almost all the models for flow simulations require appropriate parameterization for physical processes not explicitly resolved. In this chapter we take HEC-RAS as an example, which is a popular 1-D river flow model (U.S. Army Corps of Engineers, 2002), and illustrate the implication of the results presented in Chapter Four in the modelling of ice-covered river flow.

When applying the HEC-RAS model to a river channel of interest, the channel is represented by a series of cross sections in the path of the flow. The model is based on the energy equation, written between two adjacent cross sections (Figure 6.1) as

$$Y_1 + Z_1 + \frac{\alpha_1 V_1^2}{2g} = Y_2 + Z_2 + \frac{\alpha_2 V_2^2}{2g} + h_e \qquad (6.1)$$

where Y is the flow depth at a cross section, Z is the water surface elevation, V is the cross-sectional average velocity, α is the energy coefficient, g is the gravitational acceleration, and h_e is the energy head loss between the two cross sections. The subscripts 1 and 2 refer to cross sections 1 and 2, respectively.

For given channel geometry i.e. channel width, side-wall height, channel length, bottom slope, the model predicts cross-sectional mean flow velocity and flow depth. The model has widely been used for steady flow analysis, unsteady flow analysis, sediment analysis, hydraulic design functions, and run multiple plans. Most of the applications

have dealt with open water condition. The procedures for simulating river flow using the HEC-RAS model are described in Appendix E.

As shown in the model equation [Eq. (6.1)], two of the parameters are the energy coefficient and the energy head loss. Since applications of the model to ice-covered channel flow are relatively new, it is worth our while to discuss the treatment of parameters under ice-covered condition. These two parameters must be specified in order to apply the model to an ice-covered channel. To some extent, the analysis of the flow data in Chapter Four reveals the appropriate specifications of the two parameters.

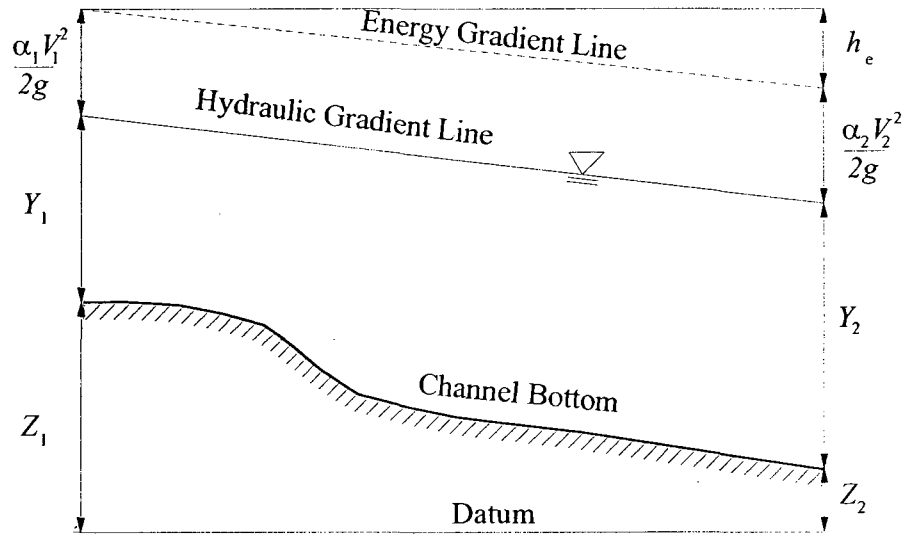

Fig. 6.1 Definition sketch of cross sections for flow modelling.

6.2 The Specification of the Energy Coefficient

The energy coefficient, α, is introduced in Eq. (6.1) in order to compute the mean kinetic energy. The analysis of the flow data given in Chapter Four suggests that the energy coefficient $\alpha = 1.1$ to 1.2 (see Table 5.6). Given the small range of variations in the energy coefficient, it appears sufficient to treat the coefficient as constant. The condition

of the ice cover can change along the path of the flow. In HEC-RAS, the energy coefficient is computed based on the conveyance in the three flow sub-section of a given river cross section: left over bank, right over bank and main channel. It would be constructive to verify during the model run time if the computed values for the energy coefficient falls in the reasonable range ($1.1 \leq \alpha \leq 1.2$). We caution that the energy coefficient of 1.1 to 1.2 corresponds to smooth ice-cover condition and the ice cover has known geometry.

6.3 The Specification of the Friction Coefficient

From the kinematic perspective, the ice cover makes a portion of the channel cross-sectional area unavailable to flow. Suppose that the uniform flow theory is applicable, the ice cover reduces the channel conveyance by increasing the wetted perimeter and reducing the hydraulic radius. More importantly the ice cover affects channel flow for a dynamic reason. A stationary, floating ice cover creates an additional fixed boundary with an associated hydraulic roughness. This hydraulic roughness of the ice cover produces friction in addition to that occurring on the channel bottom and at the side walls of the corresponding open channel flow.

In the HEC-RAS model, the energy head loss, h_e, between two cross sections due to friction is given by

$$h_e = L\bar{S}_f \tag{6.2}$$

where L is the discharge-weighted reach length, $\bar{S}_f$ is the average friction slope between the two cross sections. Additional losses of flow kinetic energy can be caused by channel expansions or contractions. In fact, the energy loss due to friction given in equation (6.2)

is a general formulation. The friction slope includes the Manning's friction coefficient, *n*, as its key determinant.

Table 6.1 Suggested n values for river ice covers (U.S. Army Corps of Engineers, 1985) for sheet ice.

Condition	Manning,s n
Smooth	0.008 - 0.012
Rippled Ice	0.01 - 0.03
Fragmented single layer	0.015 - 0.025

Different values for *n* have been suggested in the literature (Table 6.1). It is understood that the roughness along the wetted perimeter may be distinctly different from part to part of the perimeter, with different *n* values for the channel bottom and the side walls. Thus, it is often necessary to compute an equivalent *n* value for the entire perimeter and to use this equivalent value for the computation of the flow in the whole cross section. This is so-called the composite Manning's *n*. The results of our analysis presented in Chapter Four show higher *n* values (compared to the literature values listed in Table 6.1), in the range of 0.011 to 0.018. The upper limit of 0.018 is 50% higher than the suggested *n* value for smooth ice given in Table 6.1. The results also indicate that the use of *n* values exceeding 0.02 will lead to under prediction of under-ice flow velocities.

In fact, a wide range of values have been used in earlier modelling studies. White and Daly (1997) used values from $n = 0.02$ for very smooth ice underside, to $n = 0.15$ for very rough ice underside, with the mean value equal to 0.066 and standard deviation of 0.023.

Chow (1959) proposed the equivalent coefficient to be obtained by the following equation:

$$n = \left[\frac{\sum_{1}^{n} \left(P_N n_N^{1.5} \right)}{P} \right]^{2/3} \qquad (6.3)$$

This formulation has assumed that the water area is divided imaginatively into N parts of which the wetted perimeters P_1, P_2..... P_N and the corresponding coefficients of roughness n_1, n_2.....n_N are known. It has also assumed that each part of the water area has the same mean velocity, which, at the same time is equal to the mean velocity of the whole section. These assumptions were made earlier.

It is important to note that the presence of the ice cover leads to complications due to variations in an ice cover. The thickness of the ice cover can vary significantly along the path of the flow and even across the channel. This makes it necessary to specify different ice cover thickness and roughness for the main channel and for the over banks. Also, the ice cover geometry can change significantly from cross section to cross section along the channel.

Chapter Seven: Conclusions

In this thesis we have analyzed flow velocity profiles observed from a larger number of ice-covered rivers in Canada. We have also examined the thickness of ice covers. Examinations of the velocity profiles show complicated flow conditions in terms of distributions of flow velocity in the vertical. The boundary layer profiles beneath the ice cover underside and above the channel bed are rarely symmetric. This is to say that the dynamic effect of the ice cover and that of the channel bed differ. It is not surprising that many of the observed velocity profiles from the natural channels cannot exactly be described using the law of the wall distribution. However, some of the profiles do exhibit the logarithmic shape and allow us to analyze using the law of the wall.

Important implications of the above-mentioned flow characteristics include the following: a) in order to obtain reliable estimate of ice-covered river discharge, we need to rely on the mid-section method, which entails field measurements of good spatial resolutions in the vertical and across the river cross section; b) it would be difficult to numerically simulate ice-covered river flow using 1-D models. The two point method (making measurements of flow velocities at 0.2 and 0.8 of the flow depth) allows us to estimate depth average flow with reduced field efforts, but the estimated depth average velocity can contain errors of up to 20%. Based on velocity measurements from selected stations, the two-point method, the six-tenths method and the surface method contain standard deviations of 0.03, 0.07 and 0.18 m/s, respectively. This is in comparison to a depth-average velocity of about 0.5 m/s.

When an ice cover is present in a river cross section, the hydraulic radius of the cross section is reduced significantly. For ice covers with a smooth undersize, the

reduction can reach as much as 46%. This factor alone amounts to a maximum decrease in discharge by 60% from the corresponding discharge when the cross section has a free surface. The presence of an ice cover also leads to a reduction in the flow area. This reduction (expressed in percentage) is smaller for river cross sections with larger mean flow depths. This study shows flow area reductions in the range of 11% to 67%.

We have selected observed under-ice velocity profiles that can be approximated using the law of the wall in order to analyze the dynamic effects of the ice cover on the flow. Fitting the theoretic velocity distribution into the observations shows the Manning's friction coefficient, n, in the range of 0.011 to 0.018, which is higher than literature values for n. The use of n values exceeding 0.02 would under-predict the flow velocity. This means that under ice covered conditions the flow is very sensitive to the friction parameter. Therefore, when numerically simulating ice-covered river flow, the specification of the friction parameter not only on the channel bed and the sidewalls but also at the ice cover underside requires careful attention.

The field data that we examined showed a typical ice cover thickness of about 30 cm. The flow velocities appeared to change more rapidly with distance from the ice cover underside than with distance from the channel bed. This means that the ice cover has lower roughness height than the channel bed. The ratio of the depth average velocity to the maximum velocity in the water column is typically 85%. For a given river cross section, the difference in flow velocities with and without an ice cover is between 39% and 60%.

Chapter Eight: Suggestions and Recommendations

The study of ice-covered river flows is of strategic importance to Canada, with a wide range of engineering applications. Given the inadequacy of the existent knowledge of the topic, a need for further studies exists. In order to advance our understanding of the topic, we make the following suggestions and recommendation for future investigations:

(1) Although some laboratory investigations have been carried out in the past, the experimental configurations are highly idealized. More laboratory investigations with various flow depth ranges should be performed so as to systematically characterize the resistance to flow caused by an ice cover and to reveal the response of the flow structure in the vertical.

(2) It would be interesting to develop a new numerical model that has the capability to resolve the vertical variations in flow velocity. Existent river flow models typically deal with depth average flow only. The new model can be tested, aiming at reproducing the above-mentioned experimental flow conditions. Then the new model can be verified using the results presented in this thesis.

(3) The field data collected by Water Survey Canada permits a thorough assessment of methods developed so far for the determination of depth average flow and hence the determination of cross sectional mean flow. Further studies should be conducted to compare the predictability of the methods.

References

Alford, M. E. and Carmack, E. C. 1988. Observations on ice-cover and channel flow in the Yukon River near Whitehorse during 1985/86. NHRI Paper No. 40, Inland Water Divisions (IWD) Scientific series No. 162, NHRI, Saskatoon, Saskatchewan, Canada.

Ashton, G. D. 1986. "River and Lake Ice Engineering." Water Resources Publications, Littleton, Colorado, pp. 485.

Ashton, G. D. and Kennedy, J. F. 1972. Ripples on underside of river ice covers. Journal of Hydraulic Division - ASCE **98**: 1603-1624.

Beltaos, S. 1995. Ice jam processes. In river ice jams, Beltaos, S (ed.), Water Resources publications: Colorado; 71-104

Beltaos, S. 2007. Modelling of three dimensional flow velocities in a deep hole in the east channel of the Mackenzie delta, Northwest Territories. Canadian Journal of Civil Engineering **34**(10): 1312-1323.

Burrell, B. and Davar, K.S. 1980. Conveyance Capacity with Ice Cover for the Nashwaak River, N.B. 1st Workshop on the Hydraulics of Ice Covered Rivers, 1980, Burlington, ON, pp. 34-56.

Calkins, D. J., Deck, D. S. and Martinson, C. R. 1982. Resistance coefficients from velocity profiles in ice-covered shallow channels. Canadian Journal of Civil Engineering **9**(2): 236-247.

Carey, K. L. 1966. Observed configuration and computed roughness of the underside of river ice, St. Croix River, Wisconsin. U.S. Geological Survey Professional Paper **550**-B: 92-198.

Carter, R. W. and Anderson, I. E. 1963. Accuracy of current meter measurements. Journal of Hydraulic Engineering - ASCE **89**(4): 105-115.

Chow, V. T. 1959. "Open Channel Hydraulics." McGraw Hill, New York.

City of Prince George, 2008. Community information of ice jams and flood response.

Cunjak, R. A. 1996. Winter habitat of selected channel fishes and potential impacts from land-use activity. Canadian Journal of Fisheries and Aquatic Sciences **53**(suppl. 1): 267-282.

Dolgopolova, E. N. 2002. Turbulent structure of ice-covered flow and its influence on river habitat. 16th International Symposium on Ice – Ice in the Environment, Dunedin, NZ, 1: 262-267.

Hamilton, A. S., Hutchison, D. G. and Moor, R. D. 2001. Estimation of winter channel flow using a conceptual hydrological model; a case study, Wolf Creek, Yukon Territories. 11th Workshop on the Hydraulics of the Ice Covered Rivers, 14-16 May, 2001, Ottawa, Ontario: 111-125.

Hamilton, S. 2003. Winter Hydrometry: a practitioner's perspective. In workshop on monitoring and analysis of river ice processes: estimation of stream flow under ice. Saint-Foy, QC.

Heggenes, J. and Dokk, J. G. 2001. Contrasting temperatures, water flows and light: seasonal habitat selection by young Atlantic salmon and brown front in a Boreonemoral river, regulated rivers. Research and Management **17:** 623-635.

Helmiö, T. 2001. Friction measurements of ice cover: theory and practice in River Päntäneenjoki. 2nd IAHR Symposium on River, Coastal and Estuarine Morph Dynamics, 10-14 Sept., 2001. Obihiro, Japan. 179-187.

Henderson, F. M. 1966. "Open channel flow." Macmillan, New York.

Herschy, R. W. 1975. "The accuracy of existing and new methods of river gauging," PhD thesis, Department of Geography, University of Reading, Berkshire, England.

Hicks, F. E. and Healy, D. 2003. Determining water discharge based on hydraulic modelling. Canadian Journal of Civil Engineering **30**(1): 101-112.

Hicks, F. E. and Healy, D. 2004. Index velocity methods for winter discharge measurement. Canadian Journal of Civil Engineering **31**(3): 407-419

Hwang, N. H. C. And Houghtalen, R. J. 1996. "Fundamentals of Hydraulic Engineering Systems," Third edition, Prentice Hall, New Jersey.

John, F. D., Janusz, M. G., John, A. S. and Lynne, B. J. 2005. "Fluid Mechanics." 5th Edition. Pearson Education Limited, Edinburgh Gate, Harlow, England.

Katopodis, C. 2003. Case studies of inchannel flow modelling for fish habitat in Canadian Prairie Rivers. Canadian Water Resources Journal **28:** 199-216.

Katopodis, C. and Ghamry, H. K. 2007. Case studies of channel flow modeling for fish habitat in Canadian Prairie Rivers. Canadian journal of water resources.

Larsen, P. A. 1969. Head losses caused by an ice-covered open channels. Journal of the Boston Society of Civil Engineers **56**(1): 56-57.

Lau, Y. L. 1982. Velocity distributions under floating ice covers. Canadian Journal of Civil Engineering, Ottawa **9**(1): 76-83.

Martin, J. F., Robert, E. and Walker, J. F.1994. Estimation of mean flow velocity in ice-covered channels. Journal of Hydraulic Engineering - ASCE **120**(12): Paper No. 7517.

Melcher, N. B. and Walker, J. F. 1992. Evaluation of selected methods for determining channel flow during periods of ice effect. US Geological Survey, water supply paper, **2378**, Washington, D.C.

Morse, B and Hicks, F. 2005. Advances in river ice hydrology. Hydrological Processes **19**(1): 247-263.

Morse, B, Hamal, K. and Choquette, Y. 2005. River discharge measurement using the velocity index method. 13th Workshop on the Hydraulics of Ice Covered Rivers. Hanover, NH, 15 – 16 Sept. 2005.

Nezhikhovskiy, R. A. 1964. Coefficients of roughness of bottom surface of slush ice cover. Soviet Hydrology, Selected Papers **2**: 127-150.

Pelletier, P. M. 1989. Uncertainties in channel flow measurement under winter ice conditions. A case study: the Red River at Emerson, Manitoba, Canada. Water Resources Publications **25**(8): 1857-1867.

Power, G., Cunjak, R., Flannagan, J., and Katopodis, C. 1993. Biological effects of river ice. In Environmental Aspects of River Ice. NHRI Science report 5, Environment Canada, Sask. 97-119.

Prowse, T. D. 2001. River ice-ecology, B: Biological aspects. Journal of Cold Regions Engineering - ASCE **15:** 17- 33.

Rantz, S. E., and others, 1982. "Measurement and computation of channel flow." Water Supply Paper No. 2175. Vol. 1 and Vol. 5 of US Geological Survey, Washington D.C.

Rouse, H. 1961. "Fluid mechanics for Hydraulic Engineers." Dover publications, Inc. New York.

Spitzer, M. O. 1988. Peace River data review. Inland Waters and Lands, Western and Northern Region, Environmental Canada, Calgary, Canada.

Tallaksen, L. M. 1995. University of Oslo. A review of base flow recession analysis. Journal of Hydrology **165**(1-4): 349-370.

Teal, M. J., Ettema, R. and Walker, J. F. 1994. Estimation of mean flow velocity in ice-covered channels. Journal of Hydraulic Engineering – ASCE **120**: 1385-1400.

Terzi, R. A. 1981. Hydrometric field Manuel Measurement of Channel Flow, Water Resources Branch, Inland Water Directorate, Environment Canada, Ottawa, On, Canada.

Trillium Engineering and Hydrographics Inc., 2002, 2004a,b;).

Tsai, W. F. and Ettema, R. 1994. ce cover influence on transverse bed slopes in a curved alluvial channel. Journal of Hydraulic Research **32**(4): 561-582.

Urroz, G. E. and Ettema, R. 1994. Application of two-layer hypothesis to fully developed flow in ice-covered curved channels. Canadian Journal of Civil Engineering **21**: 101-110.

US Army Corps of Engineers, 1985. Ice engineering Manuel, EM 1110-2-1612, Department of the Army, Corps of Engineers, Davis, California.

US Army Corps of Engineers. 1990. HEC-2 Water Surface Profiles, Hydrologic Engineering Center, US Army Corps of Engineers, Davis, California

Uzuner, M. S. 1975. The composite roughness of ice covered channels. Journal of Hydraulic Research **13**(1): 79-102.

Urroz, G. E. and Ettema, R. 1994. Application of two-layer hypothesis to fully developed flow in ice-covered curved channels. Canadian Journal of Civil Engineering 21: 101-110.

Walker, J. F. 1994. Methods for measuring discharge under ice cover. Journal of Hydraulic Engineering – **120** (11): 1327-1336.

Walker, J. F. and Wang, D. 1997. Measurement of flow under ice covers in North America. Journal of Hydraulic Engineering - ASCE **123**(11): 1037-1040.

Wang, D. 1993. Cross-sectional velocity distribution of flow under ice. In proceedings of the CSCE annual conference. Fredericton, NB, 8 - 11 June, 1993. Canadian Society of Civil Engineering, 119-129.

White, K. D. and Daly, S. F. 1997. The effects of uncertainty in ice roughness on equilibrium ice thickness and stage. The 9th Workshop on River Ice, 24 – 26 Sept. 1997, Fredericton, N.B.

Yu, K. H. Graf, W. H. and Levine, G. 1968. The effect of ice on the roughness coefficients of the St. Croix River, Proceedings of 11th Conference on Great Lakes Research, Association of Great Lakes Research, 668-680.

Appendix A: Observed Ice Thickness

The figures in this appendix show the cross sectional view of channel width, flow depth and the thickness of the ice cover. The dashed curves mark the ice cover underside. In individual figures, the distance between the depth of zero m and the dashed curve is the thickness of the ice cover.

Cross sections 1

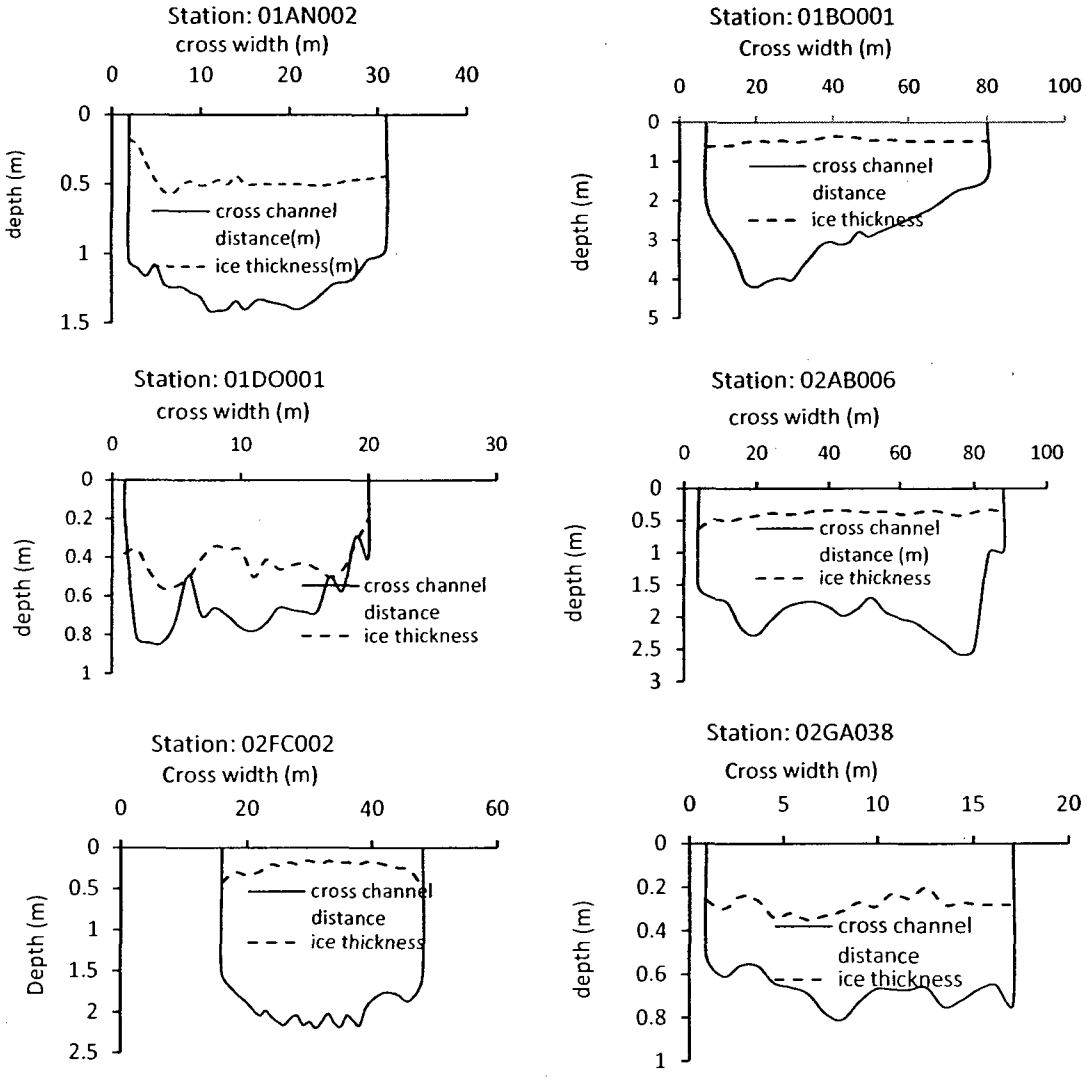

Cross-sections- 2

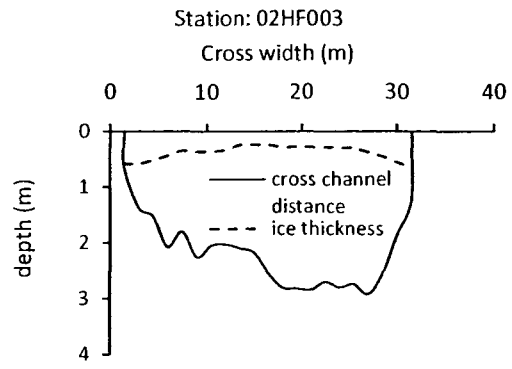

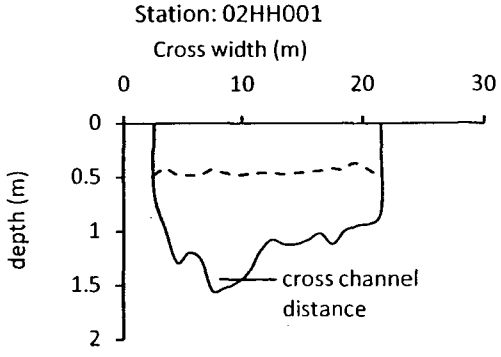

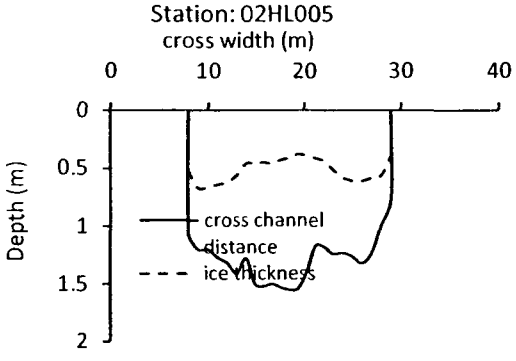

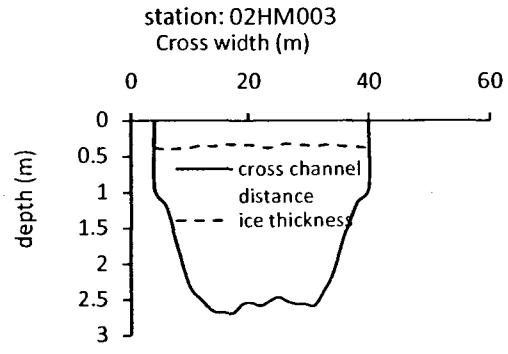

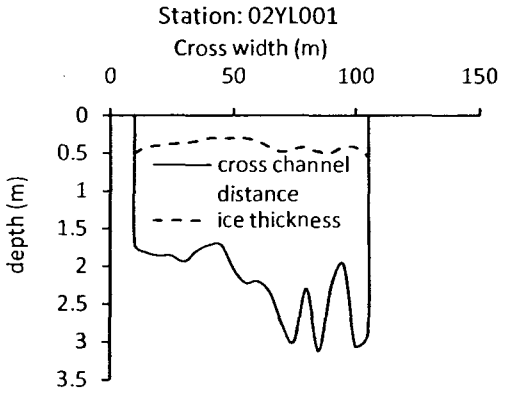

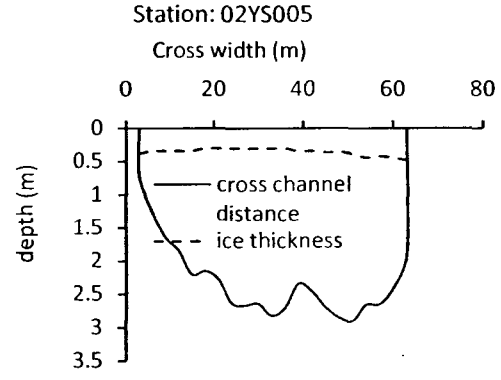

Cross-sections- 3

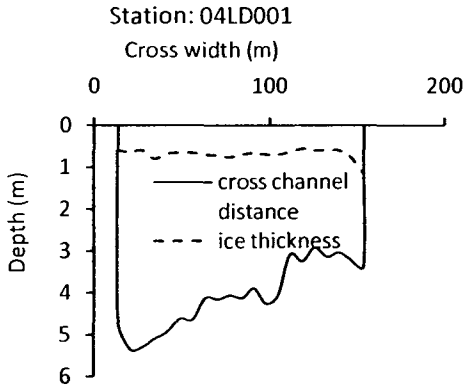

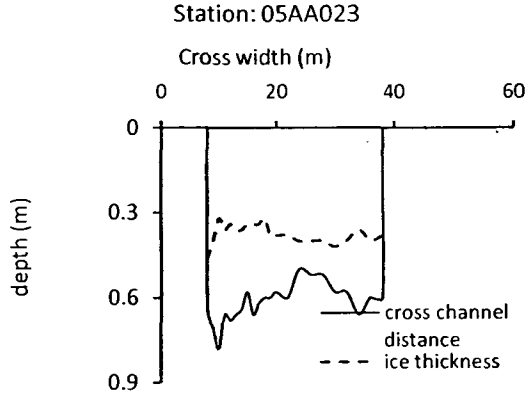

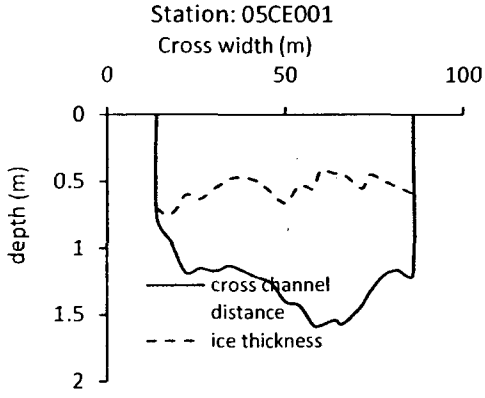

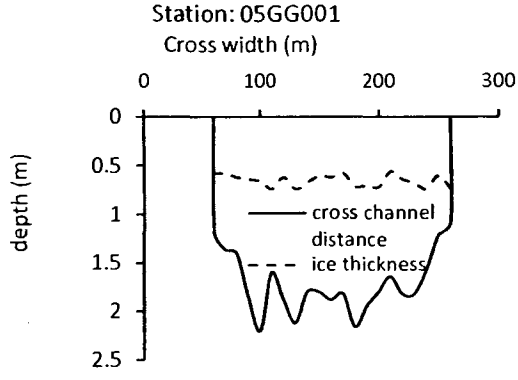

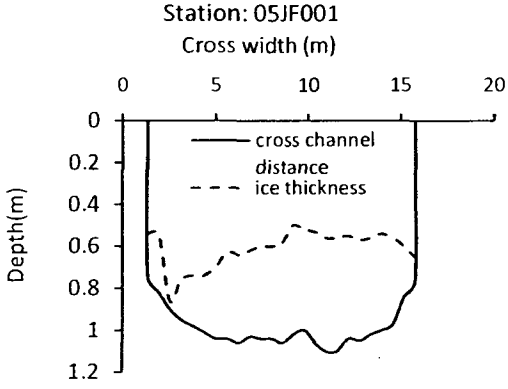

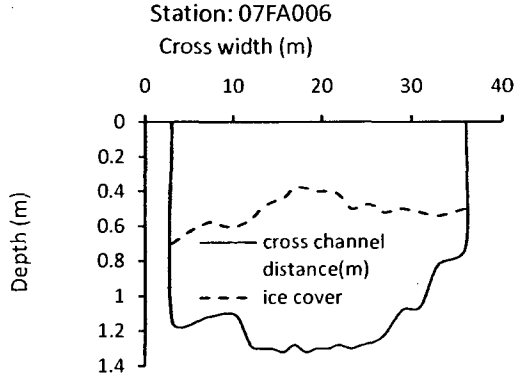

Cross-sections- 4

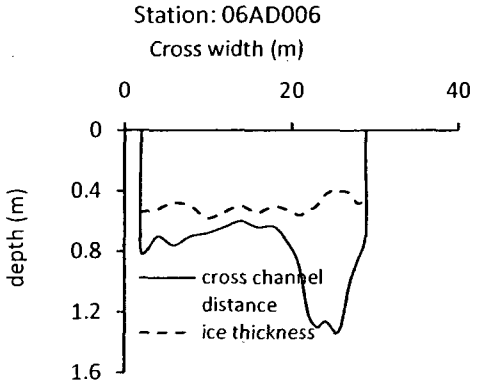

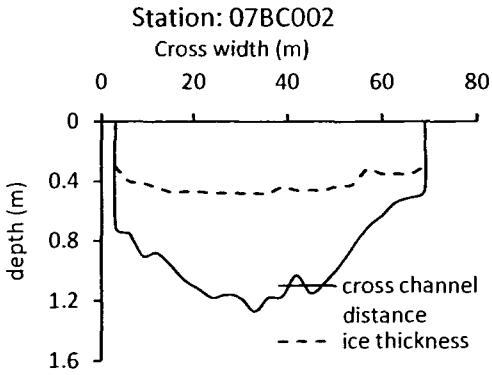

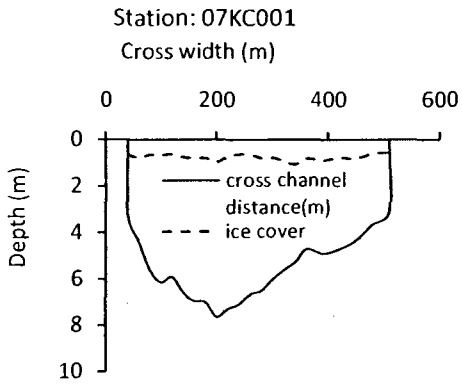

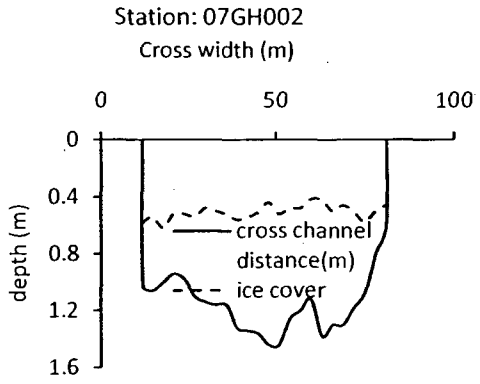

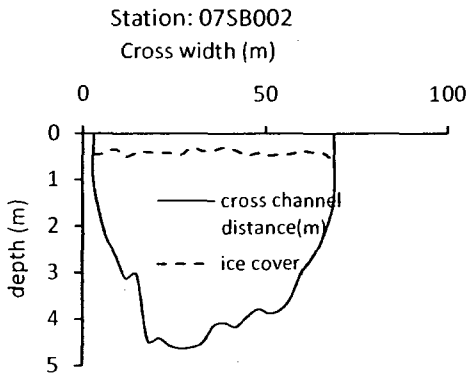

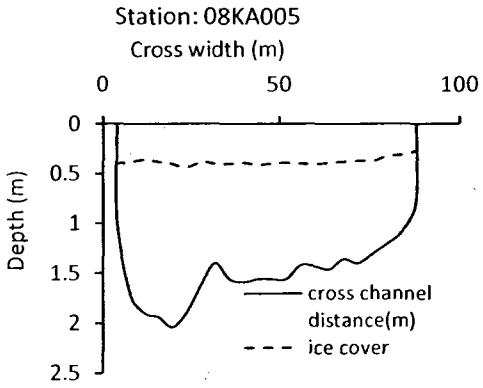

Cross-sections- 5

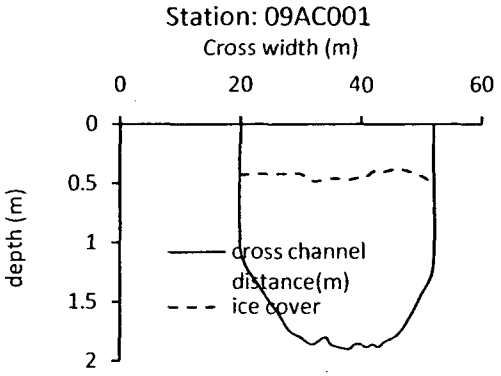

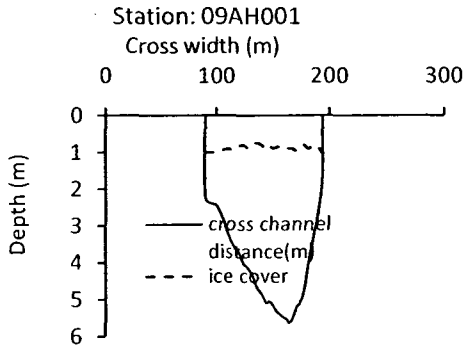

Appendix B: Observed Velocity Profiles

The figures in this appendix show observed velocity profiles. The solid curves indicate the change of the along-channel flow velocity with depth downward from the ice cover underside. The depth of zero m is set on the underside. The depth average velocities (dashed lines) are calculated from the observed velocity profiles.

Profile 1

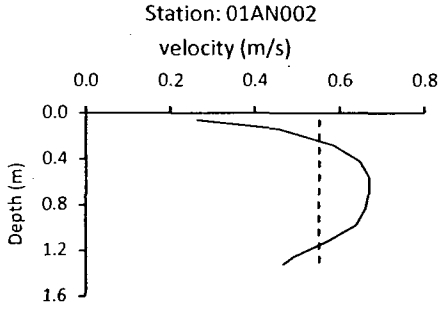

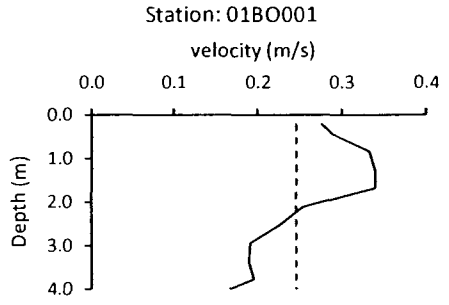

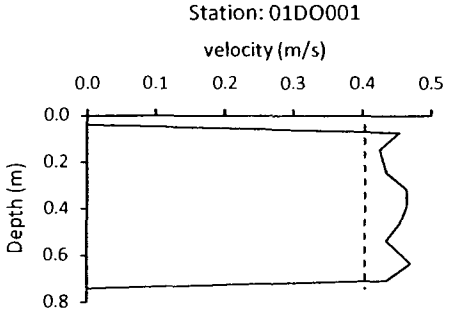

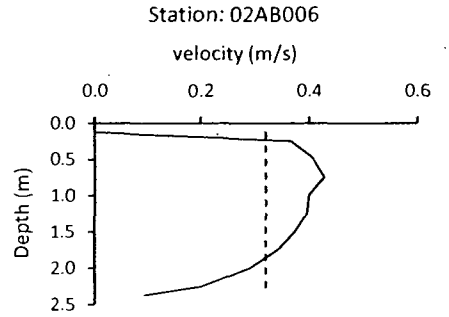

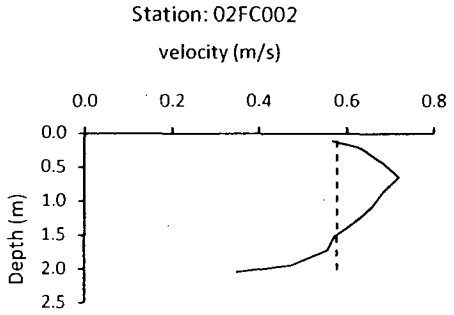

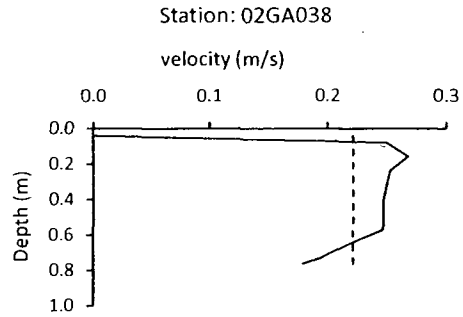

Profile 2

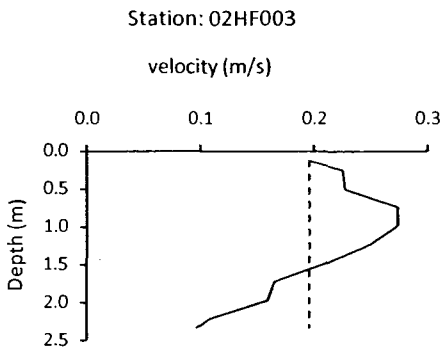
Station: 02HF003
velocity (m/s)
0.0
0.1
0.2
0.3
Depth (m)
0.0
0.5
1.0
1.5
2.0
2.5

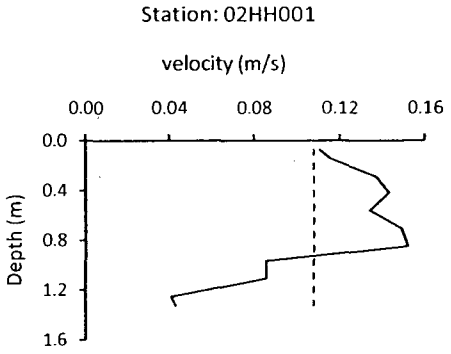
Station: 02HH001
velocity (m/s)
0.00
0.04
0.08
0.12
0.16
Depth (m)
0.0
0.4
0.8
1.2
1.6

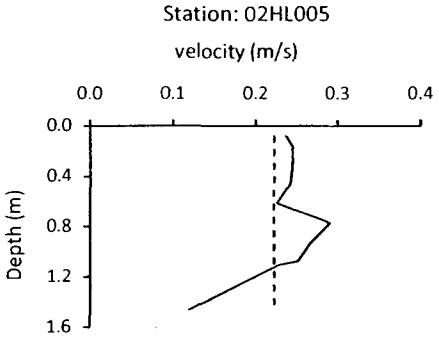
Station: 02HL005
velocity (m/s)
0.0
0.1
0.2
0.3
0.4
Depth (m)
0.0
0.4
0.8
1.2
1.6

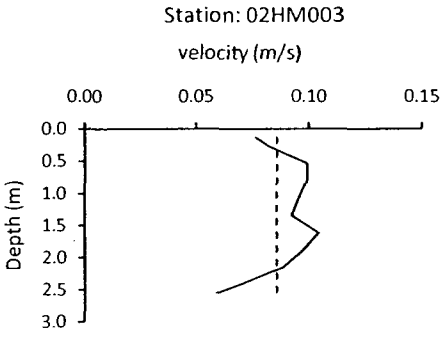
Station: 02HM003
velocity (m/s)
0.00
0.05
0.10
0.15
Depth (m)
0.0
0.5
1.0
1.5
2.0
2.5
3.0

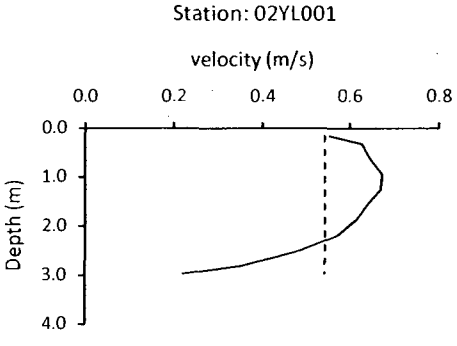
Station: 02YL001
velocity (m/s)
0.0
0.2
0.4
0.6
0.8
Depth (m)
0.0
1.0
2.0
3.0
4.0

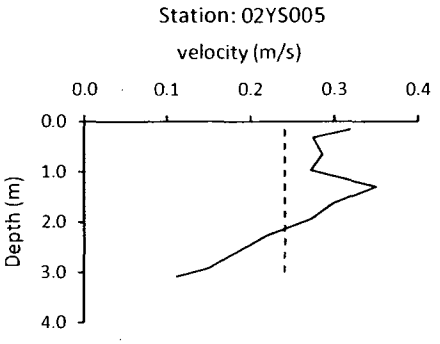
Station: 02YS005
velocity (m/s)
0.0
0.1
0.2
0.3
0.4
Depth (m)
0.0
1.0
2.0
3.0
4.0

Profile 3

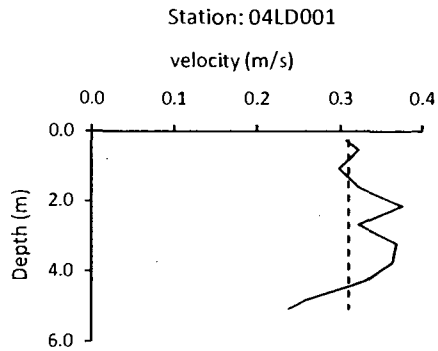
Station: 04LD001
velocity (m/s)
0.0
0.1
0.2
0.3
0.4
Depth (m)
0.0
2.0
4.0
6.0

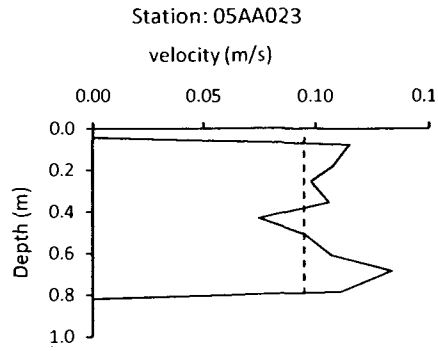
Station: 05AA023
velocity (m/s)
0.00
0.05
0.10
0.15
Depth (m)
0.0
0.2
0.4
0.6
0.8
1.0

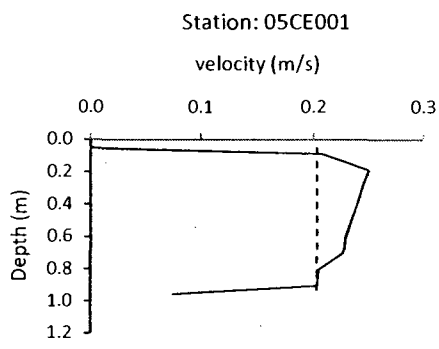
Station: 05CE001
velocity (m/s)
0.0
0.1
0.2
0.3
Depth (m)
0.0
0.2
0.4
0.6
0.8
1.0
1.2

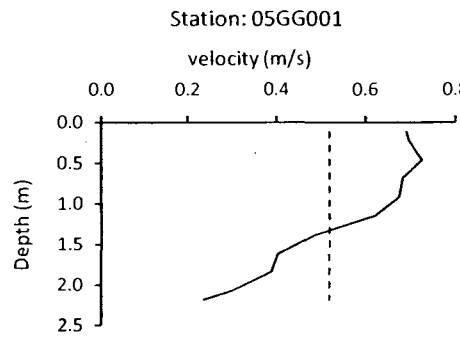
Station: 05GG001
velocity (m/s)
0.0
0.2
0.4
0.6
0.8
Depth (m)
0.0
0.5
1.0
1.5
2.0
2.5

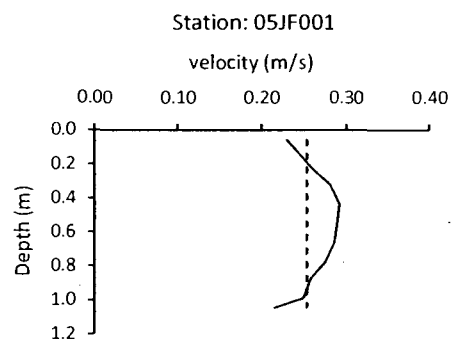
Station: 05JF001
velocity (m/s)
0.00
0.10
0.20
0.30
0.40
Depth (m)
0.0
0.2
0.4
0.6
0.8
1.0
1.2

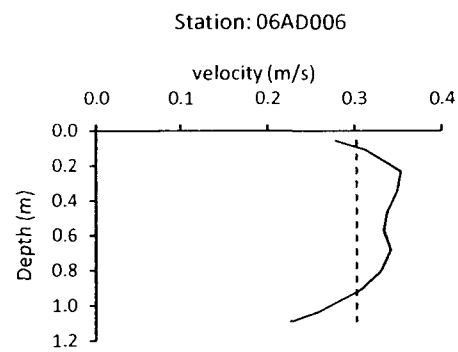
Station: 06AD006
velocity (m/s)
0.0
0.1
0.2
0.3
0.4
Depth (m)
0.0
0.2
0.4
0.6
0.8
1.0
1.2

Profile 4

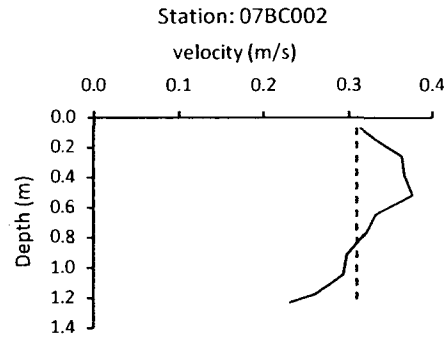
Station: 07BC002
velocity (m/s)
0.0 0.1 0.2 0.3 0.4
Depth (m)
0.0 0.2 0.4 0.6 0.8 1.0 1.2 1.4

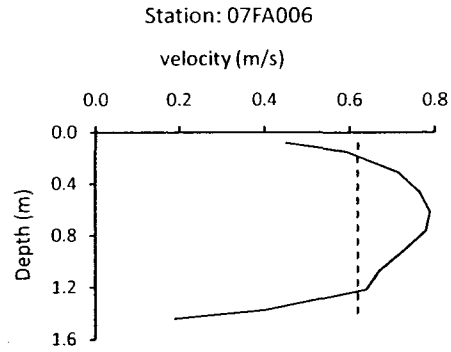
Station: 07FA006
velocity (m/s)
0.0 0.2 0.4 0.6 0.8
Depth (m)
0.0 0.4 0.8 1.2 1.6

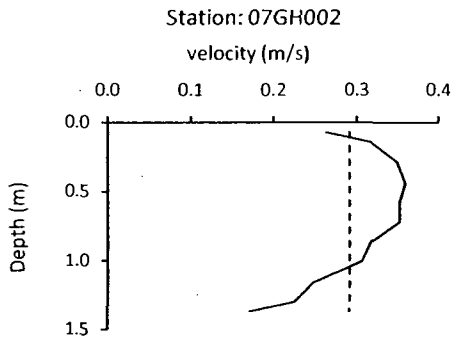
Station: 07GH002
velocity (m/s)
0.0 0.1 0.2 0.3 0.4
Depth (m)
0.0 0.5 1.0 1.5

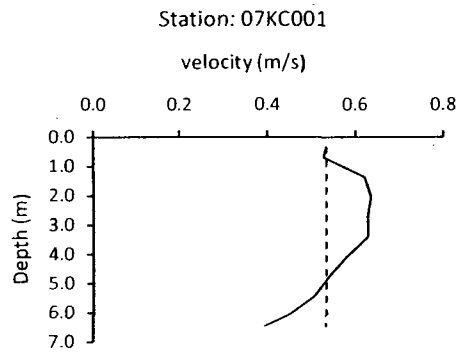
Station: 07KC001
velocity (m/s)
0.0 0.2 0.4 0.6 0.8
Depth (m)
0.0 1.0 2.0 3.0 4.0 5.0 6.0 7.0

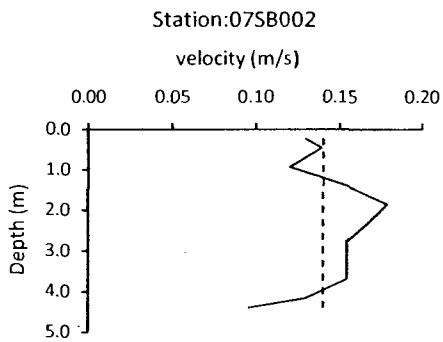
Station:07SB002
velocity (m/s)
0.00 0.05 0.10 0.15 0.20
Depth (m)
0.0 1.0 2.0 3.0 4.0 5.0

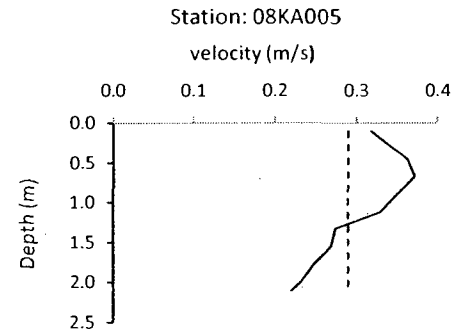
Station: 08KA005
velocity (m/s)
0.0 0.1 0.2 0.3 0.4
Depth (m)
0.0 0.5 1.0 1.5 2.0 2.5

Profile 5

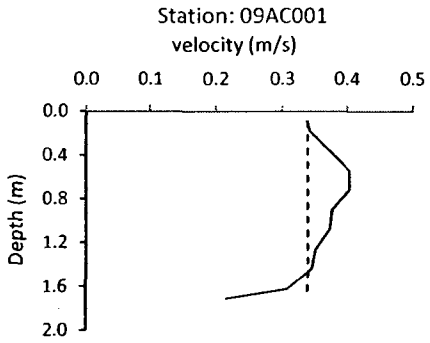
Station: 09AC001
velocity (m/s)
0.0
0.1
0.2
0.3
0.4
0.5
Depth (m)
0.0
0.4
0.8
1.2
1.6
2.0

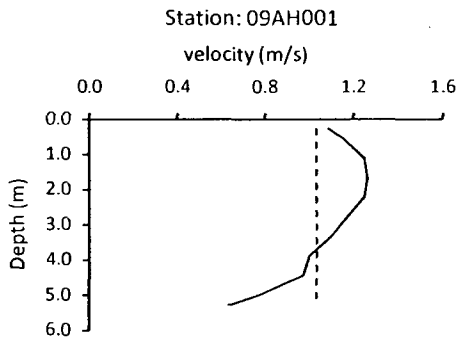
Station: 09AH001
velocity (m/s)
0.0
0.4
0.8
1.2
1.6
Depth (m)
0.0
1.0
2.0
3.0
4.0
5.0
6.0

Appendix C: Comparisons between Calculated and Observed Flow Velocities

This appendix compares the observed velocity profiles (solid curves) and the calculated logarithm velocity profiles (dashed curves). We fit the observed profiles using the best fit Manning's friction coefficient. The best fit has been obtained by trial-and-error.

Velocity Profiles-I

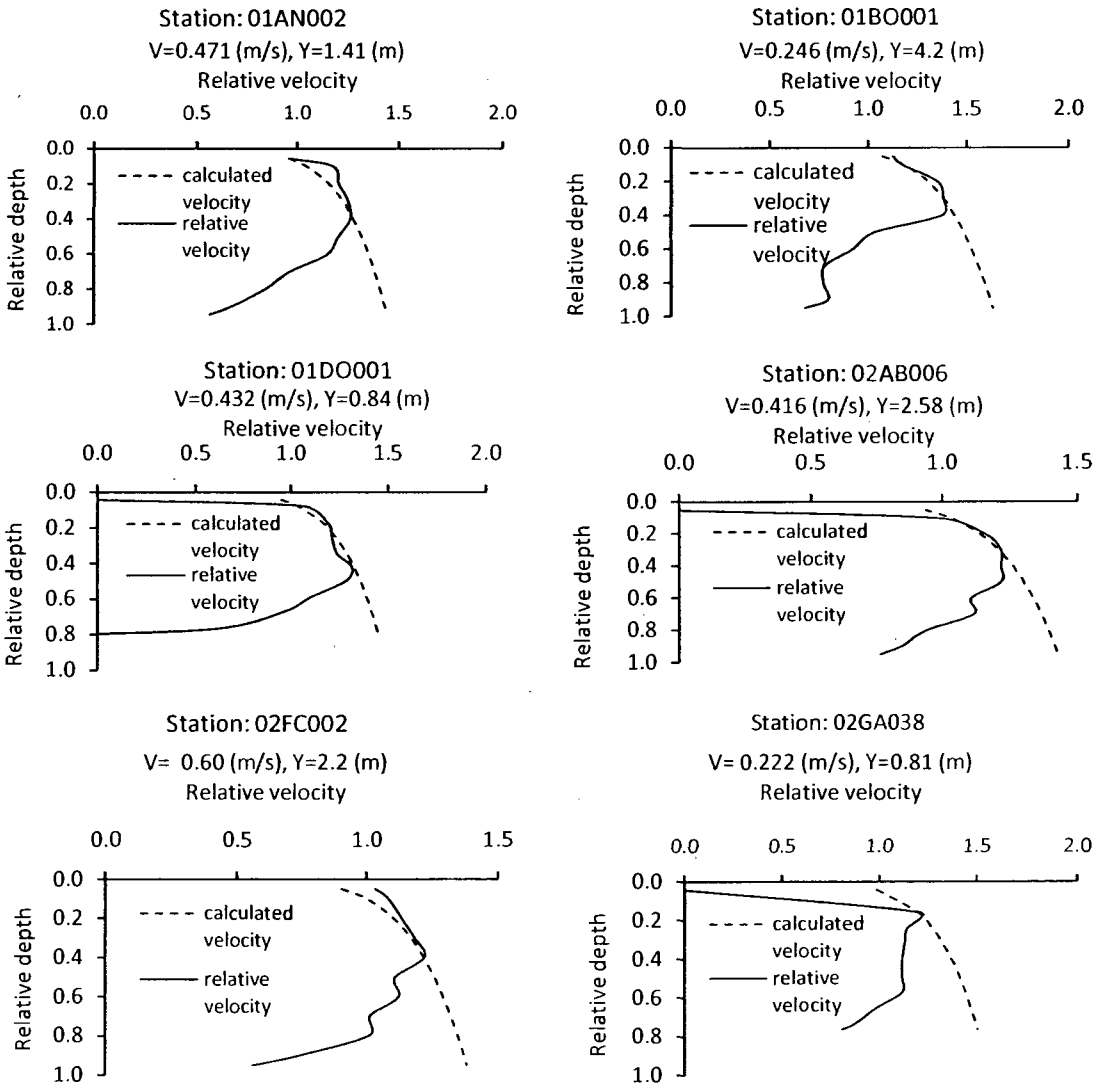

Velocity Profiles-2

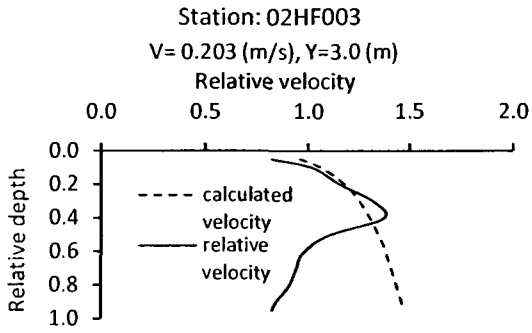

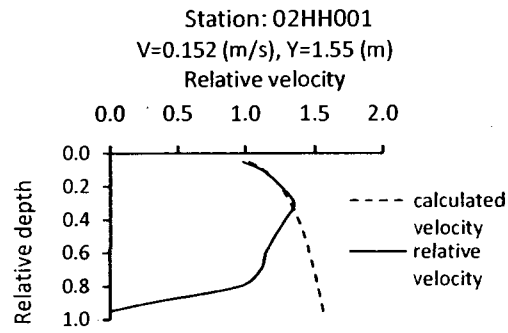

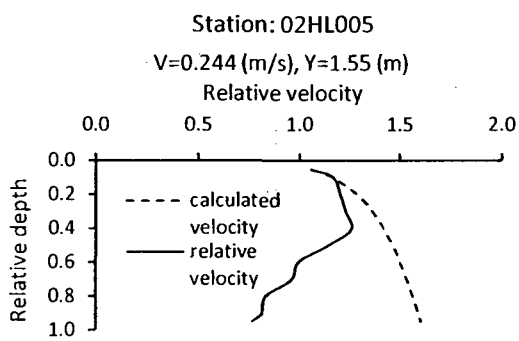

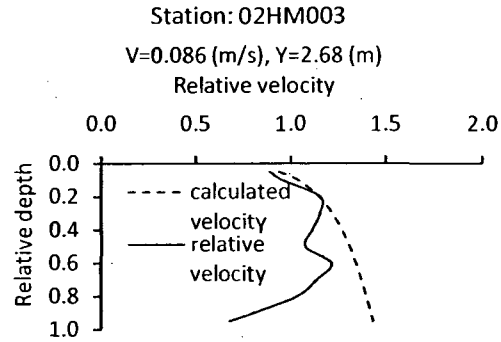

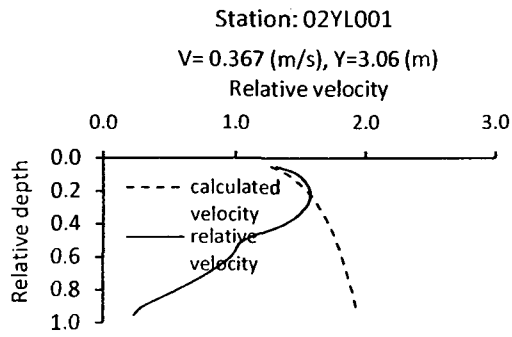

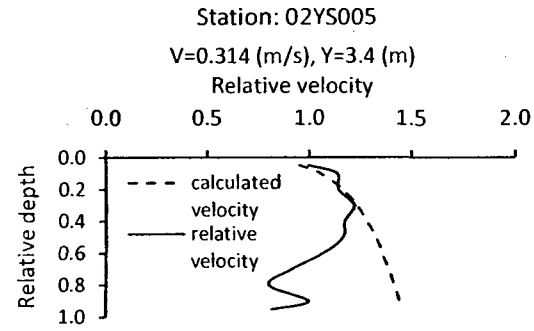

Velocity Profiles-3

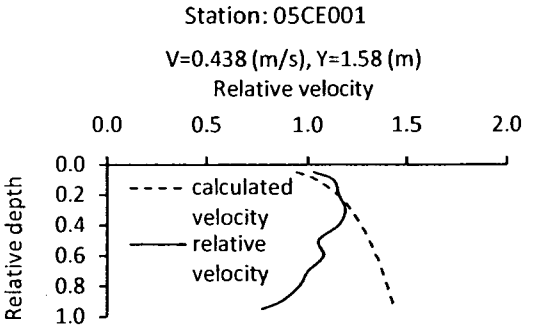

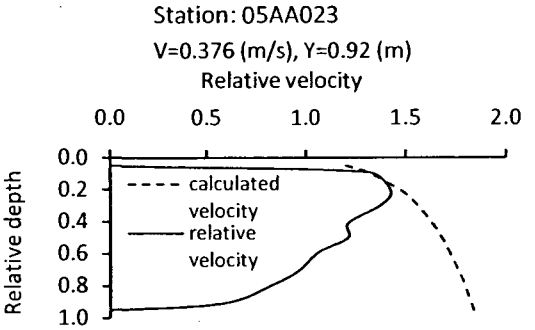

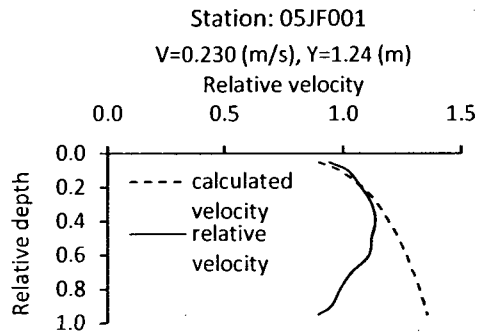

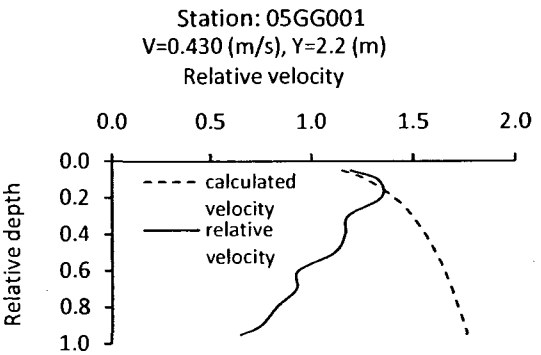

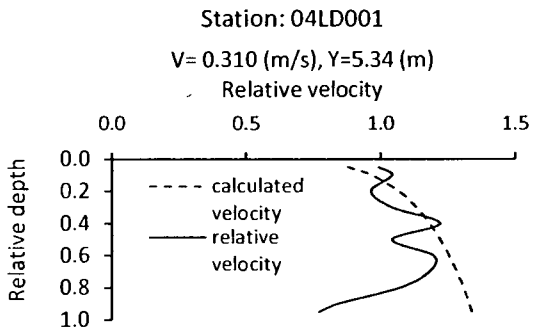

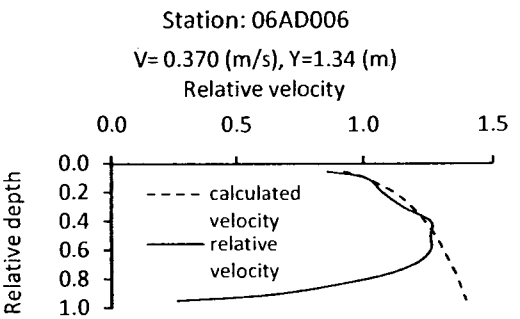

Velocity Profiles-4

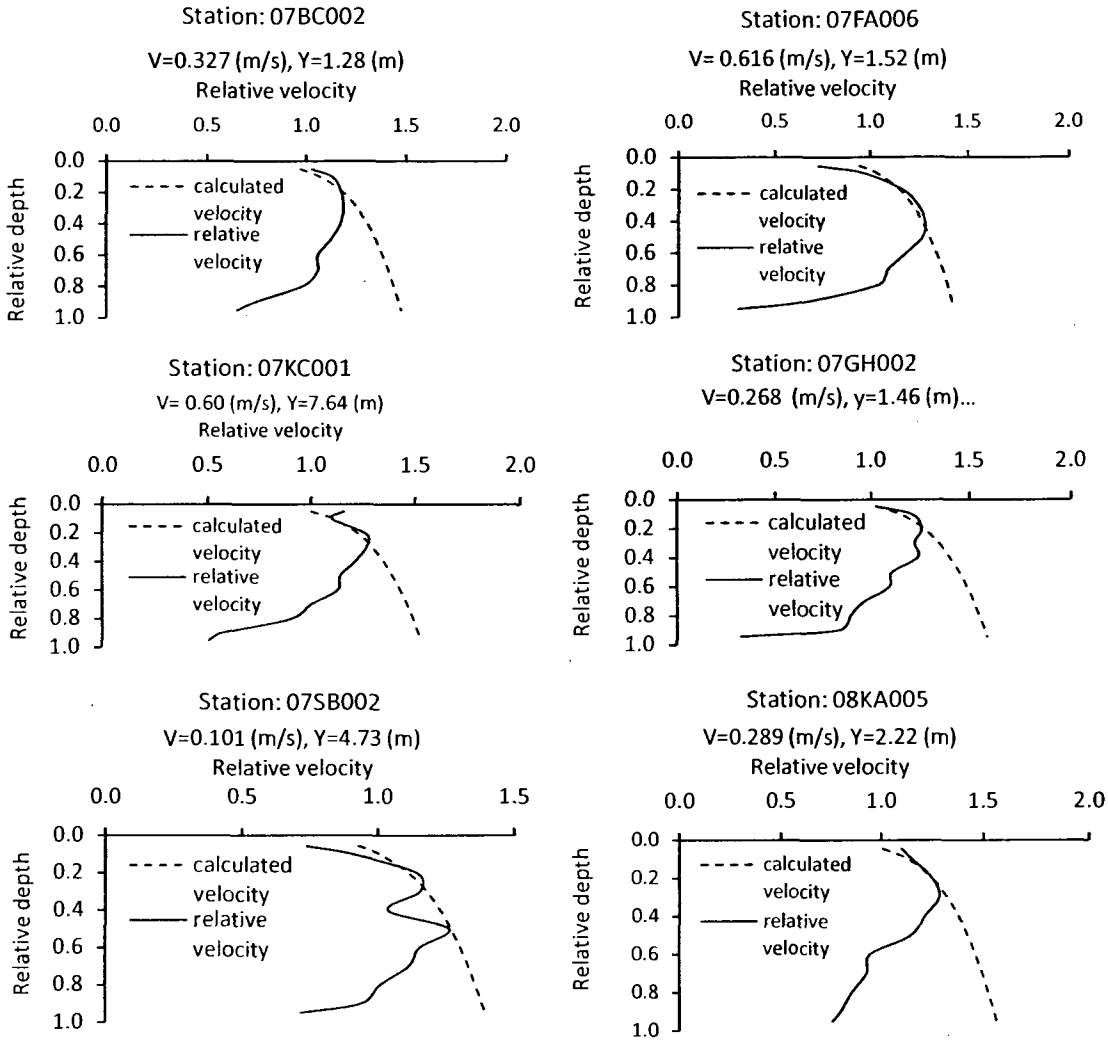

Velocity Profiles-5

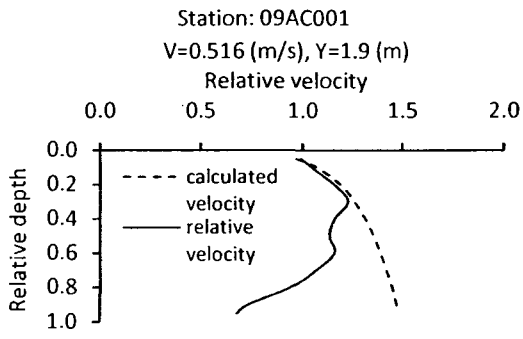

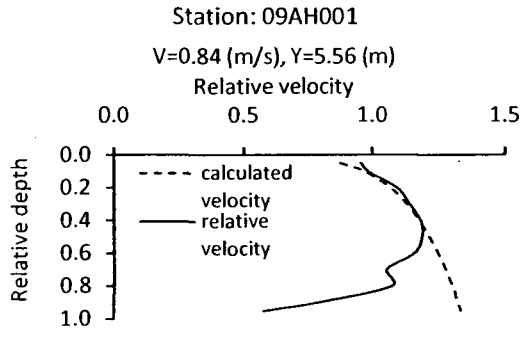

Appendix D: Flow Area Reduced by Ice thickness

The figures in this appendix show the effective flow area and the area reduced by ice thickness as calculated by using equations (4.5) and (4.6). The solid curves are the boundaries of the cross sections. The dashed curves mark the ice cover underside.

Cross section 1

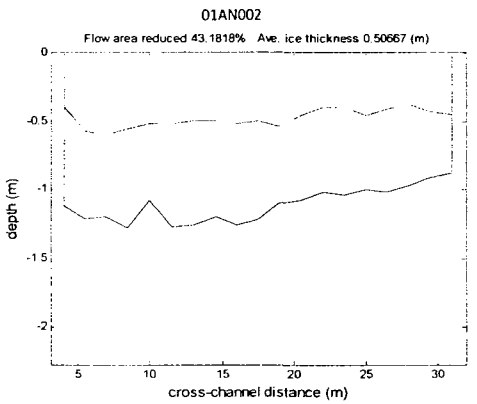

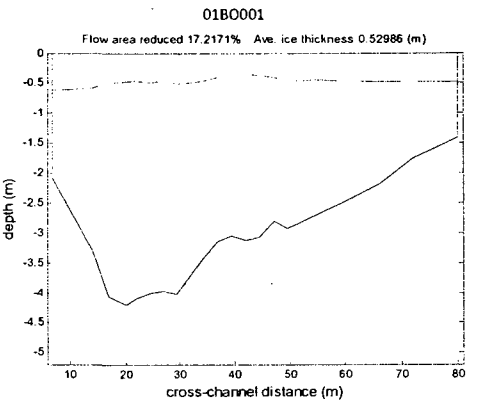

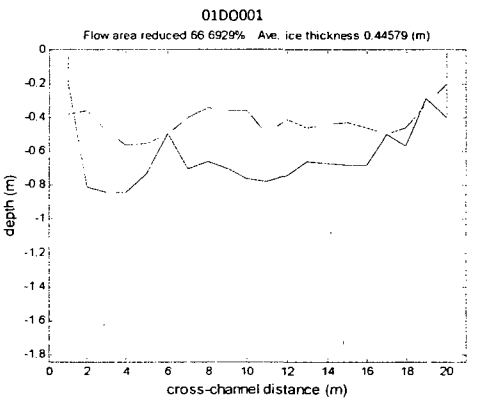

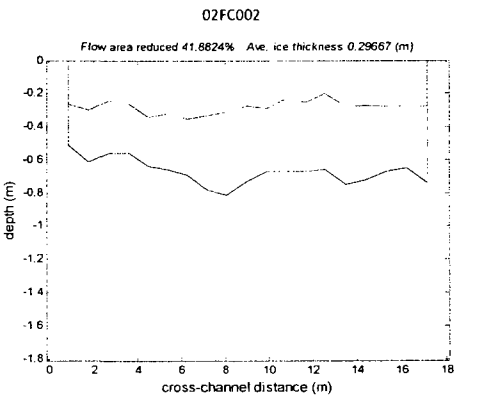

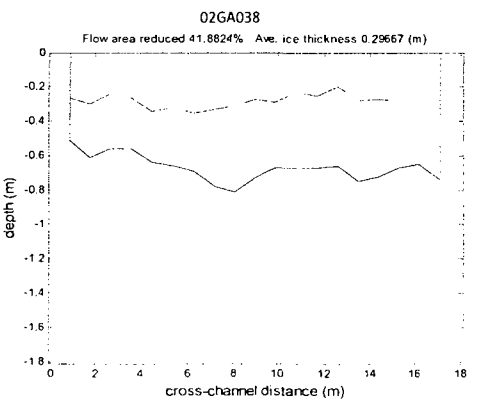

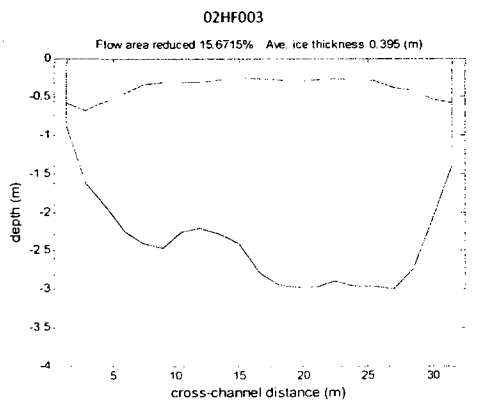

Cross section 2

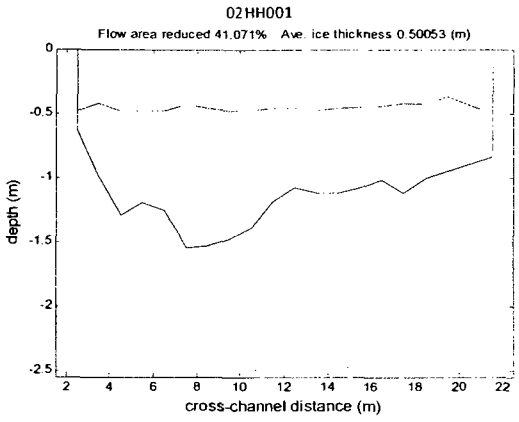

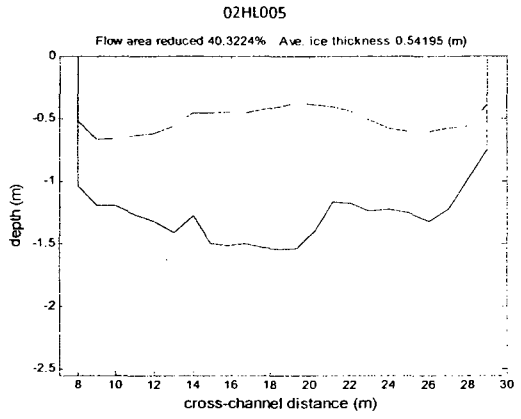

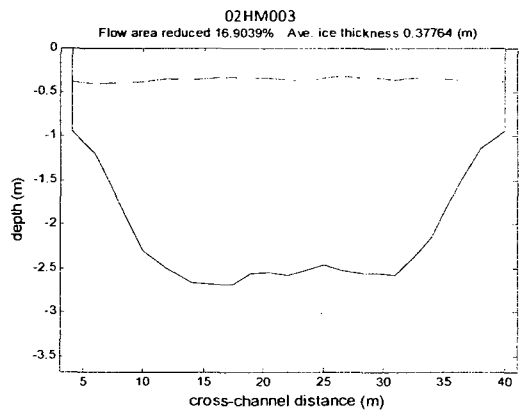

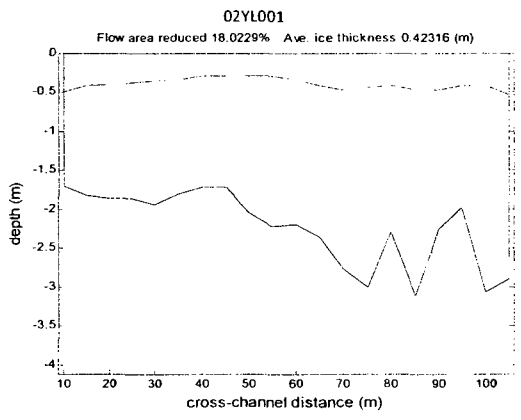

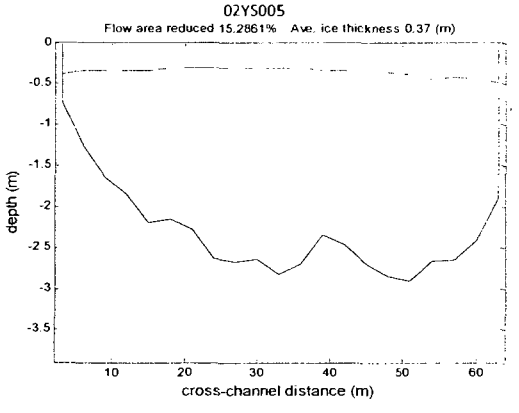

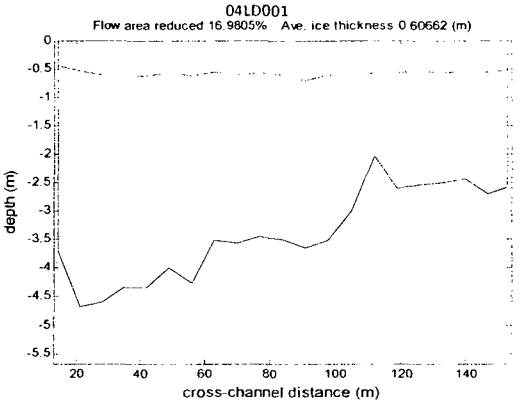

Cross section 3

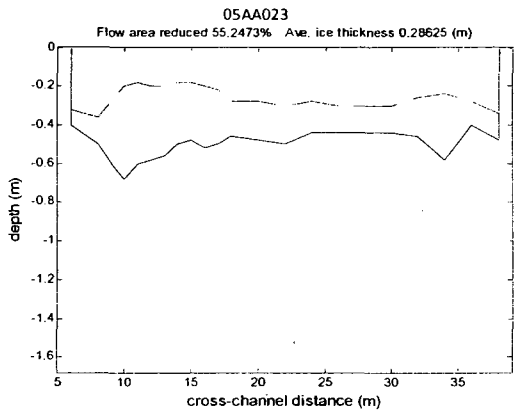

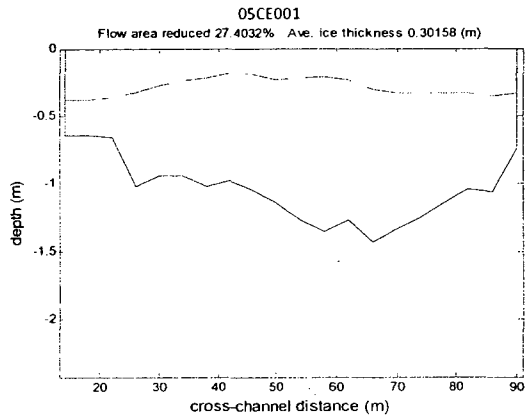

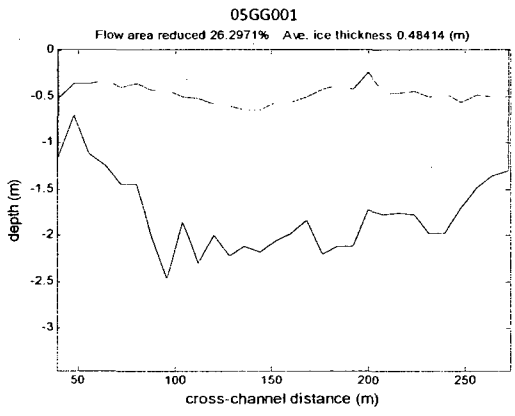

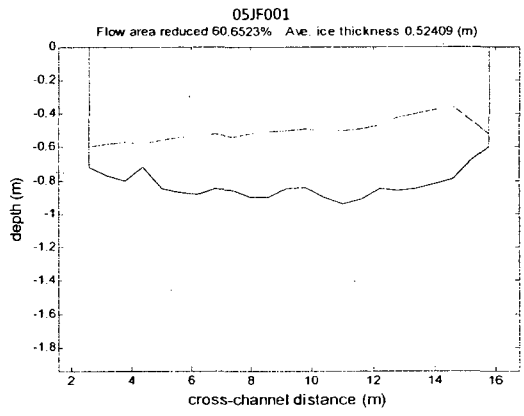

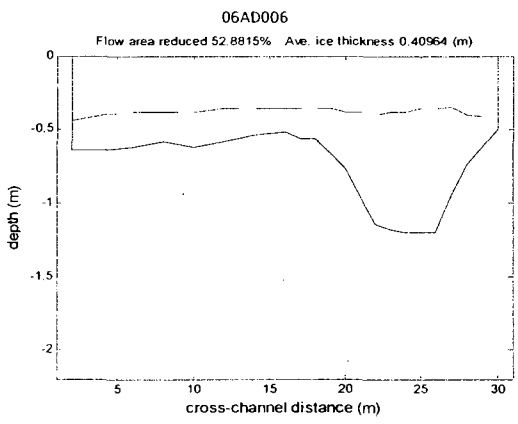

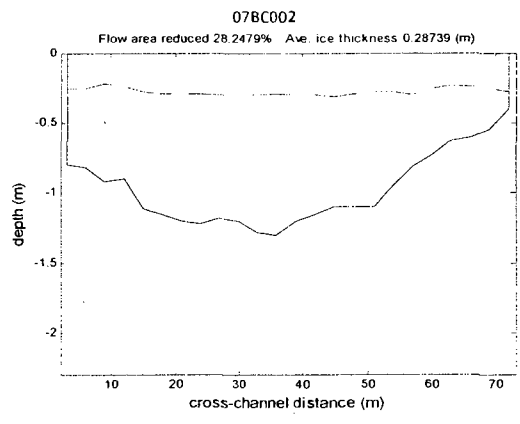

Cross section 4

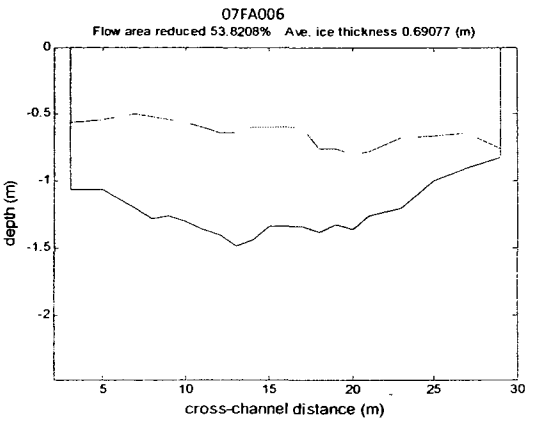

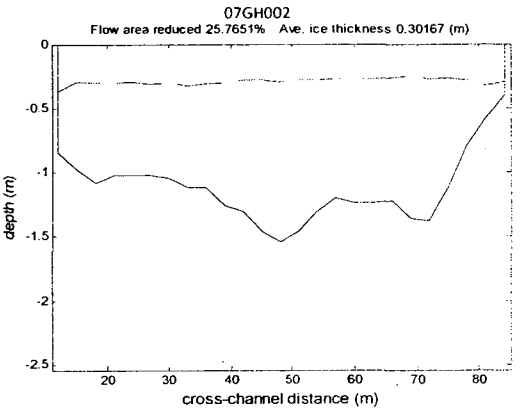

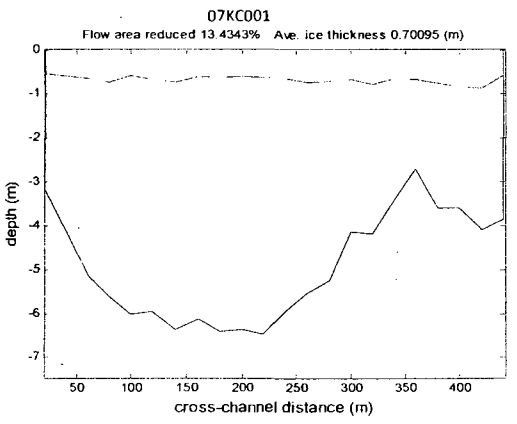

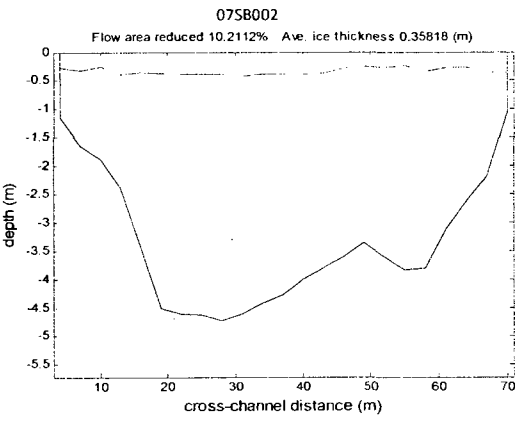

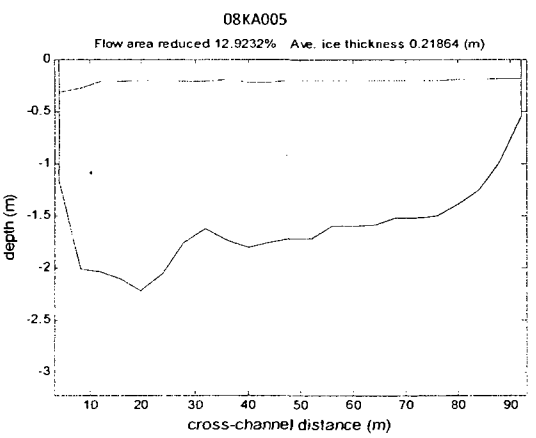

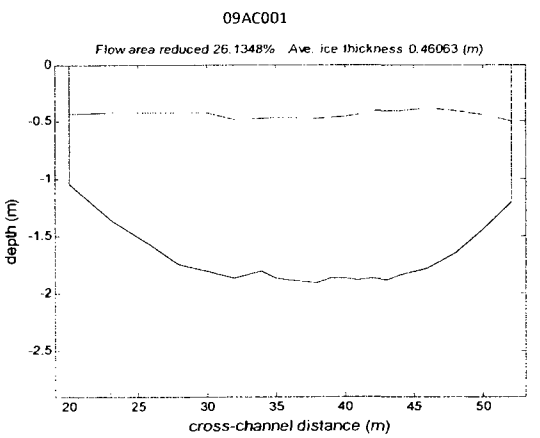

Cross section 5

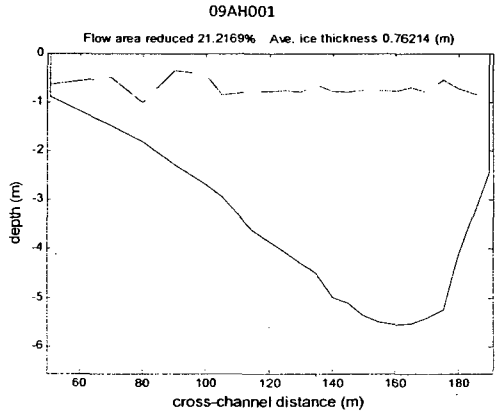

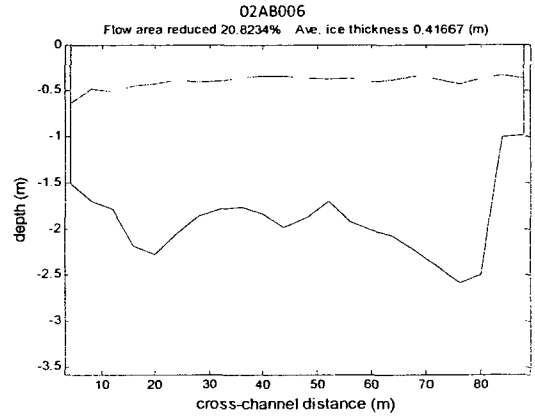

Appendix E: Modelling Application to the Yukon River

In this appendix, we show an example of applying the HEC-RAS model to the Yukon River, which is listed in Table 3.1. For this river, a representative section of 1000 m channel length was used.

The Yukon River is situated at Carmacks in Yukon Territory, Canada. It is a natural river. According to Water Survey Canada (WSC), the representing station of the river is 09AH001 and the geographic location is 62°5'45''N, 136°16'18"W. The gross drainage area of the river is 81,800 square kilometre. The average daily discharge from November to April is 350 m^3/s and 915 m^3/s from May to October. The peak discharge is in the mid June to mid July, being 3500 m^3/s. After analyzing all the data, we find out the flow area reduced by ice cover of the Yukon River is maximum of 26% and minimum of 21%. The average ice thickness is maximum 1.1 m and minimum 0.85 m. The mean flow depth is 2.5 m.

E.1 Requirement of Input data

The HEC-RAS model computes river surface profiles after input all of the required data. There are several steps of data input before running the program. The entry of geometric data is primarily important, including the river network and river reaches from up channel to down channel. The following steps to be followed in this section:

1) Name of the river and reach, including junctions.
2) The cross-sectional data is to be entered in its own editor and each cross-section is identified by reach name and river station. The cross-sectional data consists of X-Y coordinates of channel bottom, distance to down channel cross-section,

Manning's *n* values for the entire channel (the main channel, left overbank and right overbank, usually Manning's n values for overbank areas are higher than the main channel area), and contraction or expansion coefficients. During the entering of cross-section data, there is an option to enter the ice cover data. The ice cover data option consists of ice cover thickness and ice cover Manning's *n* values, both for the left overbanks, channel and right overbanks.

3) After entering all of the cross-sectional data, the steady flow data to be entered with boundary conditions for all profiles, e.g. known water surface elevations, critical depth and normal depth.
4) Completing the above steps, the program is run with subcritical, supercritical and mixed flow conditions. The result will come out with cross sectional view, rating curve, three dimensional perspective plot, velocity distribution plot, water surface profile plot, cross-section output table and profile output table.

E.2 Simulation Examples

The HEC-RAS program primarily starts the calculation of cross sections after the geometric data input. The cross sections data input starts at the downstream river station as 0.00 m for a starting distance and progressively works towards upstream within the channel length. Each entry of cross sectional data contains river station and elevation, evenly spaced intervals between two cross sections, channel bottom slope, Manning's *n* coefficients for the entire channel, and location of floodplains. The data needs to be entered separately for each cross section. After finishing all of the cross section data, the flow data is to be entered. The flow data contains the discharge rates with boundary

conditions for different flow pattern. For supercritical flow (Froude number is greater than one), calculations starts at the upstream of the channel. For sub critical flow (Froude number is less than one), calculations starts at the downstream of the channel, and for mixed flow (critical flow, the Froude number is one), calculations can start at either upstream or downstream of the channel. The types of boundary conditions are as follows:

1) Known water surface elevation,
2) Critical depth- free over fall or weir,
3) Normal depth – down channel energy slope is required, and
4) The Rating curve (water surface elevation as a function of discharge).

After finishing all of the above procedures, the program is run until reaching steady flow condition. If the program runs successfully, results of the simulation, e.g. the plan, cross sections, two and three dimensional flow profile plot, water surface profile, velocity profile plot, the rating curve and the entire detailed output table will be produced. All calculations are done in the using model equations, some of which are given in chapter five.

E.3 Results

In the following we present the results of cross sections, water surface profiles, velocity distributions, rating curves and three dimensional perspective plans. We will particularly discuss the cross section 1, as the downstream of the river.

The Yukon River (a single reach) is drawn manually. Eleven cross sectional data were interpolated and entered into the geometric data editor. The top view of the simulation reach is shown in Figure E.1. A configuration of cross sections are shown

after input the cross sectional data. The cross sections are evenly spaced. There are no junctions in the longitudinal direction. Cross section 11 is the upstream boundary of the simulation reach and cross section 1 is the downstream boundary.

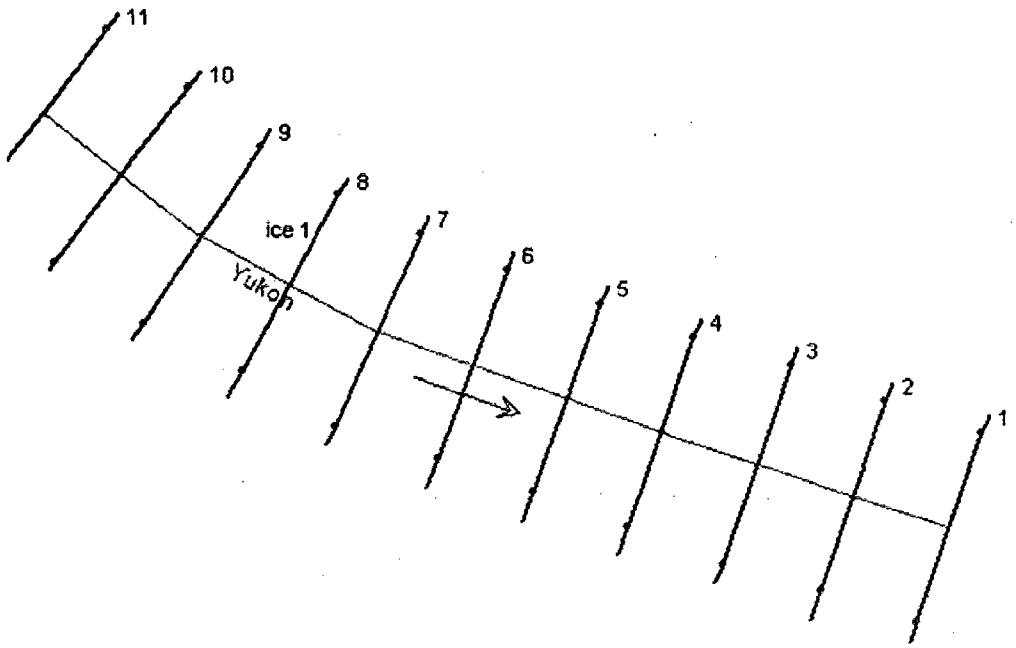

Figure E.1 Yukon River and its reach showing the cross section locations.

Figure E.2 shows a typical cross section. All cross sections contain the information of the river bank station, wetted perimeter, floodplain location of left and right over bank, bank to bank distance, main channel distance, ground surface location, energy grade profile, water surface profile and the ice cover formation. The ice cover thickness of the cross section at left over bank is 0.5 m, main channel is 0.4 m and the right over bank is 0.5 m. Manning's n values of the ice cover for the left over bank, main channel and right over bank are given in Table E.1.

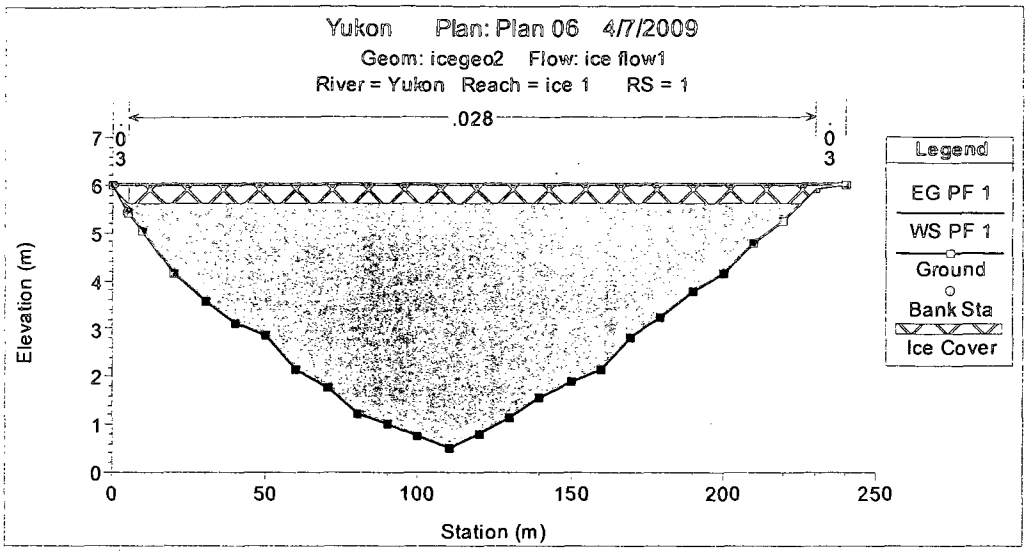

Figure E.2 Cross- section showing the ice cover, water area and bottom variations

Figure E.3 shows the water surface profile after the simulation reaches the steady state. This figure also shows the water surface elevation of the main channel, energy gradient profile, ground surface locations and the ice cover formation, considering steady flow with sub critical flow condition. The flow pattern will be changed if the flow condition is changed to supercritical or mixed flow. Usually, the upstream area of the river is wider whereas the velocity is lower and the downstream area is narrower and the velocity is higher. The energy slope of the channel maintains the flow.

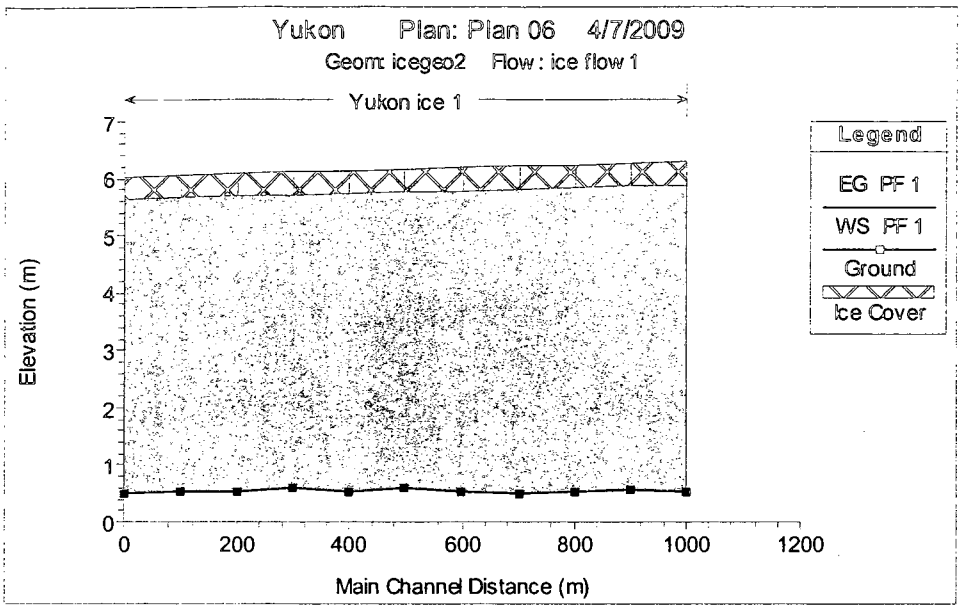

Figure E.3 Water surface profile plot

Figure E.4 shows the velocity profile of left bank, main channel and right bank are in y axis and channel distance in x axis. The figure also shows the maximum velocity at the downstream of the cross section 1 is 0.53 m/s and minimum velocity at upstream of the channel cross section 11 is 0.56 m/s. The total flow of the cross section 1 is 350 m^3/s.

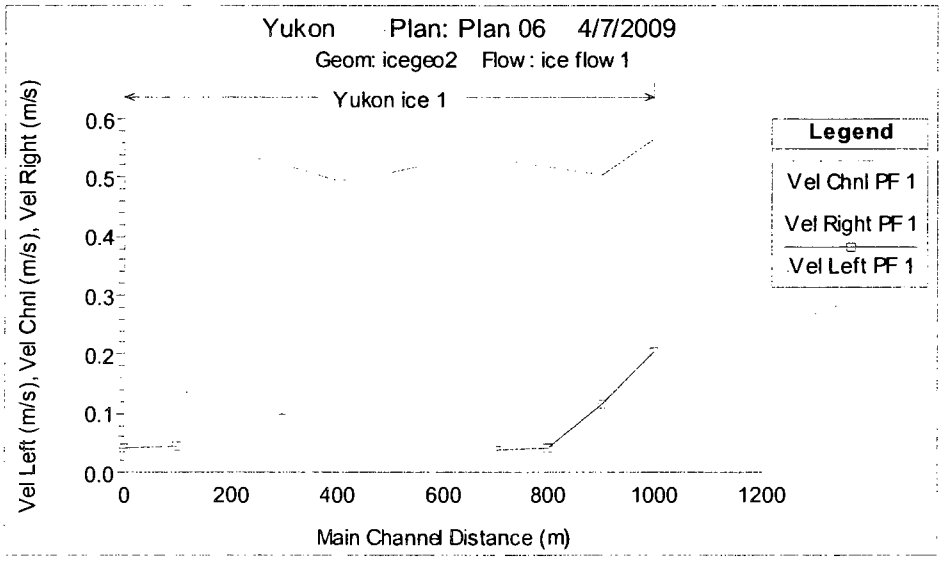

Figure E.4 Velocity variations along the channel.

The rating curve is a function of water surface elevation and discharge. Figure E.5 shows the rating curve of channel cross section 1. In this analysis, the maximum water surface elevation is 6.0 m and the corresponding discharge is 350 m^3/s. The minimum elevation is 0.49 m and corresponding discharge is 0 m^3/s. The critical water depth is 2.72 m.

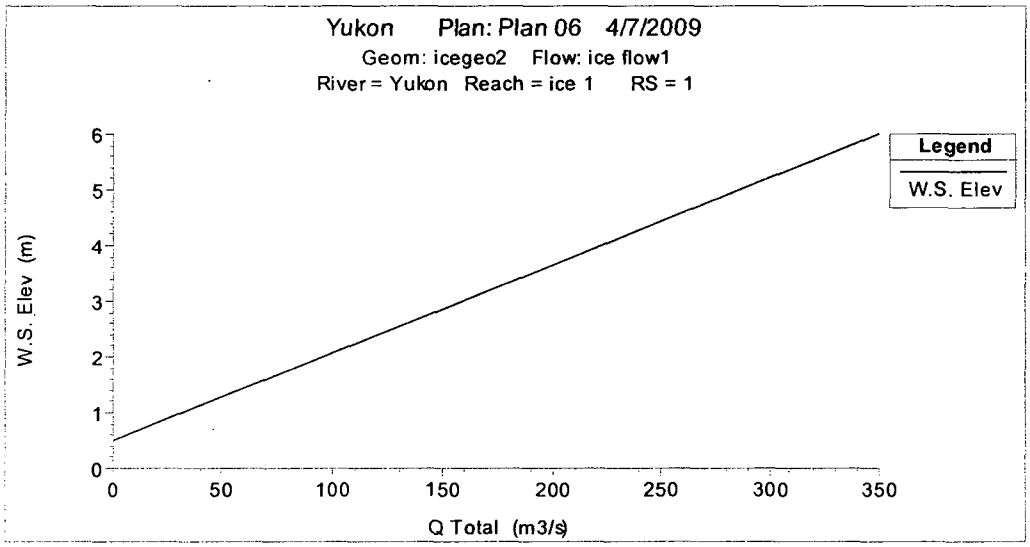

Figure E.5 The rating curve of cross section 1

Figure E.6 shows the three dimensional plan including water surface profile, ground surface, left and right bank station and ice cover thickness. This plan also indicates the water surface profile from upstream to downstream.

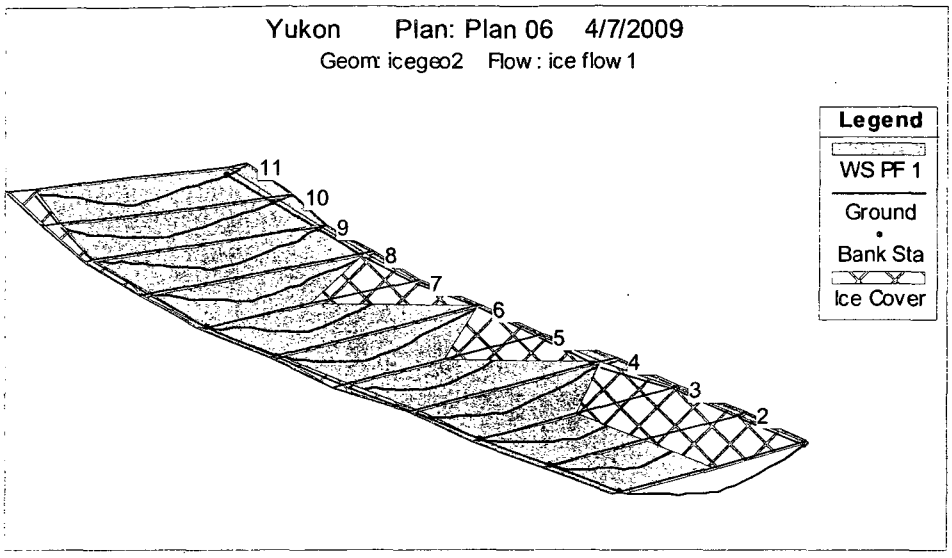

Figure E.6 Three dimensional perspective plan

Table E.1 shows the result of the river modeling for cross section 1. The reach length of one cross section to other cross section is 100 m. The energy grade elevation is 6.01 m, water surface elevation is 6.0 m, total discharge is 350 m^3/s, energy coefficient is1.0, average flow velocity is 0.53 m/s, hydraulic depth is 3.0 m, minimum channel elevation is 0.49 m and maximum channel depth is 5.51m.

Table E.1 Model results for HEC-RAS runs.

Yukon ice 1 RS: 1	Profile: PF 1				
E.G. Elev (m)	6.01	Element	Left OB	Channel	Right OB
Vel Head (m)	0.01	Wt. n-Val.	0.041	0.04	
W.S. Elev (m)	6	Reach Len. (m)			
Crit W.S. (m)	2.72	Flow Area (m2)	0.07	662.48	
E.G. Slope (m/m)	0.000257	Area (m2)	0.07	662.48	
Q Total (m3/s)	350	Flow (m3/s)	0	350	
Top Width (m)	221.76	Top Width (m)	1.12	220.64	
Vel Total (m/s)	0.53	Avg. Vel. (m/s)	0.04	0.53	
Max Chl Dpth (m)	5.51	Hydr. Depth (m)	0.07	3	
Conv. Total (m3/s)	21828	Conv. (m3/s)	0.2	21827.8	
Length Wtd. (m)		Wetted Per. (m)	2.25	441.55	
Min Ch El (m)	0.49	Shear (N/m2)	0.08	3.78	
Alpha	1	Stream Power (N/m s)	0	2	
Frctn Loss (m)		Cum Volume (1000 m3)			
C & E Loss (m)		Cum SA (1000 m2)			

Table E.2 shows the reach, river station, profile, total discharge, the minimum channel elevation, water surface elevation, critical water surface elevation, energy grade elevation, energy grade slope, channel velocity, flow area, top width, and the Froude number. The minimum channel elevation is 0.49 m at river station 1, and the maximum is 0.59 m at river stations 4 and 6. The minimum water surface elevation is 6.0 m at river station 1, and the maximum is 6.25 m at river station 11. The critical water surface elevation is 2.72 m at river station 1, the downstream of the river. The maximum elevation of energy grade line is 6.27 m at river station 11, the upstream of the river, and a minimum is 6.01m at river station 1, the downstream of the river. The minimum channel velocity is 0.49 m/s at river station 5, the upstream portion, and the maximum channel velocity is 0.56 m/s at river station 11, the upstream portion the river. The Froude number of all of the cross section is less than 1.0.

Table E.2 Model results of HEC-RAS runs.

Reach	River Sta	Profile	Q Total	Min Ch El	W.S. Elev	Crit W.S.	E.G. Elev	E.G. Slope	Vel Chnl	Flow Area	Top Width	Froude # Chl
			(m3/s)	(m)	(m)	(m)	(m)	(m/m)	(m/s)	(m2)	(m)	
ice 1	11	PF 1	350	0.51	6.25		6.27	0.000266	0.56	633.86	224.71	0.1
ice 1	10	PF 1	350	0.57	6.23		6.25	0.000208	0.5	697.89	230.03	0.09
ice 1	9	PF 1	350	0.54	6.21		6.22	0.000251	0.52	676.96	231.38	0.1
ice 1	8	PF 1	350	0.5	6.18		6.2	0.000278	0.53	656.19	231.02	0.1
ice 1	7	PF 1	350	0.52	6.15		6.17	0.000277	0.53	662.29	233.32	0.1
ice 1	6	PF 1	350	0.59	6.13		6.14	0.000241	0.51	690.96	233.86	0.09
ice 1	5	PF 1	350	0.54	6.11		6.12	0.000212	0.49	709.86	232.24	0.09
ice 1	4	PF 1	350	0.59	6.08		6.1	0.000245	0.52	674.45	236.88	0.1
ice 1	3	PF 1	350	0.54	6.05		6.07	0.000304	0.54	643.69	232.79	0.1
ice 1	2	PF 1	350	0.53	6.03		6.04	0.000276	0.53	655.54	230.3	0.1
ice 1	1	PF 1	350	0.49	6	2.72	6.01	0.000257	0.53	662.55	221.76	0.1

The Yukon River contains a single river reach and we did not consider any other branching of the river and water control structures. The simulations were done at steady flow condition. The steady flow water surface profiles shows the systems of channels, flow conditions e.g., supercritical, sub critical and mixed flow and the ice cover. The HEC-RAS model needs at least two cross sections for the upstream and downstream boundary conditions. We considered one sub-section of one kilometre long for our modelling. The river has different discharges in different seasons of the year. However, we considered an average discharge of 350 m^3/s. Simulations were done successfully.